The role of Ebf2 in normal and malignant hematopoiesis

Christoph Hinzen

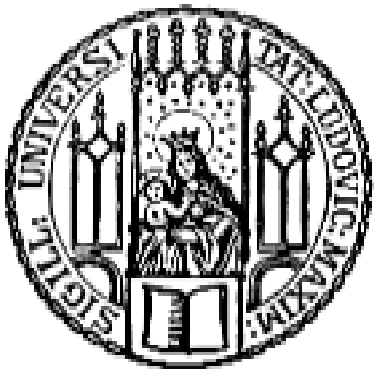

München 2012

The role of Ebf2 in normal and malignant hematopoiesis

Dissertation zur Erlangung des Doktorgrades der Naturwissenschaften (Dr. rer. nat.) der Fakultät für Biologie der Ludwig-Maximilians-Universität München

vorgelegt von
Christoph Hinzen
aus Bonn-Duisdorf

angefertigt am Helmholtz Zentrum für Gesundheit und Umwelt München

München, den 06.06.2012

Erstgutachter:	Frau Prof. Dr. Berit Jungnickel
Zweitgutachter:	Herr Prof. Dr. Michael Schleicher
Tag der mündlichen Prüfung	30.11.2012

Gewidmet meinen Eltern, Brüdern, Elke und meinem Cousin Maurits

Publications and presentations

Ebf2 expressed by osteoblastic cells mediates homing and early expansion of HSCs in the bone marrow

Hinzen C, Prokisch H, Zimber-Strobl U, Kieslinger M. (Manuscript in preparation)

Oral presentations

2/2009

TRR 54 Meeting: Growth and Survival, Plasticity and Cellular Interactivity of Lymphoid Malignancies

Title of the talk:

„Niche function of immature osteoblasts for lymphatic tumor cells“

5/2012

SKELMET 1586 Meeting: A national consortium aimed at unravelling the biology of bone metastases

Title of the talk:

„Determining the Supporting Mesenchymal Cell Lineages and Interactions with Multiple Myeloma“

Poster presentations

3/2011

Keystone meeting: „Hematopoiesis“, Big Sky Montana, USA 2011 (Poster)

„Defining *Ebf2*-mediated niches for HSCs“

Hinzen C, Kieslinger M.

4/2011

4th Interact Symposium, Munich, Germany 2011 (Poster)

„Defining *Ebf2*-mediated niches for HSCs“

Hinzen C, Kieslinger M.

3/2012

Conference: „Osteoonkologie 2012“, Tübingen, Germany 2012 (Poster)

„Differential influence of the HSC niche on hematopoietic tumour cells“

Hinzen C, Alves C, Jeremias I, Kieslinger M.

Eidesstattliche Erklärung

Ich versichere hiermit an Eides statt, dass die vorgelegte Dissertation von mir selbstständig und ohne unerlaubte Hilfe angefertigt ist.

München, den 06.06.2012 .....

Christoph Hinzen

Erklärung

Hiermit erkläre ich, dass die Dissertation nicht ganz oder in wesentlichen Teilen einer anderen Prüfungskommission vorgelegt worden ist und dass ich mich anderweitig einer Doktorprüfung ohne Erfolg nicht unterzogen habe.

München, den 06.06.2012 .....

Christoph Hinzen

List of figures

List of tables

List of abbreviations

%	percent
°C	degree celsius
AA	amino acid
AP2	adipocyte protein 2
bp	base pair
BSA	bovine serum albumine
BCR	B cell receptor
cDNA	copy-DNA
CD	cluster of differentiation
CO_2	carbon dioxide
Cre	Cre-protein
d	day
DMEM	Dulbeccos Modified Eagle Medium
DNA	deoxyribonucleic acid
dNTP	deoxyribonucleotide
DTT	dithiothreitol
E	embryonic
Ebf	early B-cell factor
EDTA	ethylenediaminetetraacetatic acid
ES	embryonic stem cell
Exon	expressed region
et al.	and others („et alii“)
FACS	fluorescence-activated cell sorting
FCS	fetal calf serum
Frt	recognition sequence of Flp recombinase
FSC	Forward Scatter
g	gram
g	force of gravity
gDNA	genomic DNA
G418	geneticin
GFP, Gfp	green fluorescent protein
h	hours
HEPES	2-[4-(2-hydroxyethyl)piperazin-1-yl]ethanesulfonic acid
HSC	hematopoietic stem cell
Intron	intervening sequence
kb	kilobase
KSL	c-Kit$^+$, Sca1$^+$, Lin$^-$ hematopoietic cell population
LacZ	bacterial beta-galactosidase
LIF	leukemia inhibiting factor
loxP	recognition sequence of Cre recombinase
M	molar
MEF	murine embryonic fibroblast
MMC	mitomycin C
MSC	mesenchymal stem cell
mg	milligram
µg	microgram
min	minute

ml	milliliter
µl	microliter
mRNA	messenger RNA
Neo	neomycin
NaN	not a number
N-terminal	amino-terminus of the protein
ng	nanogram
nm	nanometer
O/N	overnight
PBS	posphate buffered saline
PCR	polymerase chain reaction
RNA	ribonucleic acid
RNAse	ribonuclease
RT	room temperature
RT-PCR	reverse transcription polymerase chain reaction
STAT	Signal Transducer and Activator of Transcription
SDS	sodium dodecyl sulphate
SSC	Side Scatter
TAE	tris base, acetic acid and EDTA buffer
TCR	T cell receptor
Tab.	table
UTR	untranslated region
UV	ultraviolet light
V	volt
w/o	without
w/v	weight per volume

1 Summary

Hematopoietic Stem Cells (HSCs) reside in specialized bone marrow (BM) microenvironments, which govern their cell fate. During homeostasis, some HSCs within this niche are kept dormant, preserving long-term self-renewal potential, while others self-renew to replenish the hematopoietic system. The stem cell niche mediates signals inducing quiescence, proliferation or differentiation in HSCs. While HSCs themselves are well defined, the composition of the niche is still unclear. Various cell types like mesenchymal stem cells (MSCs), sinusoidal endothelial cells, osteoblasts and adipocytes have been implicated in homing, mobilization and maintenance of HSCs. The transcription factor Ebf2 is expressed in mesenchymal progenitors with osteoblastic and adipocytic differentiation potential. Noteworthy, HSCs localize to *Ebf2*-expressing cells in the bone marrow and deletion of *Ebf2* in mice results in decreased frequencies of HSCs.

In the present study, the contribution of individual mesenchymal cell lineages in *Ebf2*-mediated niche function for HSCs was defined. Therefore, *Ebf2* conditional knockout mice were generated and crossed with MSC (Prx^{Cre}), adipocyte ($AP2^{Cre}$) and osteoblast (Osx^{Cre}) specific Cre lines. The results in this thesis confirm an important role for *Ebf2* in HSC homeostasis, and more specifically that this potential resides in stromal cells with osteoblastic differentiation potential. A DNA microarray analysis of *Ebf2*-expressing cells revealed that genes involved in homing and proliferation of HSCs are downregulated in *Ebf2*-deficient cells, partly explaining the observed phenotype.
In the thymus, we found *Ebf2* expressed by mature mTECs and MTS-15^+ fibroblasts, which are implicated in a functional microenvironment for lymphoid progenitors. Interestingly, we detected a significant reduction of $CD4^+$ T cells in *Ebf2*-deficient mice. However, this phenotype was not detectable post-transplantation of $Ebf2^{-/-}$ thymic lobes under the kidney capsule of wild type mice. Therefore, we speculate that the loss of *Ebf2* in bone marrow stromal cells causes hematopoietic alterations at the level of a bone marrow derived early T cell progenitor.
To study the role of *Ebf2* in malignant hematopoiesis, human acute lymphocytic leukemia (ALL) and chronic lymphocytic leukemia (CLL) cells were co-cultured on feeder cells deficient for *Ebf2* or ectopically expressing *Ebf2*. While some CLL patient samples showed higher survival rates and cell numbers on *Ebf2*-expressing feeders, no differences were observed for ALL cells. However, ALL cells cultured on *Ebf2*-expressing feeder layers reconstituted leukemias with the same frequency as non-cultured cells, providing evidence that *Ebf2*-expressing niche cells supported the survival of cancer stem cells *in vitro*.

Zusammenfassung

Hämatopoetische Stammzellen (HSC) befinden sich im Knochenmark in speziellen Nischen, welche ihre biologische Aktivität regulieren. Bei Homöostase befindet sich ein Teil der Stammzellpopulation in einer regenerativen Ruhephase. Dadurch bleibt langfristig das Potential, selbsterneuernde Teilungen zu durchlaufen, erhalten. Andere Stammzellen hingegen proliferieren und differenzieren in spezialisierte Zellen des Blutes. Reguliert werden diese Prozesse nicht ausschließlich in Stammzellen selbst, sondern auch von ihrer Stammzellnische. Während die Organisationsstruktur hämatopoetischer Zellen gut verstanden ist, ist die zelluläre und molekulare Zusammensetzung ihrer Nische größtenteils unbekannt. Man geht heute davon aus, dass der Erhalt bzw. die Mobilisierung und Rückkehr von Stammzellen aus dem Knochenmark von mesenchymalen Stammzellen (MSCs), spezialisierten Endothelzellen, Osteoblasten und Adipozyten reguliert ist. Der Transkriptionsfaktor Ebf2 wird von einer Population mesenchymaler Vorläuferzellen, unreifen Osteoblasten und Adipozyten exprimiert. Interessanterweise findet man HSCs in unmittelbarer Nähe dieser Zellen und die gezielte Deletion von *Ebf2* in Mäusen führt zum Verlust von HSCs im Knochenmark.

Das Ziel dieser Arbeit besteht darin, die Beiträge verschiedener stromaler Zelltypen für die von *Ebf2*-vermittelte Nische für HSCs zu untersuchen. Dafür wurde ein Mausmodell mit konditional inaktivierbarem *Ebf2*-Gen hergestellt und mit mesenchymalen Stammzell-, Osteoblasten- und Adipozyten-spezifischen Cre-Linien verpaart. Wie sich herausstellte, führt die gezielte Inaktivierung von *Ebf2* in Osteoblasten zum Verlust von HSCs im Knochenmark. Interessanterweise wurden in einer DNA-CHIP-Technologie Analyse Gene, welche für die Funktion von Stammzellen wichtig sind, in *Ebf2*-defizienten stromalen Zellen weniger stark exprimiert gefunden.

Im Thymusstroma fanden wir *Ebf2* von mTECs und MTS15$^+$ Fibroblasten exprimiert. MTS15$^+$ Zellen bilden im Thymus vermutlich eine Nische für unreife T-Zellvorläufer und die Deletion von *Ebf2* in Mäusen resultiert in einer 40%igen Reduktion von CD4$^+$ T Zellen im Thymus. Überraschenderweise konnte der Phänotyp nach Transplantation von *Ebf2*$^{-/-}$ Thymuslappen unter die Nierenkapsel von Wildtyp-Mäusen nicht mehr detektiert werden. Wir vermuten daher, dass der Verlust von *Ebf2* in stromalen Zellen des Knochenmarks Veränderungen in knochenmarksständigen T Zell Vorläuferzellen zur Folge hat und dieser Defekt sich auch auf die T Zell Entwicklung im Thymus auswirkt.

Zur Untersuchung der Funktion von *Ebf2* in der malignen Hämatopoese wurden humane ALL und CLL Zellen mit *Ebf2*-defizienten und *Ebf2* überexprimierenden adhärenten Zellen kokultiviert. Einige CLL Patienten Proben reagierten auf *Ebf2* mit verbessertem Zellüberleben, während ALL Zellen keine Reaktion zeigten. Interessanterweise rekonstituierten nach Kokultur mit *Ebf2*-exprimierenden Zellen transplantierte ALL Zellen Leukämien mit gleicher Frequenz wie nicht kultivierte ALL Zellen. Dies weist darauf hin, dass *Ebf2* Leukämiestammzellen *in vitro* unterstützt.

2 Introduction

2.1 Hematopoiesis

The investigation of the hematopoietic system and stem cell biology in general began in the 1950s when scientists tried to understand the radiation syndrome. Many victims that had survived the catastrophes of Hiroshima and Nagasaki died within two weeks after, without any visible signs of injury (USSBS, 1945). To understand the cause of the radiation syndrome, scientists irradiated mice and discovered that when they protected some skeletal elements with a lead shield the mice would survive even higher dose of radiation (Jacobson et al., 1949; Lorenz et al., 1951). Soon after, transplantation experiments with bone marrow were performed. When bone marrow from a wild type animal was transplanted into an animal that had received a lethal dose of radiation, the animal survived (Jacobson, 1952).

When lower doses of radiation were applied it became clear that the bone marrow, or the blood forming system is the most susceptible organ to radiation and the first to be destroyed by a certain (lethal) dosage. To determine how many bone marrow cells are required to rescue a lethally irradiated mouse, the animals were transplanted with different numbers of bone marrow cells (Makinodan, 1956; Nowell et al., 1956). Interestingly, animals that had received relatively low cell numbers and had died during the experiment displayed white cell bumps on their spleens. The number of bumps correlated with the number of bone marrow cells the animals had received. Surprisingly, genetic analyses revealed that the cells within a bump were of clonal origin. The existence of a blood forming stem cell was functionally proven by transplantation of a single bump of clonal origin into a lethally irradiated recipient when Becker and colleagues could show that all hematopoietic cells of the surviving recipient are genetically identical to those of the bump originally transplanted (Becker et al., 1963; Juraskova and Tkadlecek, 1965; Siminovitch et al., 1963).

The isolation of hematopoietic stem cells (HSCs) on a single cell level took almost another thirty years and required the development of the hybridoma technology (Kohler and Milstein, 1975) and fluorescence activated cell sorting (FACS; Hulett et al., 1969). Monoclonal antibodies against membrane bound proteins were generated and tested by FACS for their specificity to identify defined populations of hematopoietic cells (Bernard et al., 1984; Coffman and Weissman, 1981). These

were then characterized for their function and properties (Muller-Sieburg et al., 1986; Whitlock and Witte, 1982). From the functional observations it took until 1988 when Weissman and colleagues demonstrated they had identified a population highly enriched for HSCs. It requires only sixty of these cells to rescue lethally irradiated mice and these cells gave rise to all hematopoietic lineages for a lifetime (Spangrude et al., 1988). The isolation of a population enriched for human hematopoietic stem cells was reported five years later (Peault et al., 1993).

2.2 The hematopoietic hierarchy

From elaborate analysis of surface antigens, which characterize certain hematopoietic populations, and from functional capacities of these populations the hematopoietic hierarchy was deduced (Figure 1; Weissman, 2002). All blood and immune cells displayed can be stained with labeled antibodies and can be specifically isolated by FACS. The various effector cells on the lowest levels are fully differentiated and mediate specialized functions in the blood and immune system (Janeway, 2008). Cell types higher up in the hierarchy are immature progenitor cells, which can differentiate into the specialized cells mentioned before. These processes are regulated by intrinsic and extrinsic signals (Bain et al., 1994; Rieger et al., 2009). Of all cell types shown, only the long-term HSC (LT-HSC) and the short term HSC (ST-HSC) are multipotent and can, upon certain signals, give rise to all other hematopoietic cells. The differentiaton between LT- and ST-HSCs is based on the finding that the lifespan of short-term HSCs is limited (Morrison et al., 1995b). Their capacity to form all cells within the hierarchy exhausts with time and their potential is gone about 4 months after transplantation (Morrison et al., 1995a). Although not shown yet, it is commonly assumed that only LT-HSCs have unlimited potential to undergo self-renewing divisions (Trumpp et al., 2010). A self-renewing division is defined as a cell division generating two daughter cells, on average, one of which will maintain the properties of the original cell. Thereby, the hematopoietic potential to generate billions of different blood cells every day can be maintained without exhaustion of the stem cell pool. Changes in stem cell properties are accompanied by changes in the displayed surface markers. Many studies have confirmed that long-term reconstitution potential of LT-HSCs is lost upon expression of CD34 in the mouse (Osawa et al., 1996; Reya et al., 2001; Weissman et al., 2001). The limited self-renewal capacity in ST-HSCs is lost upon expression of Flt3 (Adolfsson et al., 2001), and when the multipotent progenitor (MPP) downregulates the expression of Sca1 (Stem cell

antigen 1; Uchida et al., 1996), it differentiates into a common myeloid progenitor (CMP; Figure 1).

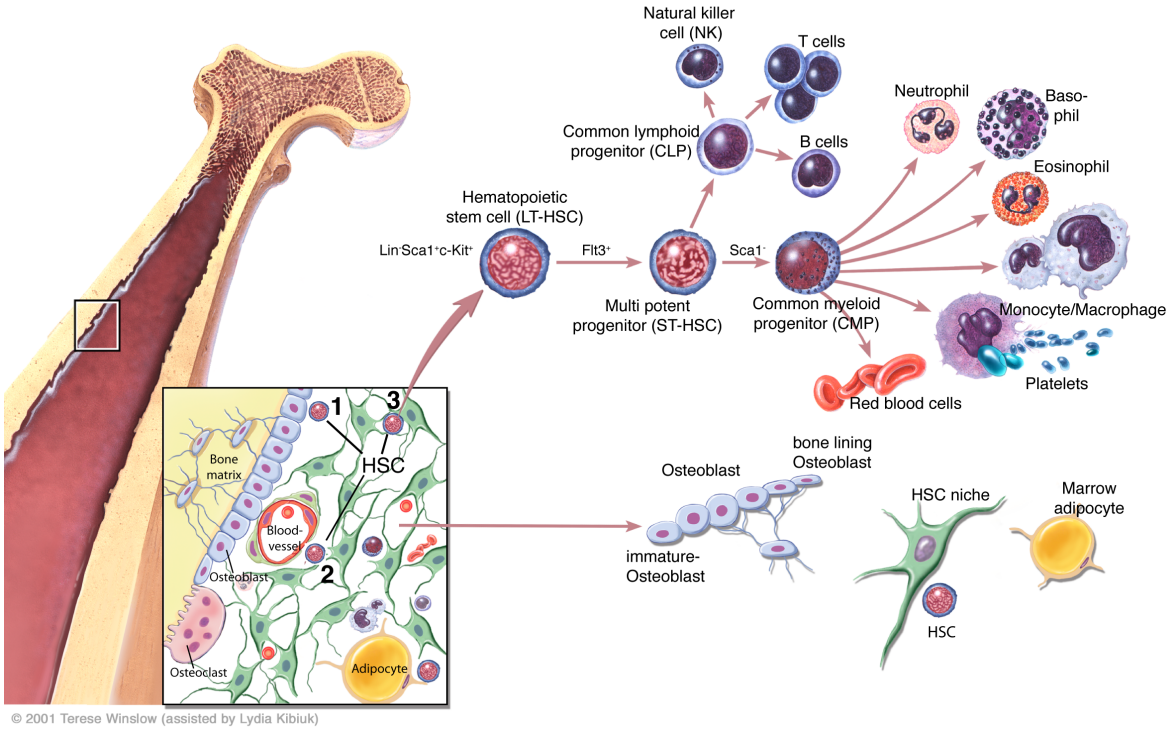

Figure 1: Hematopoiesis and bone marrow niche. Hematopoietic stem cells (HSC) give rise to mature blood cells and these processes are regulated by intrinsic and extrinsic factors in the bone marrow. Maturation of hematopoietic cells is accompanied by antigenic markers on their surface. These molecules are used for their isolation. HSCs reside in specialized microenvironments but the cellular composition remains undefined. HSCs localize to (1) osteoblasts at the inner bone surface, (2) endothelial cells of sinusoidal vessels and (3) mesenchymal stem cells (MSC) in the bone marrow. (Image was kindly provided by Terese Winslow)

Since the first description of HSCs, which are negative for the **L**ineage markers of differentiated cells (Gr-1, Mac1, B220, CD4, CD8 and TER119), but express **S**ca1 (stem cell antigen-1) and c-**K**it (stem cell growth factor receptor), they were termed „KSL“ population (Lagasse et al., 2001). Researchers applied a lot of effort to identify additional ways to increase the frequency of LT-HSCs within the KSL population (Weissman, 2002; Wilson et al., 2008). It was demonstrated that upon single cell transplantation of the KSL population only one out of seven cells had long-term reconstitution potential (Wagers et al., 2002). To further purify this population alternative methods and new surface markers were discovered. Margaret Goodell established a method independent of expressed surface molecules. Upon incubation of whole bone marrow with Hoechst-dye every cell is

stained except for HSCs (Goodell et al., 1996). Due to the expression of unique ABC-transporters, HSCs can actively efflux the dye and remain unstained. Sean Morrison added the SLAM-family markers (CD48, CD150 and CD244) to increase the purity of HSCs (Kiel et al., 2005; Lin and Goodell, 2011).

Although low numbers of LT-HSCs can be found in peripheral blood, spleen and thymus, data suggests that self-renewing divisions occur only in a specialized microenvironment, the hematopoietic stem cell niche (Lymperi et al., 2010; Seita and Weissman, 2010). Extramedullary hematopoiesis can sustain blood formation for up to months, but their potential exhausts over time and the stem cell pool depletes as shown by transplantation of splenic colonies (Schofield, 1978).

2.3 The hematopoietic stem cell niche

Hematopoietic cells depend on interaction with specialized stromal microenvironments. T cell development requires crosstalk with thymic stromal cells, which control their differentiation and proliferation (Pantelouris, 1968). Similarly, B cells cannot develop without interaction with stromal cells in the bone marrow (Nagasawa et al., 1996). Although claimed by Raymond Schofield (Schofield, 1978) already more than thirty years ago, the existence of a HSC niche has not been convincingly proven yet, mainly due to technical limitations (Lymperi et al., 2010). Within the following chapter, data will be discussed that provide strong evidence that the support of HSCs depends on different stromal cell types and the various cytokines produced by these niche cells.

Upon injection of bone marrow cells from a donor into a congenic recipient, the transplanted cells can contribute to hematopoiesis. The degree of contribution, defined as chimerism, is an indicator for the level of engraftment. In 1987, Schofield and colleagues published that the level of chimerism depends on pre-conditioning of the recipient (Massa et al., 1987). In this study, three experimental animal groups were injected eitherwise isopropyl methane sulfonate (IMS, randomly damages hematopoietic cells), or received busulfan (kills cycling hematopoietic cells) or were irradiated (kills all hematopoietic cells) before they were transplanted with an equal number of reconstituting bone marrow cells. The degree of chimerism was measured for six months. Interestingly, IMS pre-conditioned animals did not show any chimerism at all, while busulfan treated animals had a chimerism of 40-83% and the group of pre-irradiated recipients showed a chimerism ranging from 60-97%. They concluded that the transplanted HSCs need to engraft into a niche before they can actively contribute to

hematopoiesis. As niche space is limiting the niche is already occupied and without pre-conditioning the transplanted cells cannot engraft (Massa et al., 1987).

Following the same concept, Li and colleagues were the first to show that osteoblastic cells in the bone marrow limit the number of HSCs. When they specifically deleted bone morphogenic protein receptor 1 (BMPR1) in bone marrow stromal cells, they found higher numbers of osteoblastic cells (Zhang et al., 2003). This led to increased bone formation rates and a reduction in marrow space and total cellularity. However, mice deleted for BMPR1 in bone marrow stromal cells showed a twofold increase in the frequency of LT-HSCs. The authors speculate that the deletion of BMPR1 in mesenchymal stem cells (MSCs) led to increased numbers of specialized spindle-shaped osteoblastic cells that express N-cadherin. Thereby, the niche size was extended, which resulted in increased HSC frequencies (Zhang et al., 2003).

In a different study, Scadden and colleagues generated a transgenic mouse strain overexpressing a constitutively active parathyroid-hormone receptor (PTH1R) in osteoblastic cells of the bone marrow (Calvi et al., 2003). They detected increased osteoblast activity, which resulted in increased bone formation and twofold higher KSL frequencies. Interestingly, hematopoietic progenitor populations were not increased, arguing that osteoblasts are specialized niche cells for HSCs (Calvi et al., 2003).

Adipocytes are fat cells, specialized in the storage of energy, and are part of the bone marrow stroma. Their number increases with age and the amount of fat cells in the marrow inversely correlates with its hematopoietic activity. Although their function in hematopoiesis is only poorly understood, adipocytes are indicated to be negative regulators of hematopoiesis. The question whether adipocytes just fill up space in the marrow, or whether they actively contribute to hematopoietic regulation, was addressed by Daley and colleagues (Naveiras et al., 2009). When comparing mouse skeletal regions with differing adiposity, they found more stem and progenitor cells in regions with low adiposity (vertebrae of the thorax over vertebrae in the tail). These results were confirmed when transplanting wild type bone marrow into transgenic mice with inhibited adipogenesis. Overall, they found better engraftment and higher HSC frequencies in transgenic over control animals (Naveiras et al., 2009). However, the function of adipocytes and their contribution to hematopoiesis is poorly understood.

Mesenchymal stem cells (MSCs) can give rise to various cell types found in bone marrow stroma, namely adipocytes, chrondrocytes, endothelial cells, osteoblasts and fibroblasts (Pittenger et al., 1999). Nestin positive cells display characteristics

of MSCs and are in direct cell-cell contact with HSCs (Mendez-Ferrer et al., 2010). In addition, they express cytokines important for their maintenance and regulation. The deletion of Nestin positive cells in transgenic animals resulted in rapid loss of HSCs. Furthermore, upon transplantation of labeled HSCs into irradiated recipients, the HSCs homed directly to Nestin positive cells in the bone marrow (Mendez-Ferrer et al., 2010). In summary, the bone marrow microenvironment for HSCs is made up by various stromal cell types regulating their homing, maintenance, number and activity (Figure 1; Mercier et al., 2012).

While the previously cited studies demonstrated the importance of stromal cells in hematopoietic regulation by increase or ablation of these cells, the interaction of HSCs with their microenvironment has also been addressed on a molecular level. Osteoblasts produce molecules regulating major signaling pathways in hematopoietic cells. Through upregulation of parathyroid hormone 1 receptor (PTH1R) in osteoblasts, Notch signaling in HSCs can be induced, resulting in an increased stem cell pool (Calvi et al., 2003). Overexpression of the canonical Wnt inhibitor Dickkopf1 (Dkk1) in osteoblastic cells inhibited Wnt signaling in HSCs and resulted in increased proliferation and reduced reconstitution capacity of bone marrow cells in a transgenic mouse model (Fleming et al., 2008). Thrombopoietin (TPO) was identified as a molecule expressed by osteoblasts to regulate quiescence in HSCs. Quiescent HSCs express Mpl (TPO receptor) and localize to TPO-producing osteoblasts (Yoshihara et al., 2007). Upon inhibition of this signaling pathway, HSCs are released from their niche and the bone marrow in these animals can be engrafted without previous irradiation. Angiopoetin1 (Ang1) expressed by osteoblasts was identified as another molecule to induce quiescence in HSCs. Quiescent HSCs express the Ang1 receptor Tie-2 (TIE receptor tyrosine kinase 2) and localize to osteoblasts at the inner bone surface (Arai et al., 2004). Adiponectin, a growth factor expressed in adipocytes, was shown to induce proliferation in HSCs (express the adiponectin receptors 1 and 2). Interestingly, the immature state of HSCs was maintained (DiMascio et al., 2007). Although very difficult to study, varying oxygen levels are also implicated in HSC regulation and maintenance. Long-term HSCs have high levels of pimonidazole (PIM) indicating that these cells reside in hypoxic niches to preserve long-term self-renewal potential (Parmar et al., 2007; Simsek et al., 2010). High calcium levels are sensed via a calcium-receptor expressed by HSCs. Thereby, stem cells are retained in close proximity to osteoblasts at the inner bone surface (Adams et al., 2006).

Two signaling molecules, which are of high relevance in terms of this thesis, will be discussed in a broader context now. Deletion of the chemokine stromal derived factor 1 (SDF-1) in mice results in prenatal death due to hematopoietic failure

(Nagasawa et al., 1996). The fetal liver is the primary organ of early hematopoiesis from E11.5-E12.5 until the first week after birth (Morrison et al., 1995a). Examination of fetal liver in *SDF-1*$^{-/-}$ mice showed normal levels of granulocytes and monocytes and fetal liver cells from these mice yielded normal numbers of colonies in colony forming assays (Nagasawa et al., 1996). However, the bone marrow cellularity in E17.5 *SDF-1*$^{-/-}$ mice is reduced and hematopoietic cells showed greatly reduced functionality in colony forming assays compared to wild type. *SDF-1* is expressed in stromal cells of the bone marrow and although bone structures had formed normally, hematopoietic cells were almost absent. This indicates a function for *SDF-1* during very early hematopoietic processes in the bone marrow (Nagasawa et al., 1996). Two years later, *CXCR4* (C-X-C chemokine receptor type 4) deficient animals were reported to show the same phenotype as was observed in *SDF-1*$^{-/-}$ mice (Zou et al., 1998). CXCR4, which is expressed on HSCs, is the receptor for SDF-1 and 90% of wild type fetal liver cells were shown to migrate towards a SDF-1 gradient, while *CXCR4*$^{-/-}$ cells did not respond to the gradient (Zou et al., 1998). Finally, the interaction of CXCR4 and SDF-1 was shown to be responsible for the mobilization of HSCs to the peripheral blood upon G-CSF (granulocyte colony-stimulating factor) treatment (Petit et al., 2002). In human hematopoietic stem cell transplantation, the donor HSCs are mobilized and collected from the peripheral blood by administration of G-CSF. Lapidot and colleagues showed that this mobilization of HSCs from their niche is mediated by inactivation of SDF-1 due to cleavage by neutrophil elastase and cathepsin G secreted by neutrophils during G-CSF treatment (Petit et al., 2002). In summary, SDF-1 produced by bone marrow stromal cells is a strong chemoattractant for hematopoietic progenitor cells and mediates the switch from fetal liver to bone marrow based hematopoiesis. Moreover, inactivation of *SDF-1* results in the mobilization of HSCs from the bone marrow to the peripheral blood.

Matrix-metalloproteases are expressed by various stromal cells and shape the bone structure and morphology by remodeling the extracellular matrix (ECM; Kessenbrock et al., 2010). By release of membrane-bound chemokines like VEGF (vascular endothelial growth factor) they regulate angiogenesis and osteoclast activity in the bone marrow (Bergers et al., 2000; Engsig et al., 2000; Vu and Werb, 2000). Interestingly, matrix-metalloprotease-9 (MMP-9) deficient animals show no defects in hematopoiesis (Heissig et al., 2002). However, the authors show in the same study that when the bone marrow is challenged by administration of 5´Fluorouracil (5-FU, a pyrimidine analog that kills actively cycling cells), HSCs fail to repopulate and proliferate in their former niches and 72% of *MMP-9*$^{-/-}$ mice die while all control animals survive. When the levels of active MMP-9 were determined in supernatants of bone marrow from wild type animals

before and three days after 5-FU treatment, they were found elevated. The levels of soluble c-kit ligand (stem cell factor, SCF) were also found to be increased threefold in the same experiment. c-kit ligand is normally membrane bound (mKitL), but can be cleaved to soluble c-kit ligand (sKitL), which binds to c-Kit (stem cell growth factor receptor) expressed on HSCs. In an *in vitro* assay, the authors show that MMP-9 rapidly promoted sKitL release from mKitL expressing cells upon addition of MMP-9 to the cell culture medium. This release could be blocked by simultaneous addition of an MMP-9 inhibitor (Heissig et al., 2002). These data show that MMP-9 expressed by stromal cells is important to regulate the activity of HSC by releasing sKitL (SCF).

2.4 EBF proteins

2.4.1 Ebf protein family

The protein family of Ebf (early B cell factor) transcription factors comprises four members, which are highly conserved amongst each other but also in evolution (Liberg et al., 2002). Via a zinc-finger motif within their DNA binding domain (DBD) they recognize regulatory DNA elements of genes and bind to these as homo- or heterodimers, thereby inducing or suppressing transcription (Dubois and Vincent, 2001). *Ebf1*, the founding member of this protein family, plays an essential role in hematopoiesis. Deletion of *Ebf1* in mice causes a complete block in B cell differentiation (Lin and Grosschedl, 1995). Since then, Ebf1 has been intensively studied and was shown to be part of huge regulatory network, important to determine and maintain the B cell state (Nutt and Kee, 2007).

While *Ebf1* is the only family member expressed in hematopoietic cells, a largely overlapping expression pattern of the different *Ebfs* is found in other tissues. *Ebfs* were shown to be simoultaneously expressed in neuronal cells (Corradi et al., 2003; Malgaretti et al., 1997), olfactory epithelium (Wang et al., 1993), retina (Jin et al., 2010), adipocytes (Jimenez et al., 2007) and stromal cells of the bone marrow (Kieslinger et al., 2005). As all Ebf family members bind to the same DNA sequences, their activity in tissues with an overlapping expression pattern is probably redundant and a single deletion results in a hypomorphic phenotype.

2.4.2 Ebf2

Of the four Ebf proteins, most is known about the biological function of Ebf2, which displays more then 90% sequence homology with Ebf1 on protein level (Dubois

and Vincent, 2001). To study *Ebf2* expression and function in the mouse, *Ebf2-LacZ* animals were generated by gene targeting in murine ES cells (Corradi et al., 2003). *Ebf2-LacZ* mice carry an in-frame insertion of the bacterial *LacZ* gene immediately downstream of the translation initiation site of the *Ebf2* gene. At the same time, *Ebf2-Gfp* mice were generated in the laboratory of R. Reed applying the same strategy, but instead of the bacterial *LacZ* gene the animals carry an in-frame insertion of the *Gfp* gene (Wang et al., 2004). Thereby, the reporter genes mentioned (*LacZ* and *Gfp*) are expressed under control of the endogenous *Ebf2* promotor while expression of the *Ebf2* gene is disrupted.

In the context of mouse neural development, *Ebf2* regulates the migration of gonadotropin releasing hormone-synthesizing neurons (Corradi et al., 2003). The deletion of *Ebf2* in these cells results in defects of the neuroendocrine axis leading to secondary hypogonadism. Due to the contribution of *Ebf2* to neuronal development, *Ebf2-LacZ*$^{-/-}$ animals are mildly uncoordinated and walk with an unsteady and waddling gait. Furthermore, *Ebf2-LacZ*$^{-/-}$ animals exhibit a hunchback and show a strong reduction (>50%) in body weight (Corradi et al., 2003; Croci et al., 2006). Interestingly, *Ebf2* is abundantly transcribed in adipocytes and carries the potential to drive adipogenesis (Jimenez et al., 2007). However, a differentiation-block of adipocytes in *Ebf2-LacZ* mice was not reported.

In the bone marrow, *Ebf2* is expressed by a mixed population of stromal cells required for bone homeostasis (Kieslinger et al., 2005). Bones of *Ebf2-LacZ*$^{-/-}$ animals are reduced in size, mass and firmness, although bone formation rates and morphology are normal. *Ebf2*-expressing stromal cells are regulators of osteoclastogenesis and maintain bone homeostasis by acting upstream of RANKL signaling. Loss of *Ebf2* results in increased osteoclast activity, which causes an osteopenia phenotype in young animals. *Ebf2*-expressing bone marrow stromal cells express relatively high levels of *Runx2* and low levels of Sox9, alkaline phosphatase and bone sialoprotein (Kieslinger et al., 2005). Runx2 has been shown to be an essential transcription factor for the differentiation and maturation of osteoblasts from a mesenchymal progenitor (Komori et al., 1997). Alkaline phosphatase and bone sialoprotein are important for bone formation and are found to be expressed in mature osteoblasts, while Sox9 is required for determination of the chondrogenic cell lineage (Eames et al., 2004; Long, 2012). Noteworthy, *Ebf2* is not expressed in chondrocytes (Kieslinger et al., 2005). Therefore, it was concluded that *Ebf2* is expressed in a bipotent progenitor with osteoblastic and chondrocytic potential. However, due to the abundant levels of *Runx2* transcript the population was termed **I**mmature ***E****bf2*-expressing **O**steoblasts (IEOs) (Kieslinger et al., 2010).

Ebf2-LacZ$^{-/-}$ animals show a strong reduction in the total cellularity of hematopoietic organs (bone marrow, spleen and thymus, Kieslinger et al., 2010). Noteworthy, *Ebf2* is expressed in stromal cells of these organs, but not in hematopoietic cells. Bone marrow cells from *Ebf2-LacZ*$^{-/-}$ animals have greatly reduced potential to form colonies in methylcellulose and lymphoid lineages were found to be more severely affected than myeloid cells. More specifically, the frequency of hematopoietic stem cells is reduced two- to fourfold (Kieslinger et al., 2010). This defect is cell nonautonomus because upon transplantation of *Ebf2-LacZ*$^{-/-}$ bone marrow into irradiated wild type recipients the observed hematopoietic defects are gone. Furthermore, *Ebf2*-expressing bone marrow stromal cells can support HSCs *in vitro* in an *Ebf2*-dependent manner. Therefore, IEO cells represent hematopoietic niche cells that mediate stem cell homeostasis in a cell-nonautonomous manner. Altogether, this complex phenotype results in premature death of *Ebf2*-deficient animals. We routinely find dead pups in litters from *Ebf2-LacZ* heterozygous crossings and *Ebf2*-deficient survivors die roughly three to six weeks after birth for unknown reason.

2.5 Mesenchymal Cre lines

While signaling pathways involved in HSC homeostasis have been studied intensively, the role of transcription factors in this process remains relatively undefined (Lymperi et al., 2010). IEO cells represent a mixed population of stromal cells, which support HSCs (Kieslinger et al., 2010). However, their contribution at the cellular level is still unclear. To address this question within the course of this study, mice with a conditional *Ebf2* allele shall be generated based on the Cre-LoxP system. In 1988, Sauer and Henderson published to have site-specifically recombined DNA sequences in mammalian cells using Cre recombinase isolated from the bacteriophage P1 (Sauer and Henderson, 1988). Cre is a DNA recombinase that binds to 34 bp long *LoxP* sequences and recombines them while DNA elements in between are excised, leaving one *LoxP* sequence behind. The Flp-Frt system functions in an analogous way, however *Frt* sites are recombined by Flp recombinase originally isolated from *S. cerevisiae* (Chen and Rice, 2003).

In 1993, Rajewsky was the first to report successful transfer of the Cre-LoxP system to mice studying DNA polymerase beta in T cells (Gu et al., 1993). A complete deletion of that gene resulted in a lethal phenotype, making it impossible to study the protein function in T cells. Therefore, mice carrying a floxed DNA polymerase beta allele were combined with a mouse strain where Cre is

expressed under control of a T cell specific promotor. Thus, deletion specifically took place in T cells only (Gu et al., 1993).

Within the course of this study, mice with a conditional allele of *Ebf2* shall be generated and combined with appropriate Cre lines to delete *Ebf2* in certain *Ebf2*-expressing stromal cell lineages. Thereby, the contribution of these lineages in *Ebf2*-mediated niche function for HSC homeostasis can be defined *in vivo* (Figure 2).

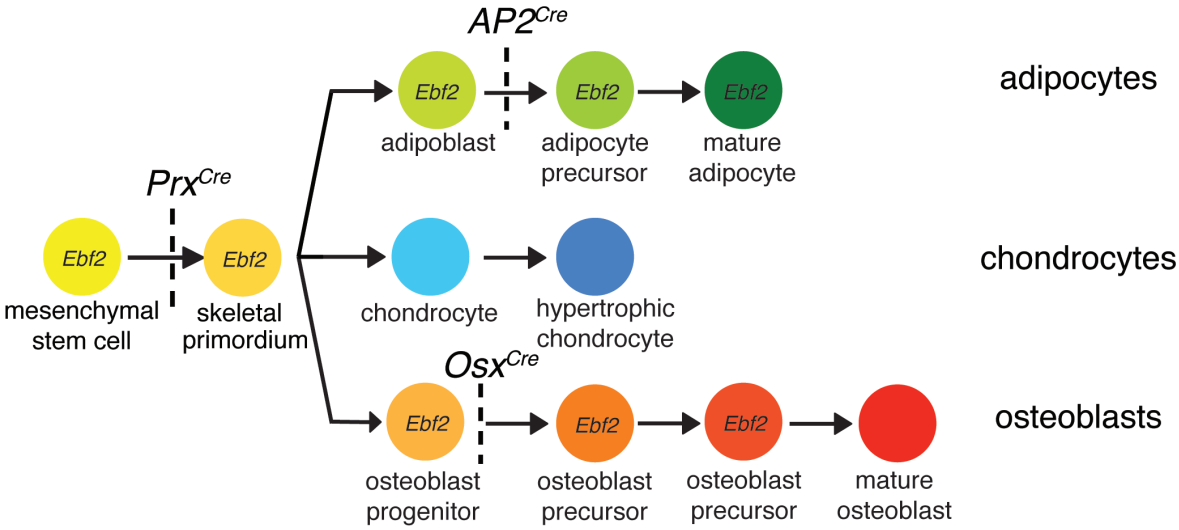

Figure 2: Schematic representation of stromal cell lineages expressing *Ebf2*. Differentiation scheme of multipotent MSCs maturating into specialized stromal lineages. Stages when *Ebf2* is expressed are indicated. Dashed lines indicate timepoints when *Ebf2* expression is disrupted due to Cre expression using the Cre lines shown ($AP2^{Cre}$, Osx^{Cre}, Prx^{Cre}).

Ebf2 is expressed by MSCs, which give rise to osteoblasts, chondrocytes and adipocytes (Pittenger et al., 1999). Paired related homeobox protein 1 (Prx) has been shown to be expressed in MSCs (Martin et al., 1995). $Prx^{-/-}$ animals show defects in skeletogenesis, involving loss or malformation of craniofacial, limb and vertebral skeletal structures. Prx^{Cre} transgenic animals express Cre recombinase under control of *Prx*-derived regulatory elements (Logan et al., 2002) and have been successfully used to study skeletal development (Kimura et al., 2010; Seo and Serra, 2007).

IEO cells can be differentiated into adipocytes *in vitro* (Kieslinger et al., 2005). To elucidate the function of *Ebf2*-expressing adipocytes in HSC homeostasis, $Ebf2^{fl/fl}$ animals shall be crossed with an adipocyte specific Cre line. Adipocyte protein 2 (AP2) is a carrier for fatty acids and is expressed in brown and white fat tissue

(Hotamisligil et al., 1996). *AP2*^{Cre} transgenic mice express Cre recombinase under control of the 5.4 kb promotor region of the *AP2* gene and have been successfully used in many studies to generate adipocyte specific deletions (He et al., 2003; Polak et al., 2008; Sabio et al., 2008).

The differentiation of mesenchymal stem cells into an osteoblast is regulated by consecutive expression of transcription factors (Long, 2012). The initial differentiation of MSCs into an osteo-chondro progenitor is driven by the transcription factor Runx2 (Komori et al., 1997). Terminal differentiation of this bipotent progenitor into the osteoblastic lineage is mediated by the transcription factor Osterix (Osx; Nakashima et al., 2002). *Osx*^{Cre} transgenic mice express Cre recombinase under control of the *osterix* promotor, which is active at very early stages of osteoblast differentiation (Rodda and McMahon, 2006).

2.6 T cell development in the thymus

Unlike other hematopoietic lineage cells, T cells develop and mature in a specialized organ, the thymus. The importance of this organ came to light when Grist and colleagues in 1962 discovered the nude mouse (these animals lack hair and a thymus; Pantelouris, 1968). A random mutation had led to the disruption of the Forkhead box protein N1 (*FOXN1*) gene, which is essential to drive differentiation of mesenchymal cells into thymic epithelium (Nehls et al., 1994). This process is crucial for proper formation of the organ (Bleul et al., 2006). Nude mice lacked T cell dependent immunity like rejection of a transplant or killing of virus-infected cells (Janeway, 2008). A similar phenotype was observed, when the thymus from young wild type mice was dissected within twenty-four hours after birth. Finally, the phenotype could be rescued by transplantation of thymic stromal cells into nude mice. These early experiments clearly demonstrated the necessity of thymic stromal cells for T cell dependent immunity (Janeway, 2008).

Since then, the architecture of this organ and the function of different epithelial cells therein have been intensively studied, creating the basis for a better understanding of T cell development (Klein, 2009). The thymus is a highly vascularized organ with an outer cortex and an inner medulla. Thymic epithelial cells comprise cortical epithelial cells (cTECs) and medullary epithelial cells (mTECs), which are located in the cortex and the medulla, respectively (Takahama, 2006). Both are derived from a common thymic epithelial progenitor and are important for early and late stages of T cell development (Bleul et al., 2006; Rossi et al., 2006).

In the early stages of T cell development, lymphoid progenitors, which are double negative for CD4 and CD8 (DN), migrate through the cortex where they rearrange their T cell receptor (TCR) gene segments variable (V), diversity (D) and joining (J). Millions of different T cell receptors are generated during these processes, ensuring recognition of any foreign antigen (Janeway, 2008). The success of an in-frame V, D, J gene rearrangement to form a functional TCR is then controlled by cTECs (Klein, 2009). Promoted by Notch-signals and signals from the IL-7 pathway, which are mediated by cTECs, the $CD4^+$ $CD8^+$ double positive (DP) T cells are stimulated to interact with major histocompatibility complex (MHC) molecules expressed on cTECs (Peschon et al., 1994; Sambandam et al., 2005). Only thymocytes, that have generated a TCR that can interact with MHCI or MHCII molecules within a certain window of affinity will receive a survival signal (Starr et al., 2003). Without this signal they die, while survivors undergo massive proliferation (Rodewald et al., 1997; Staal et al., 2004). T cells interacting with MHCI become $CD8^+$ single positive (SP) T cells, and those interacting with MHCII become $CD4^+$ (SP) T cells (Anderson et al., 1994).

The random nature of T cell receptor gene segment rearrangement bears a high risk that T cells may recognize own antigens and become self-reactive, leading to autoimmunity (Wing and Sakaguchi, 2010). To test for self-tolerance, positively selected T cells migrate from the cortex into the medulla, the inner region of the thymus (Klein, 2009). In the medulla, their unique TCR is tested regarding its tolerance towards self antigens (Derbinski et al., 2001). mTECs have the extraordinary ability to express several thousands of transcripts, which are normally restricted to specialized tissues. This phenomenon, described as promiscuous gene expression mainly depends on the transcription factor autoimmune regulator (AIRE; Anderson et al., 2002). By this mechanism, mTECs can ideally load the proteome on MHC molecules and present it to T cells. Any T cell that interacts with a presented antigen beyond a certain affinity threshold will be negatively selected (Starr et al., 2003). Thereby, mTECs ensure the tolerance of T cells to any self antigen they encounter in the periphery (Klein et al., 2009). After the process of negative selection mature T cells express G-protein receptor shingosine-1-phosphate receptor (S1P1), which is required for their egress from the thymus into the bloodstream (Matloubian et al., 2004).

While the role and function of epithelial cells in the thymus is relatively well understood, much less is known about thymic endothelial cells and thymic fibroblasts (Takahama, 2006). These cells provide extracellular matrix components, which are essential for the maturation of early T cell progenitors in the thymus (Anderson et al., 1997; Rezzani et al., 2008). In another study,

embryonic mesenchyme was shown to produce Fibroblast growth factors (FGFs), which are essential for cTEC proliferation (Jenkinson et al., 2003). In mice, FGF-7 was shown to be dispensable for T cell development, but to play an important role during thymic regeneration in irradiation and chemotherapy models (Alpdogan et al., 2006; van den Brink et al., 2004). Quite recently, a distinct population of thymic fibroblasts marked by the expression of the surface antigen MTS15$^+$ was identified (Gray et al., 2007). Interestingly, these cells localize to the blood/thymus barrier and express FGFs and various cytokines (IL-7, SCF and SDF-1) indicating an important functional role in the complex interplay between thymocytes, epithelial cells and fibroblasts (Gray et al., 2007).

2.7 Cancer

While in 1900 the global average lifespan was just 31, it had increased to 48 years by mid-20th century and rose to 66 years in 2005. By 2030 the average life expectancy at birth will be around 85 years for the populations of the Western world (WHO, 2006). These dramatic improvements are mainly due to better nutrition and great advancements in control and prevention of infectious diseases (vaccination and antibiotics; Buchman et al., 2008). Beyond question, cancer is a genetic disease and the risk to develop a cancerous disease increases with age (Dunn, 2012). Therefore, the requirements to improve cancer treatment are vital.

During treatment of leukemia and solid tumors, many patients go into remission but have a relapse with the same symptoms after a certain time (DeVita and Schein, 1973). This observation led scientists to postulate the Cancer Stem Cells (CSC) hypothesis (Bonnet and Dick, 1997; Reya et al., 2001; Visvader and Lindeman, 2008). By definition these cells have properties of normal stem cells, meaning they can infinitely sustain tumor growth (self-renewing divisions) and can regenerate all different cell types found within the heterogenous tumor (multipotent). In 1994, Dick and colleagues published the identification of cancer stem cells in acute myeloid leukemia (AML; Lapidot et al., 1994). Only upon transplantation of a CD34$^+$CD38$^-$ (immature immunophenotype) population of human acute myeloid leukemia cells into immunocompromised NOD/SCID mice, these cells caused leukemia. Any other cell population transplanted did not cause leukemia. It was therefore concluded that CSCs probably derive from an immature hematopoietic progenitor (Bonnet and Dick, 1997).

Since then, CSCs have been identified in cancers of blood, brain, breast, colon, ovary, pancreas, prostate, melanoma and multiple myeloma (Al-Hajj et al., 2003;

Bonnet and Dick, 1997; Li et al., 2007; Maitland and Collins, 2008; O'Brien et al., 2007; Schatton et al., 2008; Singh et al., 2003; Zhang et al., 2008). It has been postulated that CSCs must not necessarily derive from a stem cell, but they have to acquire its characteristics (Bjerkvig et al., 2005). This might be achieved by an accumulation of mutations that lead to dedifferentiation and activation of pathways normally restricted to stem cells, Figure 3 (Rosen and Jordan, 2009).

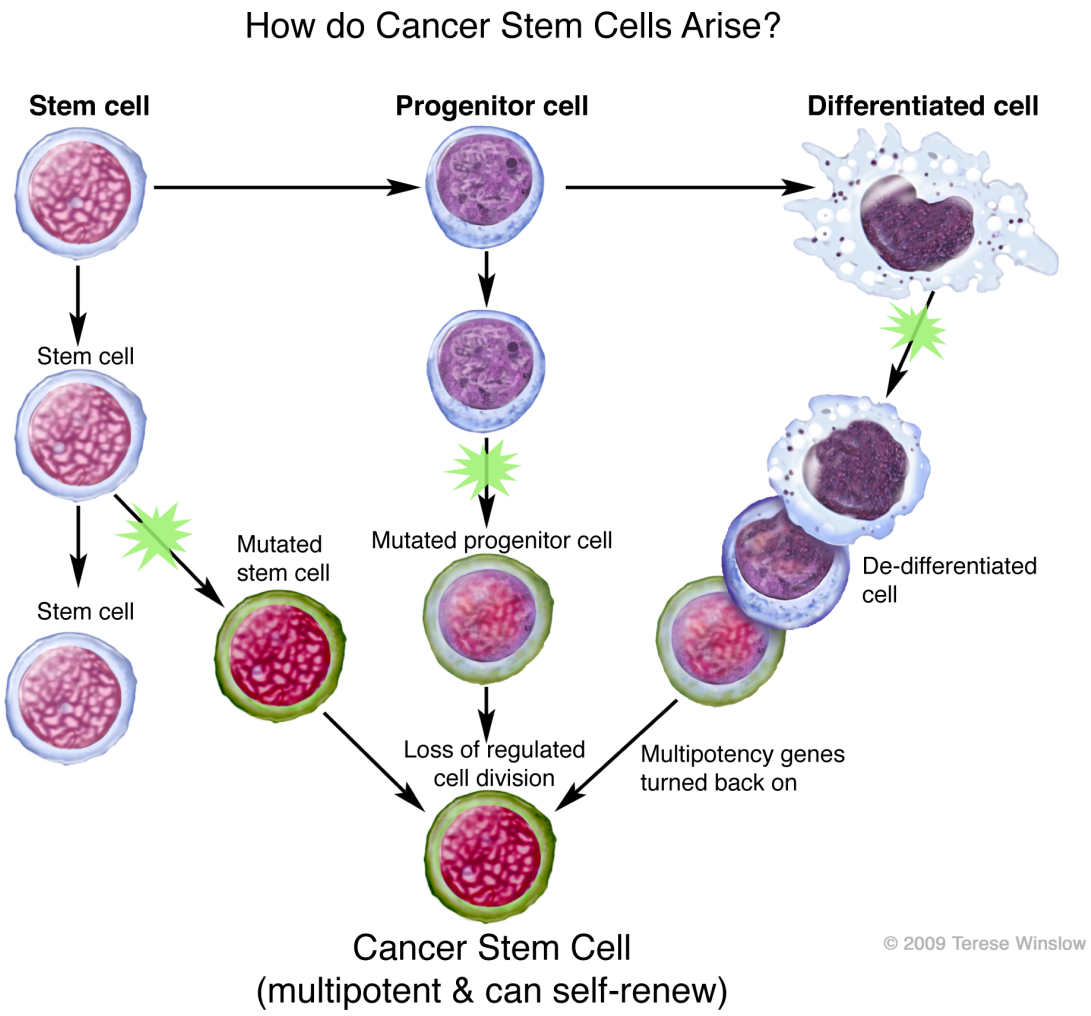

Figure 3: Cancer stem cells and normal stem cells are multipotent and can self-renew. CSCs must not necessarily derive from a normal stem cell, but any cell may turn into a CSC upon activation of pathways, which are normally restricted to stem cells. (Image kindly provided by Terese Winslow)

2.7.1 Leukemia

Leukemia is a cancer of the blood and bone marrow (Kampen, 2012). It is characterized by uncontrolled proliferation of immature leukocytes. These

malignant cells accumulate first in the bone marrow and later in secondary hematopoietic organs like spleen and lymph nodes, but also in the liver. With disease progression, normal hematopoiesis is more and more suppressed by malignant cells (Dohner et al., 2010) and as a consequence patients suffer from anemia (lack of erythrocytes) and impaired immune function (Barberan et al., 2011).

Clinically and pathologically leukemia is classified into acute and chronic forms (Michiels et al., 2007). Acute leukemias are aggressive with fast proliferating cells. Therefore, they require immediate treatment. Chronic forms develop slowly and are normally just surveyed during the first months and years after diagnosis. When a certain concentration of leukemic cells in peripheral blood is reached, patients are treated by chemotherapy (Downing, 2008).

2.7.2 B cell chronic lymphocytic leukemia (B-CLL)

B-CLL is the most common type of leukemia in the Western world (Dores et al., 2007). The median age of people newly diagnosed is above 50 years and the ratio between men and women is 2:1. Most patients are diagnosed during a routine blood test and show increased leukocyte numbers but no signs of sickness. Depending on the subtype of B-CLL, some patients die within months, while others do not need treatment throughout their lifetime. At present, B-CLL is not curable with conventional chemo- and radiation therapy. It is therefore necessary to identify new surrogate markers for a more detailed classification and prediction of the course of disease (Wadleigh and Tefferi, 2010).

The accumulation of white blood cells (lymphocytosis) displaying a B-CLL cluster of differentiation (CD) phenotype on a complete blood count to more than 5000 cells per μl is an indicator for leukemia (Harris et al., 2000; Rawstron et al., 2008). The accumulating B-CLL cells show surface expression of CD5, CD23, CD19 and $CD20^{low}$ (Lanasa, 2010). B-CLL is a clonal disease and all malignant cells in a patient are characterized by expressing either the lambda or kappa light chain. The malignant cells are slightly smaller than normal lymphocytes and tend to break when smeared onto a glass slide, reliably indicating leukemia by many broken cells (Schriever and Huhn, 2003).

Evaluation of the number of mutations found in the DNA of the IgV_H antibody gene region helps to distinguish high and low risk patients (Chiorazzi et al., 2005). A low mutation rate indicates a more immature B cell state, which correlates with a more rapid disease course. The presence of CD38 and zeta-chain-associated protein

kinase 70 (ZAP-70) on the malignant cells have also been correlated with a more aggressive disease course (Kay and Shanafelt, 2007; Malavasi et al., 2011).

Genetic changes within the neoplastic cell population are determined by fluorescence in situ hybridization (FISH) during diagnosis (Nelson et al., 2007). In a study on 325 patients newly diagnosed with B-CLL, it was found that at least one, but up to three and more chromosomal aberrations, occur in more than 80% of the patients (Dohner et al., 2000). A sole 13q deletion (causes delayed development in children) was found in 36% of the patients and correlated with a median survival of 133 months. Patients (7%) with a 17p deletion (affecting the tumor suppressor p53) had a median survival of only 32 months (Dohner et al., 2000). From this study, it can be concluded that B-CLL is characterized rather by prolonged survival of malignant B cells than by aggressive and invasive proliferation. Therefore, the cause of the disease is most likely a defect in apoptosis (Hallaert et al., 2007).

Presumably, B-CLL cells depend on growth and survival factors provided by stromal cells in the bone marrow, as when cultured *ex vivo*, an apoptotic program is activated and the cells die within days (Collins et al., 1989). This is prevented when B-CLL cells are supported by a stromal feeder layer (Lagneaux et al., 1998). However, proliferation of B-CLL cells can be detected by *in vivo* labeling in patients, but the CD phenotype of these proliferating CSCs in the bone marrow remains undefined (Chiorazzi, 2007). From these observations and due to rarely observed invasive proliferation into other organs it can be assumed that B-CLL cells depend on factors produced by the bone marrow stromal microenvironment.

2.7.3 B cell acute lymphocytic leukemia

B-ALL is characterized by the accumulation of lymphoblasts with clonal origin in the bone marrow and peripheral blood (Cobaleda and Sanchez-Garcia, 2009; Onciu, 2009). Lymphoblasts are immature cells, which would normally differentiate into leukocytes, but instead proliferate in an uncontrolled manner in the bone marrow and aggressively infiltrate other organs. This form of leukemia is found mainly in children from 2-5 years and then peaks again in elderly people (>50 years; Borkhardt et al., 1997). Because these immature cells proliferate quickly, patients require treatment within weeks after diagnosis (McGregor et al., 2012). Today, the overall cure rate with combined radiation- and multi chemotherapy is about 80% in children and 50% in adults (Gokbuget and Hoelzer, 2009; Yeoh et al., 2002). The diagnosis is based on a complete blood cell count and a blood smear. A bone marrow biopsy is a final proof.

The analysis of chromosomal translocations is routinely done in B-ALL diagnosis and serves as prognostic marker to identify patients who require more intense therapy (Harrison, 2009). The *TEL-AML1* fusion t(12;21) is the most commonly detected chromosomal abnormality and found in 25% of patients (Zelent et al., 2004). The *TEL* gene and the *AML1* gene both encode transcription factors, which are essential for early hematopoietic development/stem cell maintenance (Ford et al., 2009). The TEL-AML1 translocation links the helix-loop-helix domain of TEL to the DNA binding and transactivation domains of AML1. Detection of this fusion is a favorable prognostic marker (Zelent et al., 2004).

As part of an epidemiologic study, it was shown that the TEL-AML1 translocation could rarely be detected in neonatal blood spots (Greaves and Wiemels, 2003). Still, it took 5-10 years until leukemia was diagnosed in these children. Recurrent chromosomal translocations are a hallmark of B-ALL and are commonly found in TEL-AML1 leukemias, indicating that B-ALL develops from an immature cell accumulating additional mutations until it can drive leukemogenesis (Armstrong and Look, 2005).

Fusion of the Abelson (ABL1) tyrosine kinase to the BCR (breakpoint cluster region) gene is a commonly found chromosomal translocation t(9;22)(q34;q11) in B-ALL (Nowell and Hungerford, 1960). The resulting Philadelphia chromosome encodes the constitutively active BCR-ABL tyrosine kinase, which drives tumorigenesis by increased cell division, inhibiting DNA repair mechanisms and providing anti apoptotic factors via constitutive STAT5 (Signal transducer and activator of transcription) signaling (Malin et al., 2010). The BCR-ABL fusion is found in 40% of adult patients and is associated with a poor prognosis (Gleissner et al., 2002).

To this day, cancer stem cells have not been identified in B-ALL by a certain CD phenotype (Buss and Ho, 2011; Cox et al., 2009). However, their existence was functionally proven and their frequency can be defined using mouse models (Cox et al., 2004). To determine their frequency, patient derived cells are transplanted at limiting dilutions into immunocompromised mice. The CSC frequency is then calculated from the number of engrafted mice for each cell dose injected, using ELDA software (Hu and Smyth, 2009).

3 Aim of the study

Hematopoietic stem cells (HSCs) have the unique ability to undergo self-renewing divisions. Thereby they maintain steady levels of hematopoiesis without depleting the stem cell pool. The balance between quiescence, proliferation and differentiation is regulated by intrinsic and extrinsic factors, provided by specialized microenvironments in the bone marrow. While HSCs themselves are well defined, the molecular and cellular composition of the niche they reside in is poorly understood. The transcription factor *Ebf2* is expressed in stromal cells of the bone marrow and has been shown to regulate HSC homeostasis. Still, the underlying mechanisms and the contribution of *Ebf2* on a cellular level remain undefined.

The aim of this study was to examine whether all *Ebf2*-expressing bone marrow stromal cells contribute to *Ebf2*-mediated niche function for HSCs or whether this potential lies in a certain cell lineage. Therefore, mice carrying a conditional allele of *Ebf2* were generated and combined with Cre lines to disrupt *Ebf2*-expression specifically in mesenchymal stem cells, adipocytes or osteoblasts.

HSCs and leukemic Cancer Stem Cells (CSC) share certain characteristics. CSCs have the unique ability to propagate a heterogeneous disease upon transplantation of a single cell. Therefore, CSCs like HSCs are multipotent and can undergo self-renewing divisions. As IEO (immature *Ebf2*-expressing osteoblastic) cells support HSCs *in vitro* in an *Ebf2*-dependent manner, we addressed the question whether CSCs depend on the same *Ebf2*-mediated bone marrow niches. Therefore, co-culture experiments of human B-ALL and B-CLL leukemic cells with IEO cells and stromal cell lines were carried out. Thereby, the influence of *Ebf2* on proliferation, survival and maintenance of CSCs was investigated.

Finally, the role of *Ebf2* in T cell development was studied. *Ebf2*-deficient mice show a strong reduction in thymic cellularity. In the thymus, *Ebf2* is expressed by a small population of stromal cells at the boundary between the outer cortex and the inner medulla. Applying FACS, the nature of this cell population was characterized and we investigated whether different T cell types are equally affected by the loss of *Ebf2* in thymic stromal cells. Furthermore, thymic embryonic lobes were transplanted into wild type recipients to determine whether the observed phenotype originates in the thymus or on the level of a bone marrow-derived T cell progenitor.

4 Results

4.1 *Ebf2* in normal hematopoiesis

4.1.1 Generation of mice with a conditional *Ebf2* allele

Ebf2-LacZ$^{-/-}$ animals have a two- to fourfold reduction in HSC frequency, show a strong reduction in total cellularity of hematopoietic organs and die for unknown reasons at the age of roughly three to six weeks (Kieslinger et al., 2010). Most likely, various tissues and organs contribute to this complex phenotype leading to premature death. However, the underlying mechanisms, which cause the observed phenotype are poorly understood. To identify the *Ebf2*-expressing stromal cells responsible for the hematopoietic defects and to study their role in normal and malignant hematopoiesis, we generated a conditional knockout of *Ebf2*, based on the Cre-LoxP system. This strategy aimed at overcoming the premature death and at precisely defining the contribution of mesenchymal cell lineages expressing *Ebf2*, like MSCs, adipocytes and osteoblasts in *Ebf2*-mediated niche function for HSCs. As a consequence of this tissue specific deletion, the animals are expected to be in a better health condition, which allows to perform transplantation experiments.

4.1.2 Targeting strategy

The introduction of *LoxP* sites into genes needs awareness. Their presence can result in alternative start codon usage, alteration of regulatory elements or expression of a truncated version of the protein. As a result, the generated mouse model might be useless. Thus, analyses of Ebf2 protein structure and bioinformatic approaches on the *Ebf2* genomic locus were combined to minimize such risks. To fulfill their function as transcription factors Ebfs contain a DNA binding domain (DBD). Within their DBD lies a zinc-finger motif and for Ebf1 it was shown that each of the four central amino acids encompassing the zinc ion is essential for DNA binding (Hagman et al., 1995). Due to sequence homology of more than 90% at the protein level and 100% conservation of the four central zinc-finger amino acids between Ebf1 and Ebf2, we assumed that they are functionally indispensible in both proteins (Dubois and Vincent, 2001, Figure 4). Thus, exons which encode this structure are considered eligible targets. Upon Cre-mediated removal of DNA sequences encoding this zinc-finger, protein function should be disrupted.

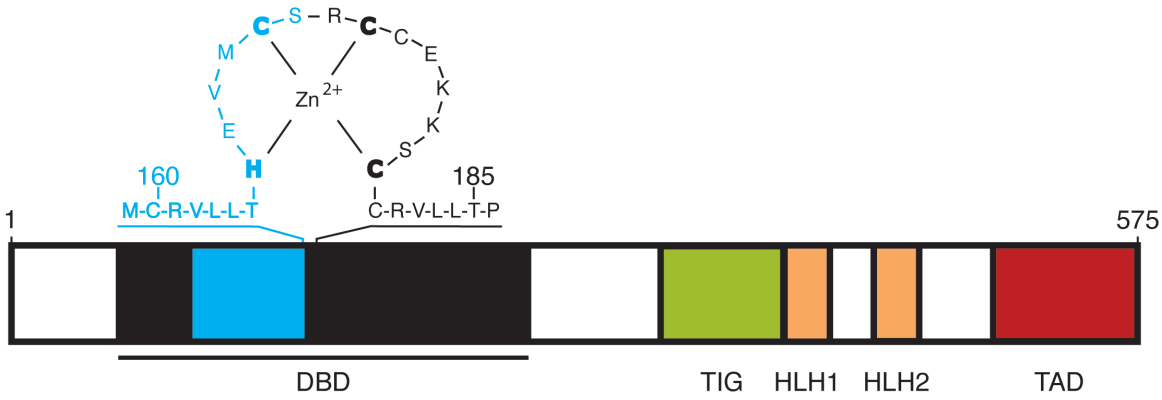

Figure 4: Schematic representation of the Ebf2 protein structure and its functional domains. The 575 amino acids comprise four different structural domains: a DNA binding domain (DBD), a transcription factor immunoglobulin domain (TIG), two helix-loop-helix domains (HLH) and a transactivation domain (TAD). The DBD contains a centered zinc finger motif, which is conserved between Ebf family members. For Ebf1, each of its four central amino acids (highlighted in bold letters) is essential for DNA binding (Hagman et al.,1995). The region coloured in blue is encoded by exons four to six.

Ebf2 stretches over 196 kb on mouse chromosome 14 and consists of 17 exons. The zinc-finger motif is encoded by exon six and seven with an intron of seven kilobases (kb) in between. As the recombination efficiency starts to drop when the distance between two *LoxP* sites exceeds 400 bp (Ringrose et al., 1999; Schnutgen et al., 2006) and the success rate for homologous recombination for an insert of almost nine kb was considered rather low, just one of the two exons was targeted (exon six encodes 50% of the zinc finger). However, this approach carries the risk that due to alternative splicing mechanisms a truncated protein might be expressed. This truncated version might still interact with other Ebf proteins potentially altering their function and causing an undefined biological setting. Therefore, the targeting strategy was improved by making use of the non-sense mediated mRNA decay pathway (NMD; Ishigaki et al., 2001). Additional removal of exons four and five in addition to exon six, upon recombination of the *LoxP* sites, will cause an out-of-frame splice from exon three to exon seven. This frameshift generates an artificial stop codon in exon eight. As a consequence, the *Ebf2* mRNA encodes a truncated protein of only two hundred amino acids which lacks 50% of its essential DBD. This should trigger NMD and result in degradation of the mRNA (Figure 5).

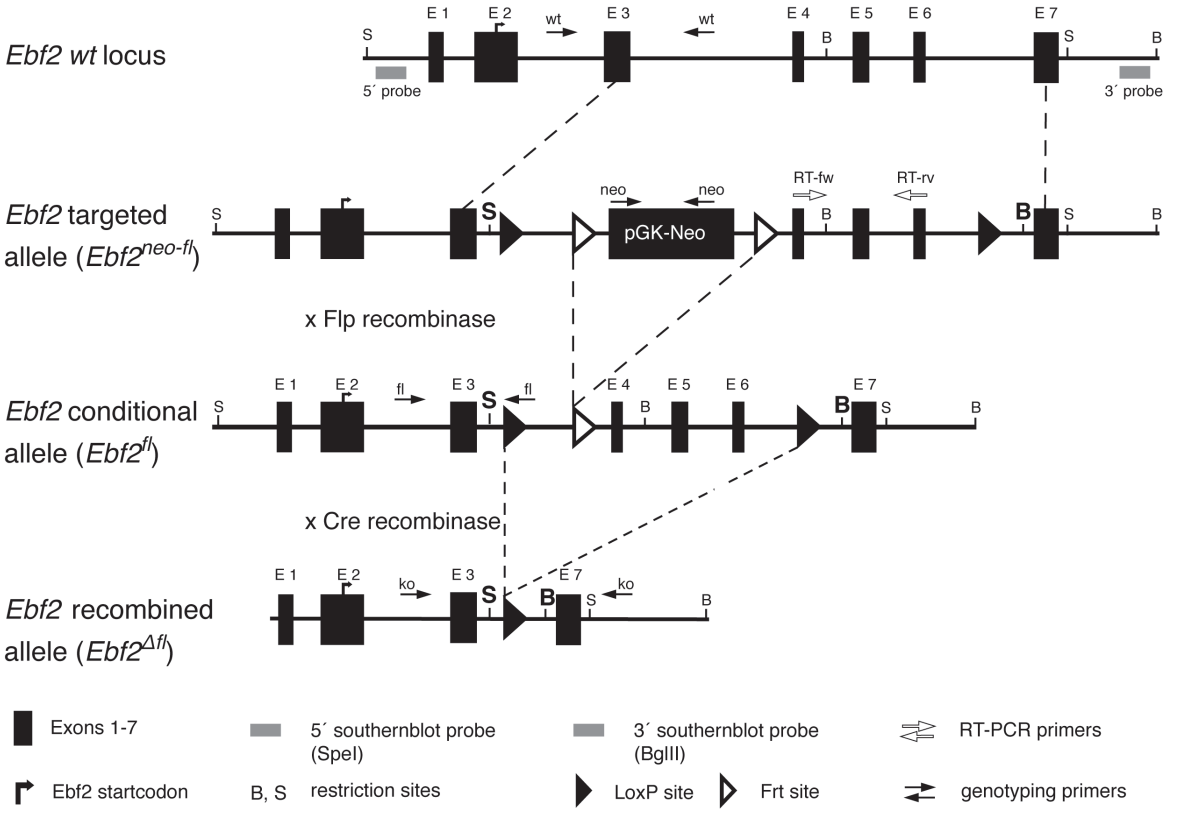

Figure 5: Schematic representation of the targeting strategy to generate mice carrying a conditional *Ebf2* allele. The first seven exons of the *Ebf2* wild type locus and the targeting construct are displayed. *LoxP* sites were introduced in front of exon four and after exon six. Flp or Cre recombinase activity leads to recombination and excision of DNA fragments in between *Frt* or *LoxP* sites, respectively. Probes and restriction sites used in southern blot experiments are shown. Primer pairs used to genotype the different genetic situations are indicated by filled arrows. The primer pair used to detect *Ebf2* transcripts in RT-PCR reactions is shown by open arrows.

Introns, although non-coding, can contain regulatory elements important for gene regulation (Banerji et al., 1983). Although *LoxP* sites are only 34 bps in size, they can influence gene expression and splicing. If these minor changes manifest in a phenotype, the mouse model becomes useless for conditional approaches. Most likely not only genes, but also their regulatory elements are conserved in evolution. Therefore, cross-species alignments between *Ebf2* of C57BL/6 mice (set as reference), macaque, beagle and human were performed and regions of very low sequence homology within introns three and six were identified (Figure 6; Ovcharenko et al., 2004). These regions are unlikely to be of functional relevance and were therefore chosen for the placement of *LoxP* sites.

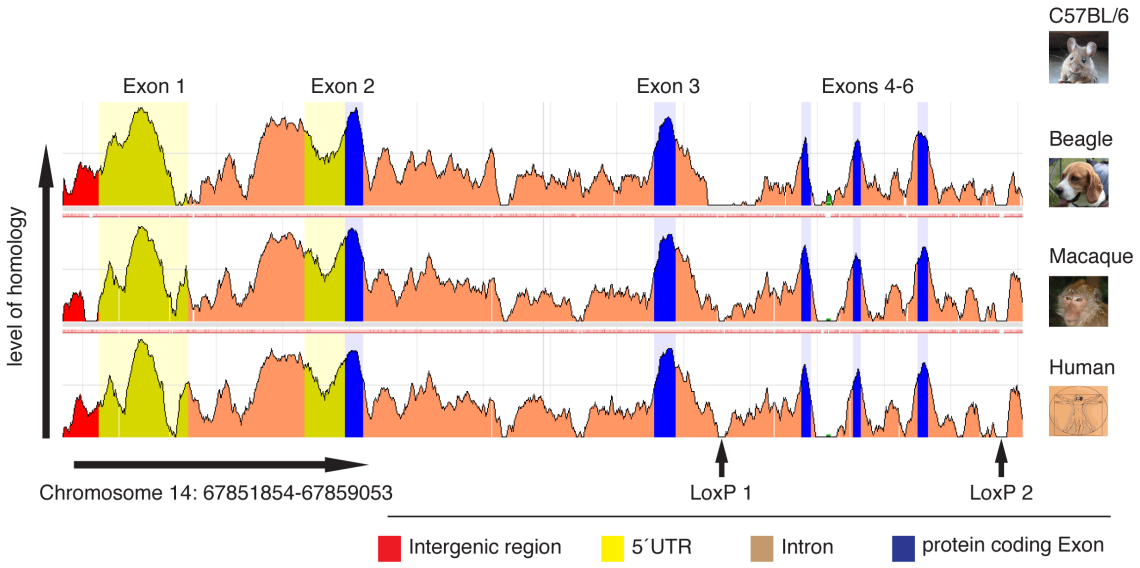

Figure 6: Cross-species alignment of the C57BL/6 *Ebf2* genomic locus. The DNA sequences of various organisms were aligned with the *Ebf2* genomic region of C57/BL6, set as reference. Arrowheads indicate two regions with low sequence homology, which qualify for the introduction of *LoxP* sites.

pEZ FrtLox DT served as vector backbone (Figure 7). It contains a *diphteria toxin A* gene, whose expression is lethal and kills all ES cells that have randomly integrated the linearized plasmid into their genome. This greatly increases the frequency of correctly targeted ES cell clones and reduces screening efforts. Moreover, the vector contains a neomycin resistance cassette, which is flanked by two *Frt* sites. The neomycin cassette is required for selection of ES cell clones, which have correctly integrated the construct. The *Frt* sites have a length of 48 bp and are recognized by Flp recombinase that recombines *Frt* sites and excises the DNA fragment lying inbetween (Chen and Rice, 2003). Adjacent to *Frt* sites, the vector contains two *LoxP* sites between which the insert has to be cloned. At the outsides of these *LoxP* sequences, a left and right arm with homology to the targeted genomic region are required. These arms allow homologous recombination in ES cells.

4.1.3 Cloning strategy

Homologous recombination events can occur between two similar or identical stretches of DNA. The chance for such an event correlates directly with the level of identity. Therefore, the DNA fragments that mediate the recombination during gene targeting shall be identical to the targeted DNA sequence. To generate the targeting vector for Bruce4 and IDG3.2 ES cells, about 10 kb *Ebf2* genomic DNA from C57BL/6 were needed comprising a 5.7 kb left arm of homology, a 1.7 kb insert and a 2.7 kb right arm of homology. To generate these fragments, a PCR

based approach using the „Phusion high fidelity DNA polymerase“ (Finnzymes) with an error rate of $4.4x10^{-7}$ was chosen.

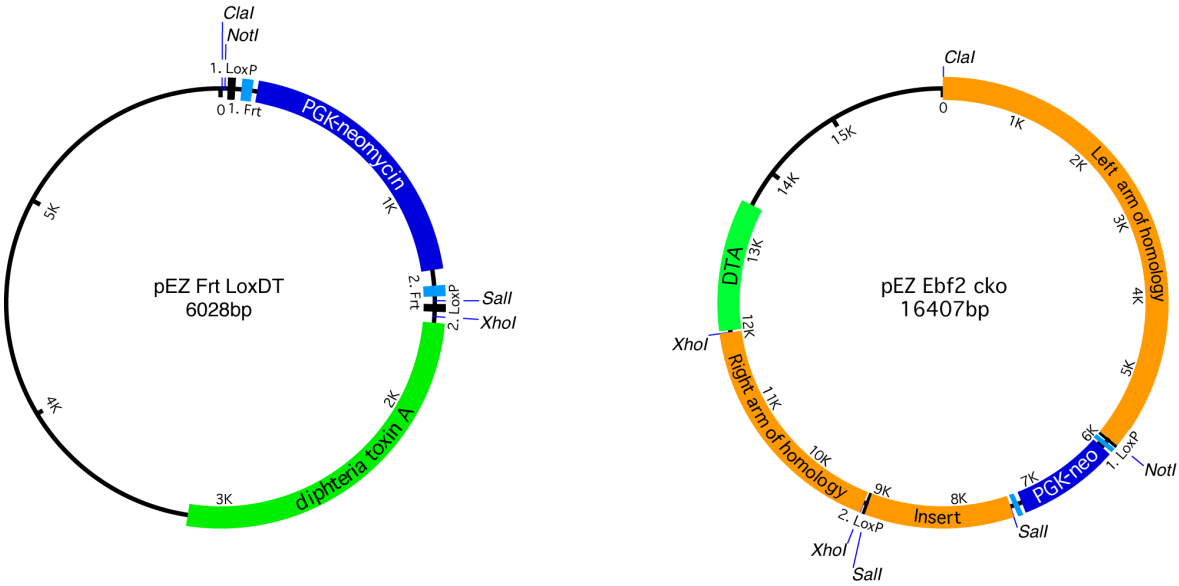

Figure 7: Vector backbone and completed construct used to target the *Ebf2 locus*. pEZ Frt LoxDT contains a *Frt*-flanked PGK-neomycin resistance cassette (PGK-neo), two *LoxP* sites and the *diphteria toxin A* gene (DTA). The insert was cloned in between the second *Frt* and *LoxP* site using the unique *Sal*I restriction site. Left- and right arm of homology were cloned adjacent of the two *LoxP* sites. To clone the left arm of homology, *Cla*I and *Not*I were used. The right arm of homology was cloned using the indicated *Xho*I site.

A BAC clone (RP23-148I22) from a C57BL/6 library served as template in the reactions. The generated blunt ended PCR products were cloned into pJet1.2/blunt and sequenced. Hereafter, they were consecutively subcloned into pEZ Frt LoxDT. Restriction sites used for cloning steps and restriction sites to identify ES cell clones with a targeted *Ebf2* allele in southern blot analysis were introduced via primer overhangs on the oligonucleotides used in the PCR reactions. Newly introduced restriction sites, which were used for clonings are shown in Figure 7. In preparation for southern blot analyses we introduced a *Spe*I site at the 3´-end of the left arm of homology and a *Bgl*II site at the 5´-end of the right arm of homology (not shown). When the vector was complete as shown in Figure 7, restriction analyses with different enzymes were performed and the newly introduced DNA fragments were sequenced.

4.1.4 ES cell targeting and screening

In this study, two different ES cell lines were manipulated. Bruce4, a pure C57BL/6 ES cell line, was used to quickly achieve a congenic genetic background for transplantation experiments. IDG3.2, a F1 hybrid ES cell line derived from a crossing of 129/Sv x C57BL/6, was used because it is reported to be very robust and reliable in terms of germline transmission (personal communication with U. Zimber-Strobl and R. Kühn, HMGU).

Bruce4 and IDG3.2 ES cells were electroporated and after selection with geneticin, 500 Bruce4 ES cell clones and 400 IDG3.2 ES cell clones were isolated and analyzed by southern blot. In the first screen using the BglII probe, four Bruce4 ES cell clones (ES cell clone B5-36 is shown as an example in Figure 8 a) and three IDG3.2 clones gave a signal at the expected height of a recombined allele (4 kb, see Figure 8b). This corresponds to a targeting efficiency of 0.8% in both ES cell lines (supplementary Table 1). Those seven clones were then analyzed with the SpeI probe and all gave a signal at the expected height for a recombined allele (5 kb, see Figure 8c). Correctness of *LoxP* sites was confirmed by sequencing and *LoxP* sites were functionally tested adding tat-Cre (Peitz et al., 2002) to cultured ES cells. Genomic DNA from tat-Cre treated cells was isolated and a recombined *Ebf2* allele could be detected by PCR (Figure 5, data not shown).

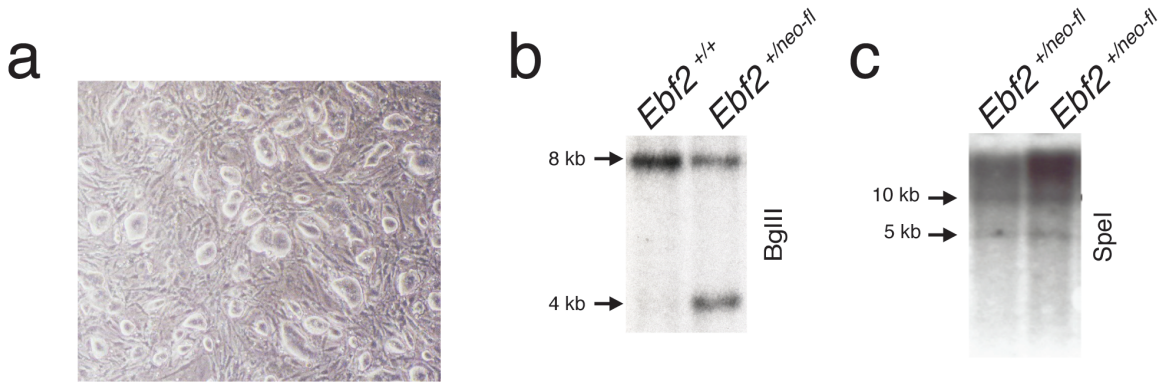

Figure 8: Embryonic stem cell clones cultured on mouse embryonic fibroblasts and southern blot analysis of the latter. (a) Brightfield image of Bruce4 ES cell clone B5-36 just before injection into blastocysts. (b) Southern blot analysis of genomic ES cell DNA after cleavage with *Bgl*II showing a wild type (8 kb) and the targeted allele (4 kb, clone B5-36). (c) Southern blot analysis of ES cell clones (B5-36 and B5-71) after cleavage with *Spe*I. Both clones show the correct integration of the construct (wt: 10 kb, targeted allele: 5 kb).

Two clones of each ES cell type were then expanded for injection into blastocysts (Bruce4 clones: B5-36 and B5-71. IDG3.2 clones: I3-31 and I4-96). Blastocysts were isolated from three-week-old wild type C57BL/6 and Balb/C females by induced superovulation. Six days prior to isolation, 7.5 units of pregnant mare serum gonadotropin were injected intraperitoneally. Two days later, mice were injected with 7.5 units human chorionic gonadotropin and bred with males. Another 3.5 days later, E3.5 blastocyts were harvested and 20-24 ES cells were injected each. Bruce4 ES cells were injected into Balb/C blastocysts (generates chimeras with black and brown coat colour) while IDG3.2 ES cells were injected into C57BL/6 blastocysts (generates chimeras with white and black fur colour). Thereafter, blastocysts were transplanted into Balb/C foster mothers.

Overall, 15 chimeric animals showing a chimerism ranging from 5-90% were obtained (one female and no males from IDG3.2, five females and nine males from Bruce4). Male chimeras where crossed to C57BL/6 wild type females for germline transmission. In this breeding setup, animals with a black (sperms derive from Bruce4 ES cells injected into the blastocyst) or brown (sperms derive from the germline generated from cells of the fertilized Balb/C blastocyst) fur colour can be obtained. Due to heterozygosity of the injected ES cells (*Ebf2*$^{+/neo\text{-}fl}$), the chance of successful inheritance of the transgene in an offspring with black fur colour is 50%. In two out of nine chimeras the engineered ES cells had contributed or completely formed the germline and the targeted *Ebf2* allele was passed on to their progeny. One male, derived from clone B5-36 generated only black pups. This male is the founder animal of the new mouse strain. In addition to fur colour, genotypes were confirmed by PCR and southern blot analysis with the SpeI probe (data not shown). *Ebf2*$^{+/neo\text{-}fl}$ animals were then crossed with C57/BL6 *FlpE* females to remove the neomycin resistence cassette (Figure 5). This transgenic mouse strain expresses Flp recombinase under control of the human beta actin promotor which is active in all tissues (Rodriguez et al., 2000). Flp mediated recombination of the *Frt* sites leads to excision of the PGK-neomycin selection cassette in the mouse germline. Thereby, the *PGK* promotor, which might interfere with the endogenous *Ebf2* promotor is removed. Offsprings from these breedings have the genotype *Ebf2*$^{+/fl}$. Removal of the PGK-neomycin selection cassette was controlled by PCR (Figure 5, data not shown).

4.1.5 Analysis of *Ebf2*$^{\Delta fl/\Delta fl}$ animals

To evaluate the functionality of the newly generated mouse strain, it was crossed with *Del*^{Cre} transgenic animals, which express Cre recombinase in the germline (Schwenk et al., 1995). Cre mediated recombination of the two *LoxP* sites leads to

excision of Exons 4-6 (Figure 5). Offsprings from these breedings have the genotype *Ebf2*$^{+/\Delta fl}$. Heterozygous progeny with one recombined *Ebf2* allele (*Ebf2*$^{+/\Delta fl}$) were then intercrossed to generate *Ebf2*$^{\Delta fl/\Delta fl}$ animals. Mice with this genotype carry two recombined *Ebf2* alleles and their phenotype should recapitulate the phenotype of *Ebf2-LacZ*$^{-/-}$ animals. Recombination of *LoxP* sites was confirmed by PCR on genomic tail DNA as shown in Figure 9a. To control for a loss of *Ebf2* transcript, thymic epithelium from *Ebf2*$^{\Delta fl/\Delta fl}$ animals was isolated and cDNA was synthesized from the extracted total RNA. In RT-PCR no *Ebf2* transcript could be detected (Figure 9b).

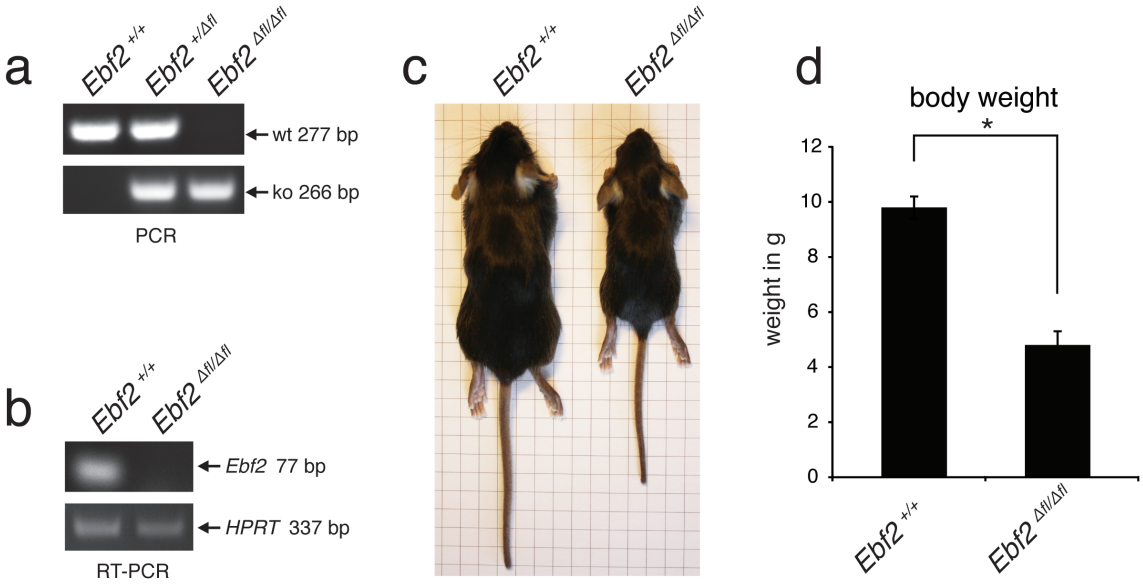

Figure 9: Genotyping and RT-PCR to detect recombination of *LoxP* sites and loss of *Ebf2* transcript in *Ebf2*$^{\Delta fl/\Delta fl}$ mice. (a) Heterozygous *Ebf2*$^{+/\Delta fl}$ animals were bred to generate *Ebf2*-deficient mice. A genotyping result is shown. (b) A reverse transcription reaction on cDNA from thymic stromal cells of wild type and *Ebf2*$^{\Delta fl/\Delta fl}$ animals failed to amplify the 77 bp product from *Ebf2*$^{\Delta fl/\Delta fl}$ cDNA. The shown HPRT product was used for normalization and serves as control for successful reverse transcription. (c) General appearance of a *Ebf2*$^{\Delta fl/\Delta fl}$ animal at the age of three weeks compared to a wild type littermate of the same age. (d) Three week old *Ebf2*$^{\Delta fl/\Delta fl}$ mice weight about 50% less compared to wild type littermates (n=3, p=0.0001).

In Corradi et al. (2003), *Ebf2-LacZ*$^{-/-}$ knockin animals are described to show a 50% reduction in body mass compared to *Ebf2-LacZ*$^{+/+}$ and *Ebf2-LacZ*$^{+/-}$ littermates, to be mildly uncoordinated and to walk with an unsteady and waddling gait. Furthermore, Corradi and colleagues report that *Ebf2-LacZ*$^{-/-}$ animals exhibited a hunchback and *Ebf2*$^{\Delta fl/\Delta fl}$ animals show the same behavioral disorders. When we determined the body weight of three-week-old *Ebf2*$^{\Delta fl/\Delta fl}$ mice we detected strong

reductions comparable to those previously reported for the *Ebf2-LacZ* mutation (Figure 9 c, d).

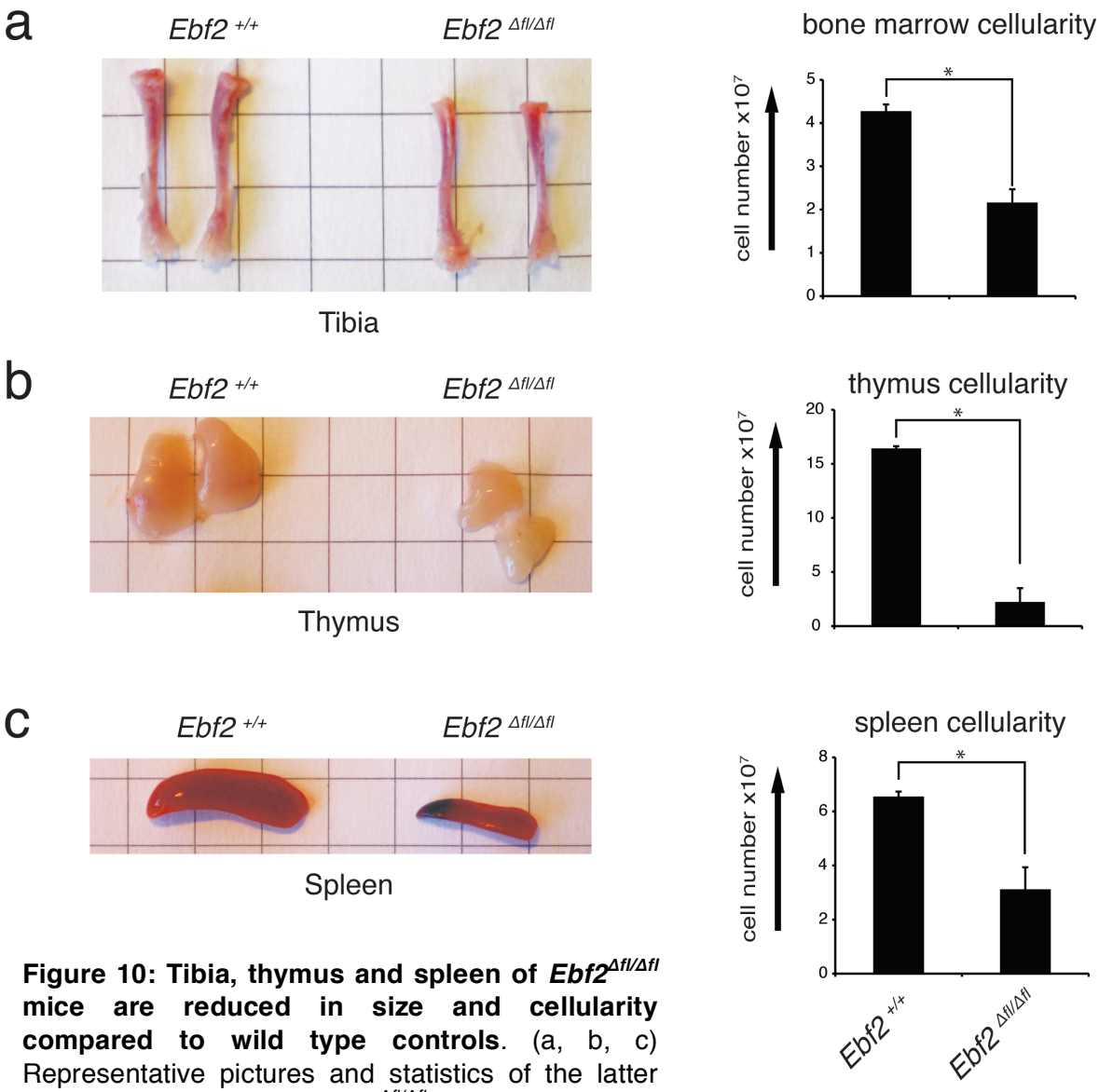

Figure 10: Tibia, thymus and spleen of *Ebf2*$^{\Delta fl/\Delta fl}$ mice are reduced in size and cellularity compared to wild type controls. (a, b, c) Representative pictures and statistics of the latter organs from control and *Ebf2*$^{\Delta fl/\Delta fl}$ animals at the age of three weeks are shown (n=3, bone marrow p=0.0001, thymus p=0.0001, spleen p=0.002).

At the age of three weeks, *Ebf2*$^{\Delta fl/\Delta fl}$ animals were sacrificed and total cellularity of thymus, spleen and bone marrow were found to be strongly reduced (Figure 10). The strongest reduction was found for thymus cellularity (sevenfold), followed by spleen (twofold) and bone marrow (twofold). Except for the reduction in spleen cellularity, which was reported to be decreased about fivefold at the age of three weeks, this data is comparable to the report on the *Ebf2-LacZ*$^{-/-}$ mutation (Kieslinger et al., 2010).

Ebf2-LacZ$^{-/-}$ animals have a two- to fourfold reduction in KSL (c-Kit^{+}, Sca1^{+}, Lin^{-} cells, a population highly enriched for hematopoietic stem cells) frequency (Kieslinger et al., 2010). The KSL compartment in *Ebf2*$^{+/+}$ and *Ebf2*$^{\Delta fl/\Delta fl}$ littermates was therefore analyzed and a sevenfold reduction could be detected (Figure 11). FACS gating strategy to determine the KSL frequency is shown in supplementary Figure S2.

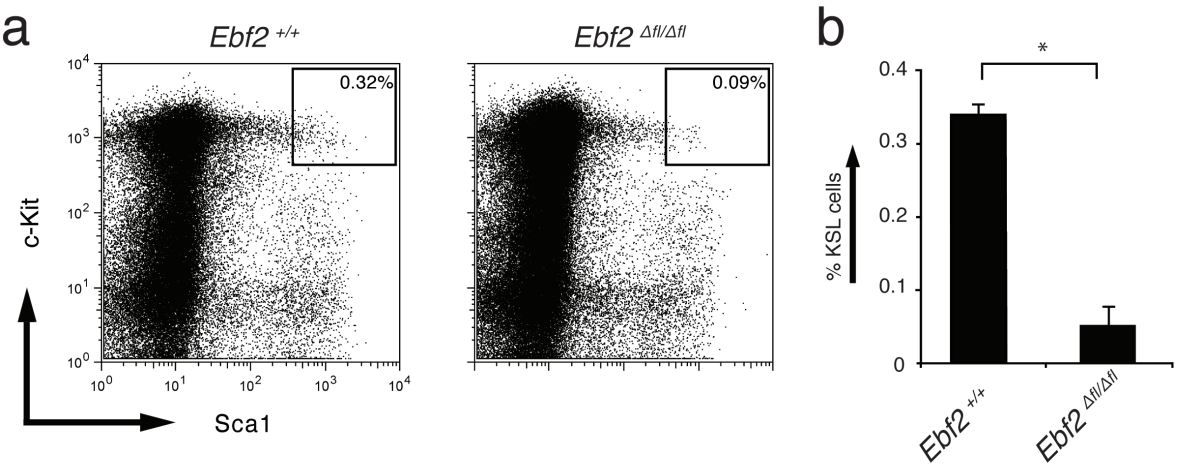

Figure 11: *Ebf2*$^{\Delta fl/\Delta fl}$ animals have reduced KSL frequencies. (a) Analysis of the KSL compartment in three-week-old animals by flow cytometry. Lymphocytes from the bone marrow were gated as living cells (PI^{-}), lineage marker negative (Lin^{-}) and were analyzed for the expression of Sca1 and c-Kit. (b) *Ebf2*-deficient animals show a sevenfold reduction in KSL frequency compared to control animals (n=3, p=0.0001).

In summary, Cre-mediated recombination of *LoxP* sites leads to a loss of *Ebf2* transcript. *Ebf2*$^{\Delta fl/\Delta fl}$ animals fully recapitulate the phenotype of *Ebf2-LacZ*$^{-/-}$ mice (Corradi et al., 2003; Kieslinger et al., 2010).

When we measured body weight, cellularity of hematopoietic organs and KSL frequencies in *Ebf2*$^{fl/fl}$ animals (not deleted in *Ebf2*), no differences compared to wild type littermates were detected (data not shown). Therefore, mice with a conditional allele of *Ebf2* were successfully generated and the new mouse strain is applicable to investigate the function of *Ebf2* in different stromal cell types by crossing *Ebf2*$^{fl/fl}$ animals with stromal cell type specific Cre lines.

4.1.6 Analysis of *Prx*^{Cre}*Ebf2*$^{fl/fl}$ animals

To investigate whether *Ebf2* expressed by MSCs is crucial for the support of HSCs in the bone marrow niche, *Ebf2*$^{fl/fl}$ animals were crossed with *Prx*^{Cre} transgenic

mice (Logan et al., 2002). Thus, *Ebf2* is specifically deleted in MSCs. *Prx*^{Cre}*Ebf2*$^{fl/fl}$ animals behave normally and do not show any signs of growth retardation. Their movement is ordinary and the animals are healthy. At the age of ten weeks, animals were sacrificed and primary and secondary hematopoietic organs were analyzed (Figure 12).

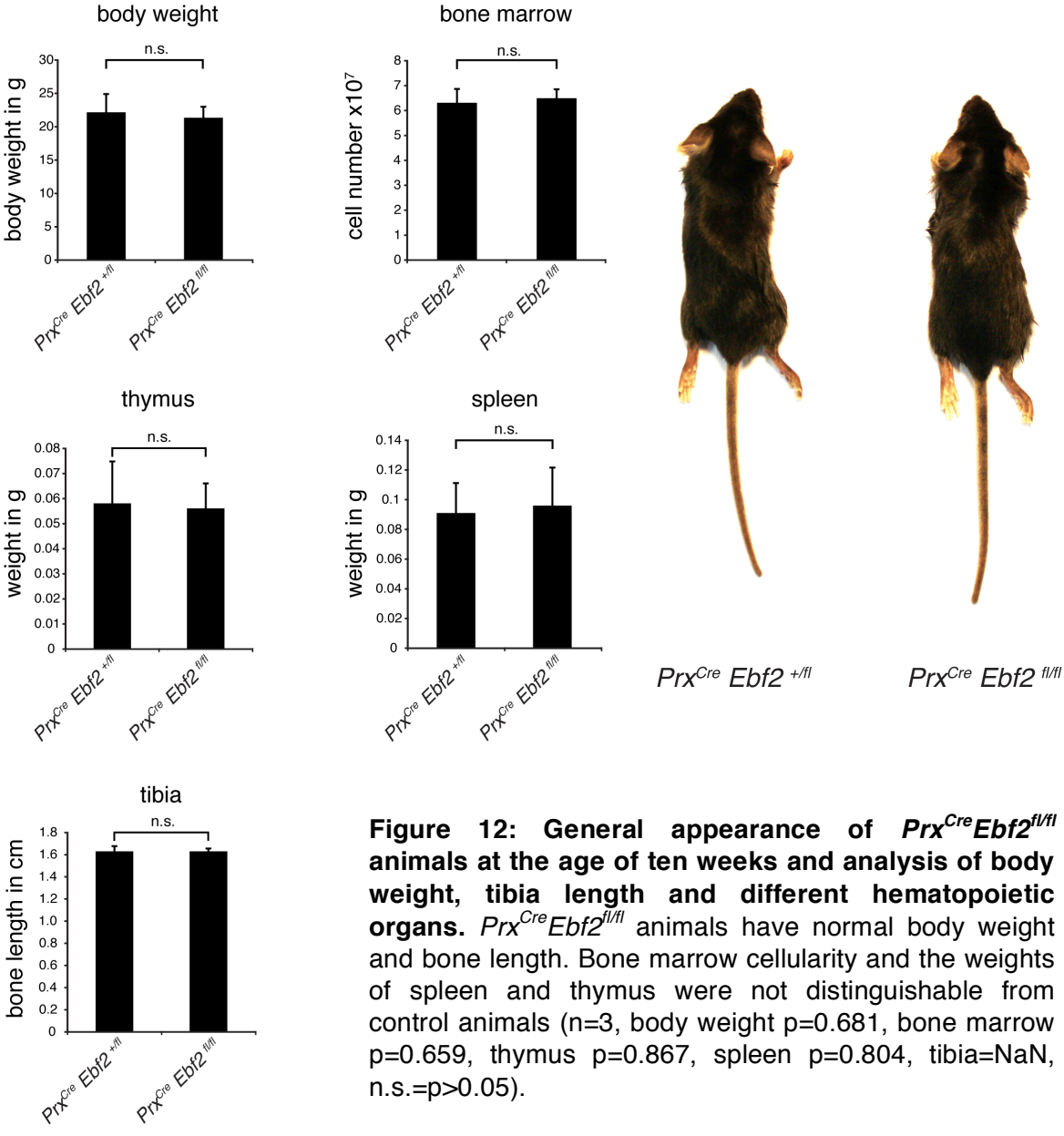

Figure 12: General appearance of *Prx*^{Cre}*Ebf2*$^{fl/fl}$ animals at the age of ten weeks and analysis of body weight, tibia length and different hematopoietic organs. *Prx*^{Cre}*Ebf2*$^{fl/fl}$ animals have normal body weight and bone length. Bone marrow cellularity and the weights of spleen and thymus were not distinguishable from control animals (n=3, body weight p=0.681, bone marrow p=0.659, thymus p=0.867, spleen p=0.804, tibia=NaN, n.s.=p>0.05).

Spleen and thymus were of normal size. Bones were normal in size and firmness (observation during preparation of bones). Bone weight was also unaffected by the loss of *Ebf2* (data not shown). When the weight of spleen, thymus and bone marrow cellularity was determined, the organs from *Prx*^{Cre}*Ebf2*$^{fl/fl}$ were not

distinguishable from control animals. Finally, the KSL compartment in *Prx*^{Cre}*Ebf2*$^{fl/fl}$ animals was analyzed and found to be unchanged (Figure 13). We performed a genotyping PCR on genomic DNA (gDNA) isolated from bone marrow cells of *Prx*^{Cre}*Efb2*$^{fl/fl}$ animals to confirm that *Cre* expression resulted in successful deletion of Exons 4-6. Detection of a recombined *Ebf2* conditional allele confirmed recombination of the *LoxP* sites at the *Ebf2* locus by Cre recombinase (supplementary Figure S2).

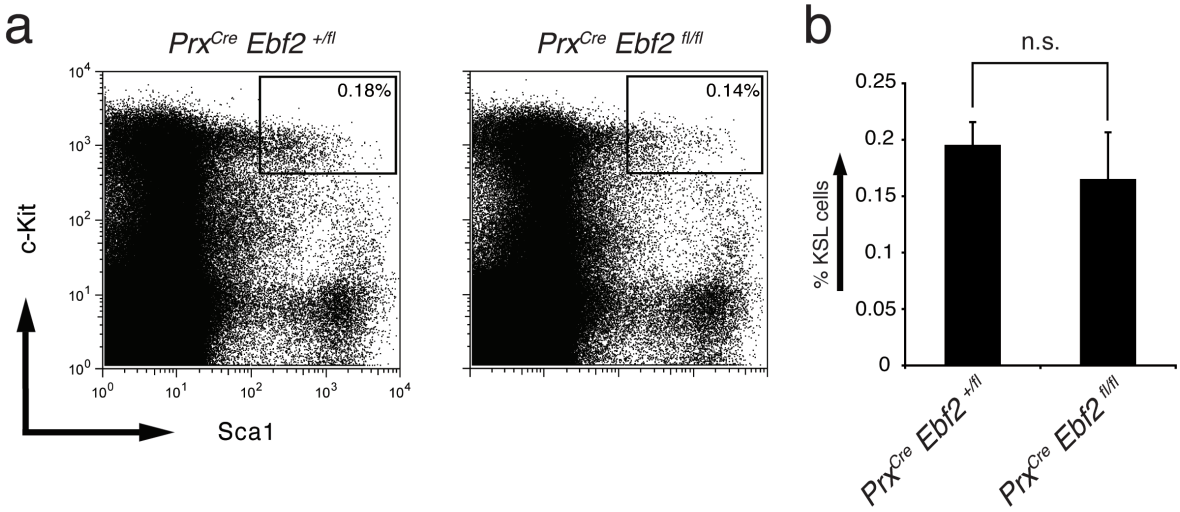

Figure 13: *Prx*^{Cre}-mediated deletion of *Ebf2* does not affect HSC homeostasis. (a) Total bone marrow from ten-week-old *Prx*^{Cre}*Ebf2*$^{fl/fl}$ animals and controls was analyzed by flow cytometry. Lymphocytes were gated as living cells (PI$^-$), lineage marker negative (Lin$^-$) and were analyzed for the expression of Sca1 and c-Kit. (b) Statistics on KSL frequencies measured in different experiments (*Prx*^{Cre}*Ebf2*$^{+/fl}$ n=4, *Prx*^{Cre}*Ebf2*$^{fl/fl}$ n=3, p=0.264, n.s.=p>0.05).

4.1.7 Analysis of *AP2*^{Cre}*Ebf2*$^{fl/fl}$ animals

Adipocytes are part of the bone marrow stromal microenvironment for hematopoietic cells. Adiponectin, a secreted metabolic hormone, is exclusively produced by adipocytes and promotes proliferation of HSCs in the bone marrow (DiMascio et al., 2007). As *Ebf2* is expressed in adipocytes (Jimenez et al., 2007) *Ebf2*$^{fl/fl}$ animals were crossed with *AP2*^{Cre} transgenics, which express Cre under control of the adipocyte protein 2 (AP2) promotor to delete *Ebf2* specifically in adipocytes (He et al., 2003).

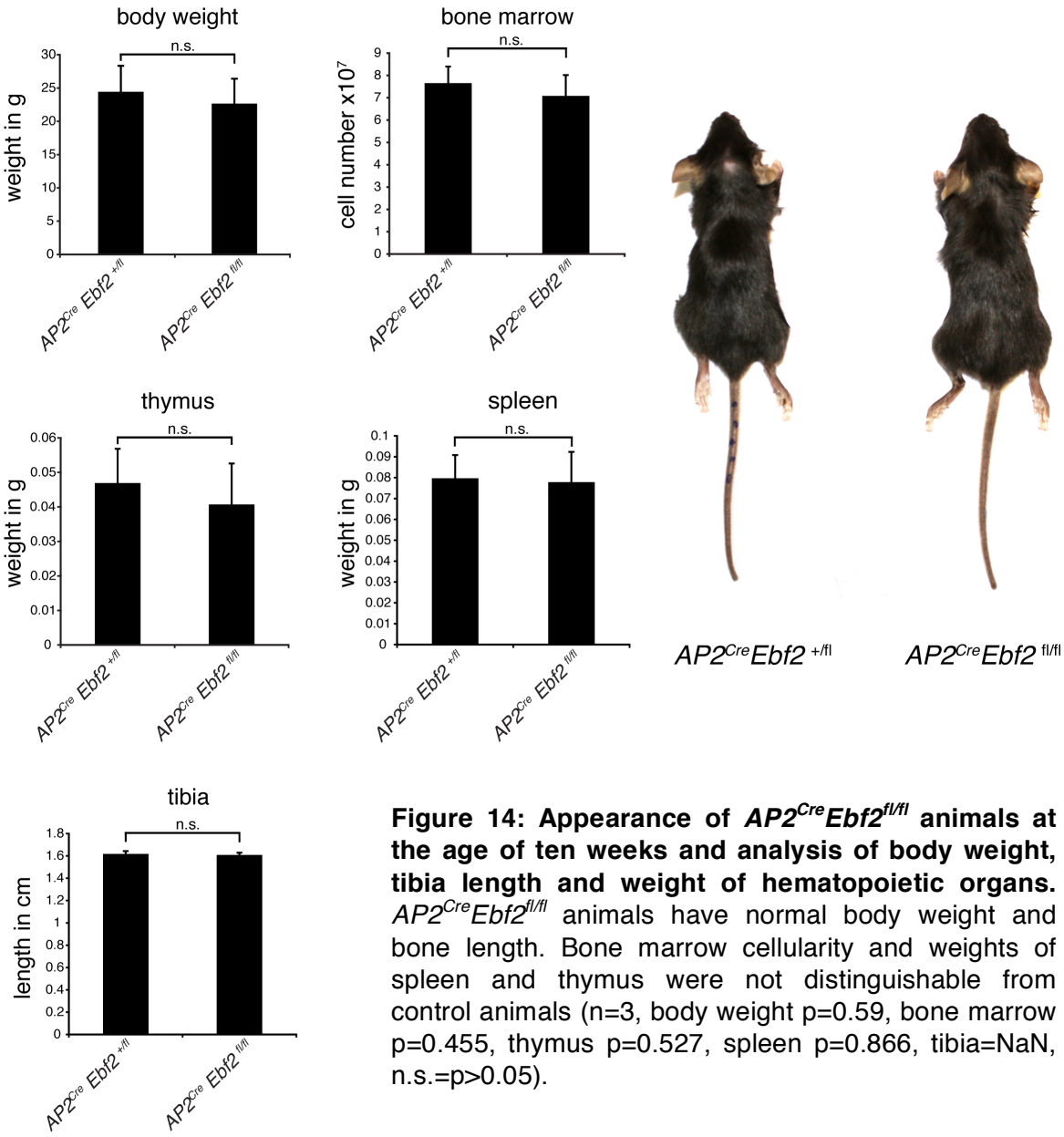

Figure 14: Appearance of *AP2^{Cre}Ebf2$^{fl/fl}$* animals at the age of ten weeks and analysis of body weight, tibia length and weight of hematopoietic organs. *AP2^{Cre}Ebf2$^{fl/fl}$* animals have normal body weight and bone length. Bone marrow cellularity and weights of spleen and thymus were not distinguishable from control animals (n=3, body weight p=0.59, bone marrow p=0.455, thymus p=0.527, spleen p=0.866, tibia=NaN, n.s.=p>0.05).

Recombination of the *LoxP* sites of the conditional *Ebf2* allele was confirmed by PCR on gDNA isolated from adipose tissue and flushed bone marrow cells of *AP2^{Cre}Ebf2$^{fl/fl}$* mice (supplementary Figure S3). *AP2^{Cre}Ebf2$^{fl/fl}$* animals developed normally and were not distinguishable from control animals (Figure 14). At the age of ten weeks body weight was determined and found to be unaltered and no reduction in subcutaneous fat was detected. Moreover, we did not observe a difference in bone firmness of *AP2^{Cre}Ebf2$^{fl/fl}$* animals compared to control mice (own observation during dissection of femur and tibia). Appearance of hematopoietic organs was ordinary and the weights of thymi and spleens were similar to those of control animals. Furthermore, the total bone marrow cellularity was not reduced and when the KSL frequency was determined by FACS, no difference to control animals was detected (Figure 15).

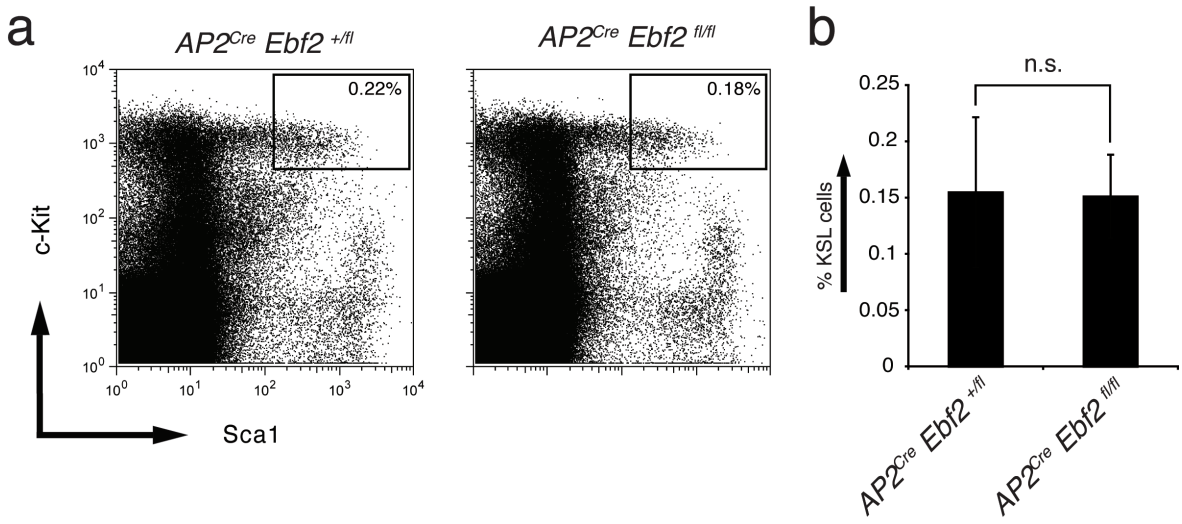

Figure 15: Deletion of *Ebf2* in adipocytes does not result in reduced KSL frequencies. (a) Analysis of KSL frequency in total bone marrow isolated from femurs and tibias of ten-week-old $AP2^{Cre}Ebf2^{fl/fl}$ and control animals by flow cytometry. Lymphocytes were gated as living cells (PI^-), lineage marker negative (Lin^-) and were analyzed for the expression of Sca1 and c-Kit. (b) Bar chart and statistics on the detected KSL frequencies (n=3, p=0.938, n.s.=p>0.05).

4.1.8 Analysis of $Osx^{Cre}Ebf2^{fl/fl}$ animals

Osteoblasts play a key role in regulating the hematopoietic stem cell niche and immature osteoblasts express *Ebf2* (Kieslinger et al., 2010; Zhang et al., 2003). To investigate the role of *Ebf2*-expressing osteoblasts, $Ebf2^{fl/fl}$ animals were crossed with Osx^{Cre} transgenic animals, which express Cre recombinase under control of the *osterix* promotor (active during early osteoblast differentiation; Rodda and McMahon, 2006). $Osx^{Cre}Ebf2^{fl/fl}$ pups were not distinguishable from control animals right after birth. However, at the age of one week $Osx^{Cre}Ebf2^{fl/fl}$ animals started displaying developmental retardation and were smaller than littermates of other genotypes. The severity of this phenotype increased with age and $Osx^{Cre}Ebf2^{fl/fl}$ animals had significantly reduced body weight at the age of four weeks (Figure 16).

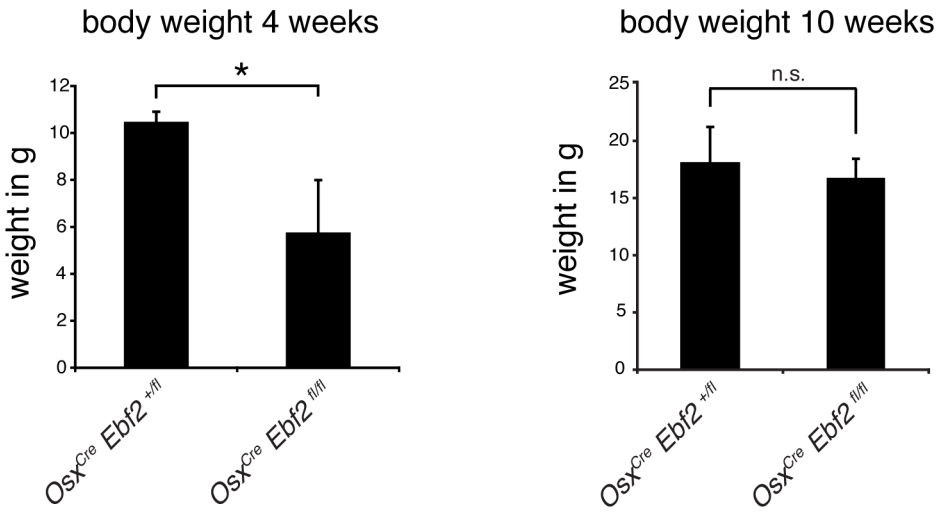

Figure 16: Deletion of *Ebf2* in immature osteoblasts results in a time-dependent body mass reduction. At the age of four weeks $Osx^{Cre}Ebf2^{fl/fl}$ animals have significantly reduced body weight while ten-week-old $Osx^{Cre}Ebf2^{fl/fl}$ animals have relatively normal body weight compared to controls (four-week-old: n=3, body weight p=0.023; ten-week-old: n=3, p=0.447, n.s.=p>0.05).

To reduce the extent of this phenotype to a minimum, the animals were fed pulp. Although this mildened the phenotype, $Osx^{Cre}Ebf2^{fl/fl}$ mice still show reduced body mass. During the first weeks of life, $Osx^{Cre}Ebf2^{fl/fl}$ animals were regularly observed. No behavioral disorders, like a waddling gait were detected. $Osx^{Cre}Ebf2^{fl/fl}$ animals behaved comparable to control littermates, although displaying dwarfism they were in a better physical condition than $Ebf2^{\Delta fl/\Delta fl}$ animals. Due to the observed reduction in body mass, which is also detectable in $Ebf2^{\Delta fl/\Delta fl}$ animals, we decided to analyze hematopoietic organs and long bones of four-week-old $Osx^{Cre}Ebf2^{fl/fl}$ animals (Figure 17).

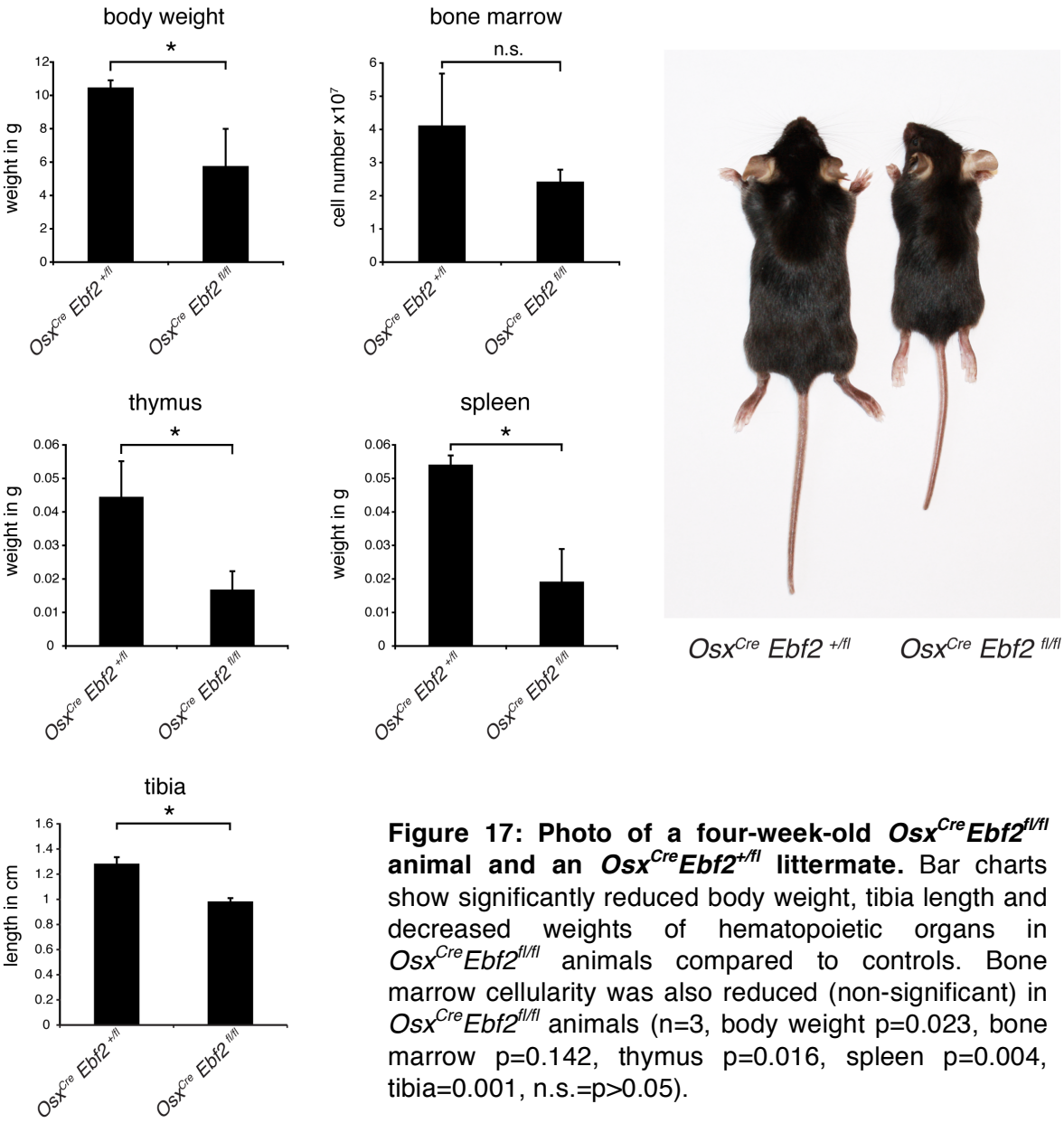

Figure 17: Photo of a four-week-old *Osx^{Cre}Ebf2$^{fl/fl}$* animal and an *Osx^{Cre}Ebf2$^{+/fl}$* littermate. Bar charts show significantly reduced body weight, tibia length and decreased weights of hematopoietic organs in *Osx^{Cre}Ebf2$^{fl/fl}$* animals compared to controls. Bone marrow cellularity was also reduced (non-significant) in *Osx^{Cre}Ebf2$^{fl/fl}$* animals (n=3, body weight p=0.023, bone marrow p=0.142, thymus p=0.016, spleen p=0.004, tibia=0.001, n.s.=p>0.05).

The size of femur and tibia was reduced by about 20%. Although the bones were reduced in size, they were rather solid and firm like bones of control animals (own observation during dissection of femur and tibia). *Osx^{Cre}Ebf2$^{fl/fl}$* animals had about 40% less bone marrow cells than control mice (non-significant). The weight of spleen and thymus was found to be significantly reduced, 2.5-fold for thymus and 2.8-fold for spleen, see Figure 17.

When the frequency of KSL cells in three- to four-week-old *Osx^{Cre}Ebf2$^{fl/fl}$* animals was determined by FACS analysis, we detected a two- to fourfold reduction (Figure 18).

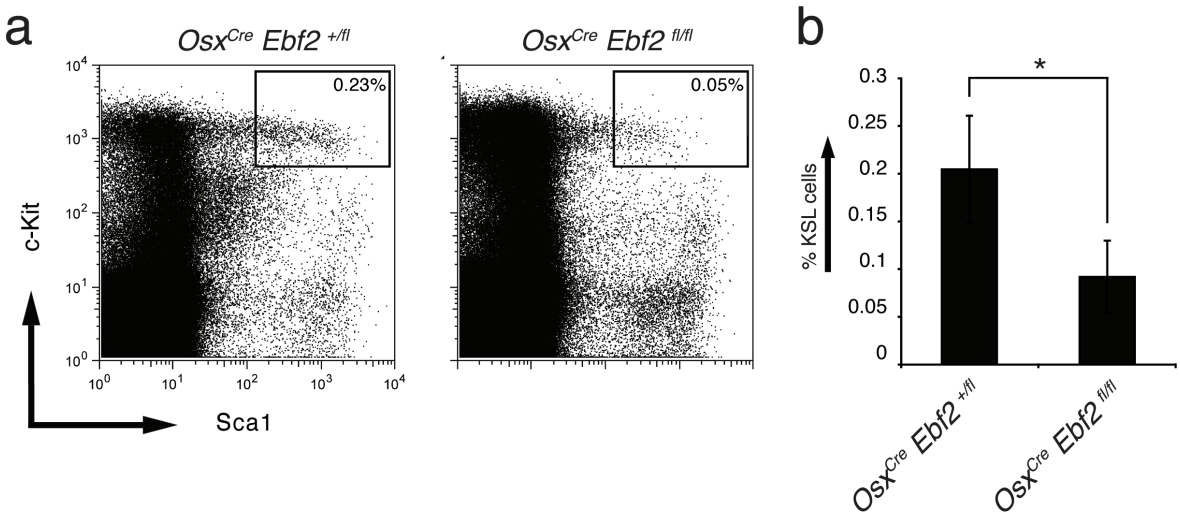

Figure 18: Deletion of *Ebf2* in immature osteoblasts results in reduced KSL frequencies in three- to four-week-old *Osx^{Cre}Ebf2$^{fl/fl}$* animals compared to controls. (a) Analysis of total bone marrow from three- to four-week-old animals by flow cytometry. Lymphocytes were gated as living cells (PI^-), lineage marker negative (Lin^-) and were analyzed for the expression of Sca1 and c-Kit. (b) KSL frequencies in *Osx^{Cre}Ebf2$^{fl/fl}$* animals are reduced about 2.3-fold compared to controls (*Osx^{Cre}Ebf2$^{+/fl}$* n=4, *Osx^{Cre}Ebf2$^{fl/fl}$* n=5, p=0.009).

Surprisingly, the body weight of *Osx^{Cre}Ebf2$^{fl/fl}$* animals increased rapidly from week four onwards. At the age of ten weeks, the body weight of *Osx^{Cre}Ebf2$^{fl/fl}$* animals had strongly increased and we could not detect a significant difference compared to controls (Figure 16).

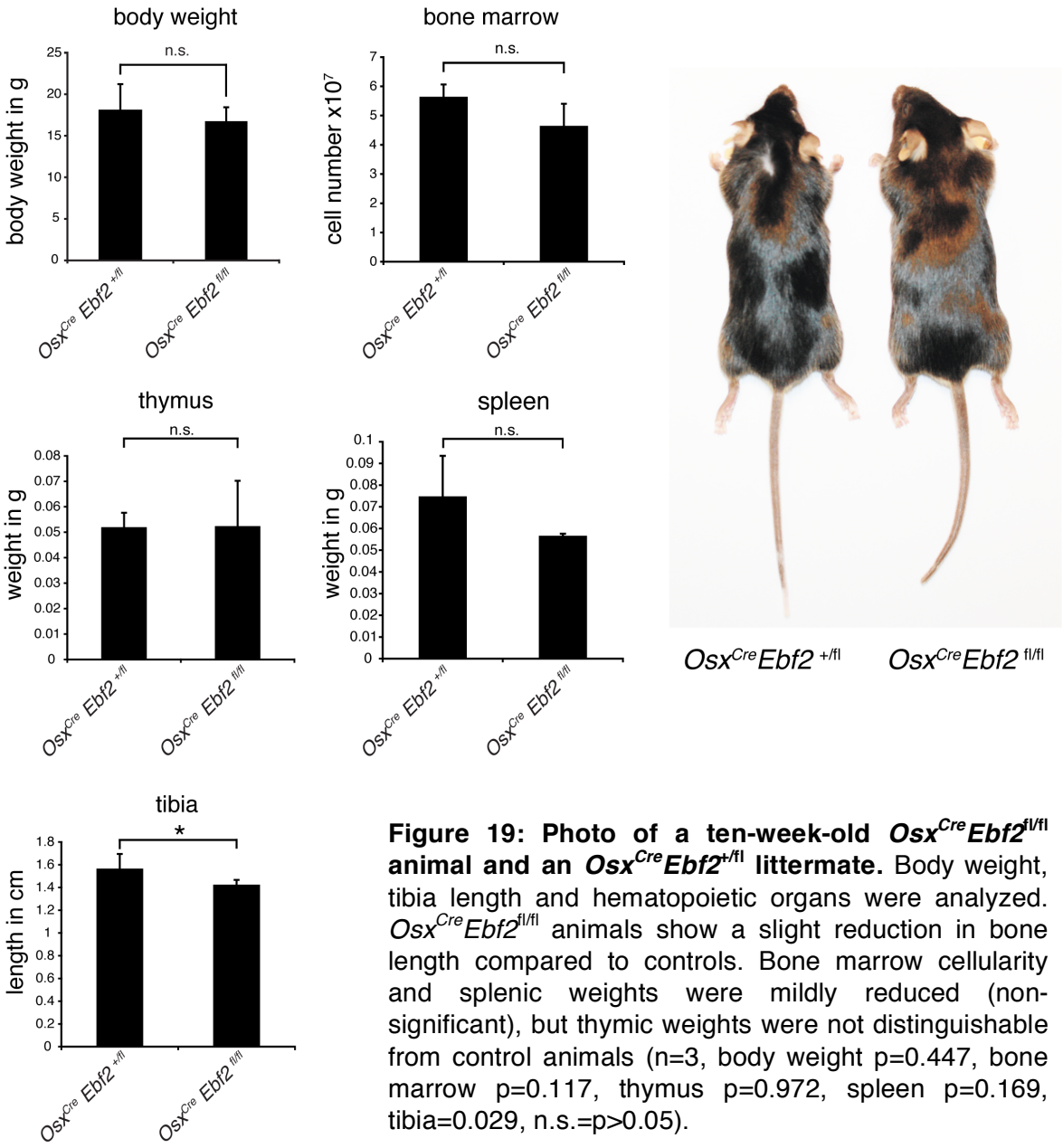

Figure 19: Photo of a ten-week-old *Osx^{Cre}Ebf2$^{fl/fl}$* animal and an *Osx^{Cre}Ebf2$^{+/fl}$* littermate. Body weight, tibia length and hematopoietic organs were analyzed. *Osx^{Cre}Ebf2$^{fl/fl}$* animals show a slight reduction in bone length compared to controls. Bone marrow cellularity and splenic weights were mildly reduced (non-significant), but thymic weights were not distinguishable from control animals (n=3, body weight p=0.447, bone marrow p=0.117, thymus p=0.972, spleen p=0.169, tibia=0.029, n.s.=p>0.05).

When the weight of hematopoietic organs from ten-week-old mice was determined, a slight reduction in spleen size was detected, but thymic weight was found to be normal (Figure 19). The bone marrow cellularity was slightly reduced (non-significant). Further, long bones from *Osx^{Cre}Ebf2$^{fl/fl}$* animals were shorter (10%). Investigation of the stem cell compartment by FACS showed no reduction in KSL frequency (Figure 20).

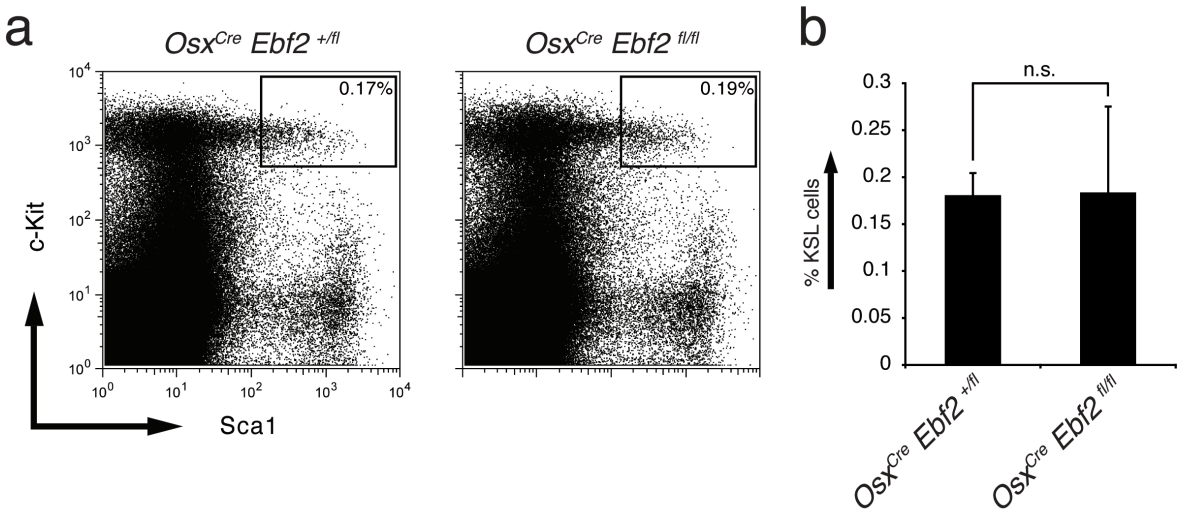

Figure 20: *Osx*^{Cre}-mediated deletion of *Ebf2* in osteoblasts does not result in decreased KSL frequencies in ten-week-old animals. (a) Total bone marrow of ten-week-old *Osx*^{Cre}*Ebf2*$^{fl/fl}$ and control animals was analyzed by flow cytometry. Lymphocytes were gated as living cells (PI$^-$), lineage marker negative (Lin$^-$) and were analyzed for the expression of Sca1 and c-Kit. Frequencies of KSL cells in the indicated gate were not reduced as shown in the diagramm (b), (n=3, p=0.958, n.s.=p>0.05).

4.1.9 DNA microarray analysis of IEO-*Ebf2*$^{+/-}$ and IEO-*Ebf2*$^{-/-}$ cells

Ebf2 is strongly expressed in adipose tissue. We and others speculated that *Ebf2* may be essential for steady state metabolic processes in fat cells. Loss of *Ebf2* in this tissue is most likely the reason why *Ebf2*-deficient mice display dwarfism and show a strong reduction in body weight (Corradi et al., 2003). When we combined newly generated *Ebf2*$^{fl/fl}$ mice with *AP2*^{Cre} and *Osx*^{Cre} transgenic mice we expected *AP2*^{Cre}*Ebf2*$^{fl/fl}$ animals to recapitulate the body weight phenotype but *AP2*^{Cre}*Ebf2*$^{fl/fl}$ animals had unchanged weights compared to control animals. Intriguingly, juvenile *Osx*^{Cre}*Ebf2*$^{fl/fl}$ mice had reduced body weight but almost fully recovered from this reduction until the age of ten weeks. This observation links early mouse developmental processes to the transcription factor *Ebf2* expressed in osteoblasts.

To gain a better understanding of the observed phenotype in *Osx*^{Cre}*Ebf2*$^{fl/fl}$ animals, the gene expression profiles of IEO-*Ebf2*$^{+/-}$ and IEO-*Ebf2*$^{-/-}$ bone marrow stromal cells were compared by DNA microarray analysis. Osteoblastic cell fractions were isolated from *Ebf2-Gfp*$^{+/-}$ and *Ebf2-Gfp*$^{-/-}$ embryos at the developmental stage E18.5 and Gfp positive IEO (**I**mmature ***E****bf2*-expressing **O**steoblastic) cells were FACS sorted into trizol (sorting scheme and information on breeding procedures are shown in supplementary Figure S4). Prior to amplification and labeling of total RNA samples, an aliquot was run on a bioanalyzer for quality control. Finally, six samples of each genotype with high

RNA quality were amplified, labeled, hybridized and scanned using an Illumina DNA microarray plattform. The top 100 downregulated genes detected in IEO-*Ebf2*$^{-/-}$ cells compared to IEO-*Ebf2*$^{+/-}$ cells are shown in table S 2. The complete list of deregulated genes can be found on the CD provided with this thesis.

4.1.10 Characterization of *Ebf2*-expressing thymic stromal cells

In the thymus, *Ebf2* is expressed by a small stromal cell population at the boundary between cortex and medulla (Kieslinger et al., 2010). Nature and function of these cells is still unknown. Due to the strong decrease in thymic cellularity detected in *Ebf2*-deficient mice, these cells might have a functional role in homing and support of bone marrow derived common lymphoid progenitors (CLPs) in the thymus. In order to investigate which thymic stromal cells express *Ebf2*, single cell preparations from minced and collagenase/dispase digested thymi were analyzed by FACS. As beta-galactosidase does not fluoresce, it cannot directly be detected in FACS. Therefore, *Ebf2-Gfp* mice were used to characterize *Ebf2*-expressing thymic stromal cells. *Ebf2-Gfp*$^{-/-}$ animals were shown to have the same stem cell phenotype as published by Grosschedl and colleagues (Hiechinger, S., 2010) and fully recapitulate the phenotype of the *Ebf2-LacZ* mutation (Wang et al., 2004, own observation).

Thymi from *Ebf2-Gfp*$^{+/+}$ and *Ebf2-Gfp*$^{+/-}$ animals were isolated and single cell suspensions were stained with antibodies to identify stromal cell populations that express *Ebf2-Gfp*. DAPI was added to exclude dead cells. (1) Non-epithelial cells were identified as CD45^{-}G8.8^{-}Ly51^{-}. Amongst this population a fraction of cells expresses *Ebf2-Gfp*. (2) cTECs were identified as CD45^{-}G8.8^{int}Ly51^{+} and showed no *Ebf2-Gfp* expression. However, we identified *Ebf2*-expressing cells among the (3) mature mTEC population which was identified as CD45^{-}G8.8^{+}Ly51^{-}CD80^{high}. Hence, *Ebf2-Gfp* is expressed in a fraction of mature mTECs (Figure 21).

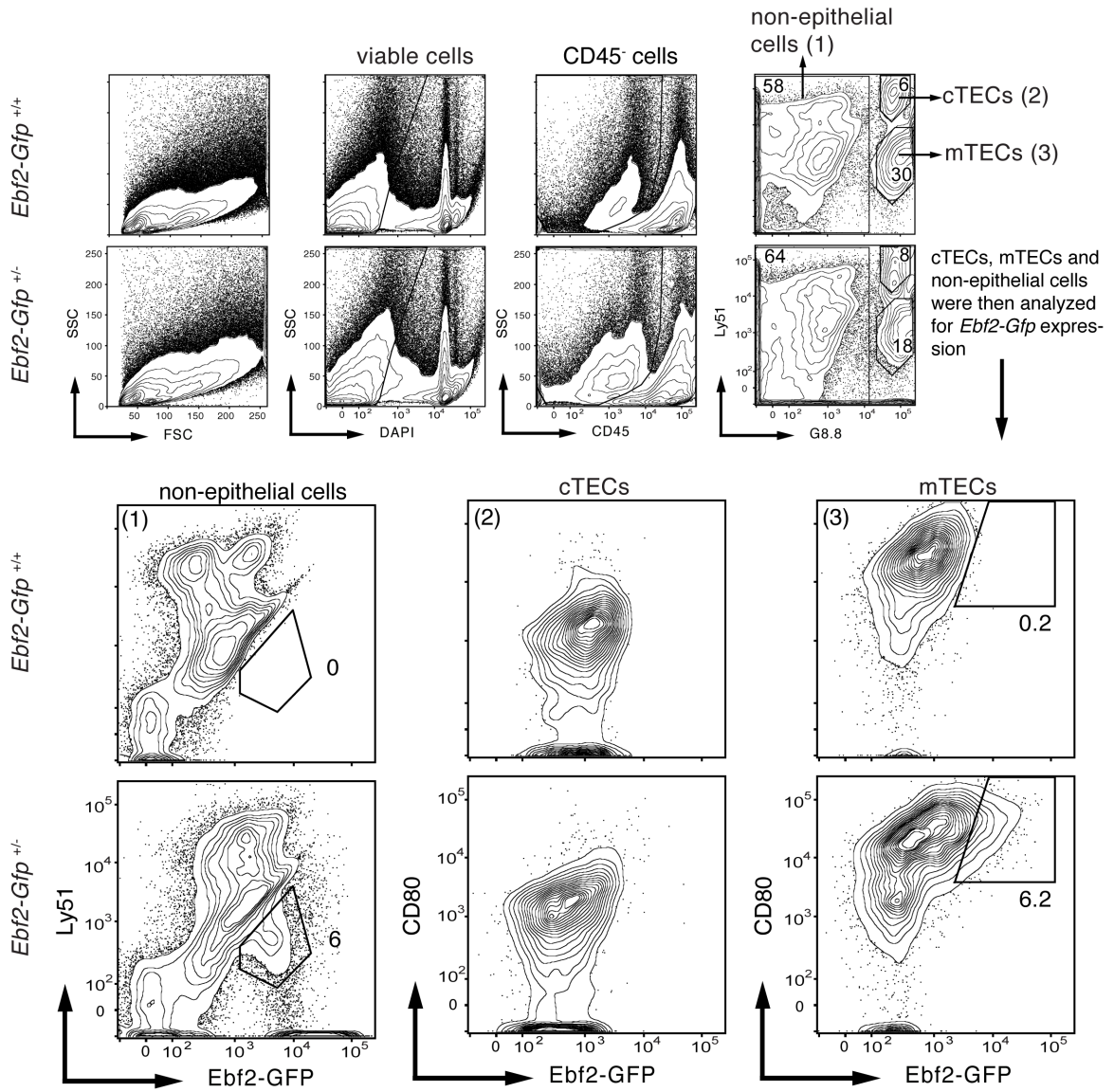

Figure 21: *Ebf2* is expressed by mature CD80$^+$ mTECs and a population of non-epithelial cells. Cells were gated for living cells (DAPI$^-$) and non-hematopoietic cells (CD45$^-$). Next, cells were analyzed for Ly51 and G8.8 expression. (1) non-epithelial cells, (2) cTECs and (3) mTECs were identified and separately analyzed further. (1) A fraction of non-epithelial cells expresses *Ebf2*. (2) cTECs do not express *Ebf2*. (3) Within the mTEC population a fraction of mature mTECs expresses *Ebf2*.

For a more in-depth analysis of the *Ebf2*-expressing cell population, markers for endothelial cells (CD31), subcapsular epithelial cells (gp38) and MTS15$^+$ fibroblasts (MTS15) were tested in thymic cell preparations from *Ebf2-Gfp*$^{+/+}$ and *Ebf2-Gfp*$^{+/-}$ animals. While *Ebf2* is not co-expressed with CD31 and gp38 (data not shown) a population of MTS15/Gfp double positive cells could be identified (Figure 22). Digested thymi were stained with DAPI, CD45, G8.8 and MTS15. To exclude dead and hematopoietic cells, gates on DAPI$^-$ and CD45$^-$ cells were set (not shown). Living stromal cells were then analyzed for G8.8 expression. Non-epithelial cells were then examined for expression of MTS15 and Ebf2-Gfp and a

population of double positive cells was identified. Hence, *Ebf2* is expressed in MTS15$^+$ mesenchymal fibroblasts (Figure 22).

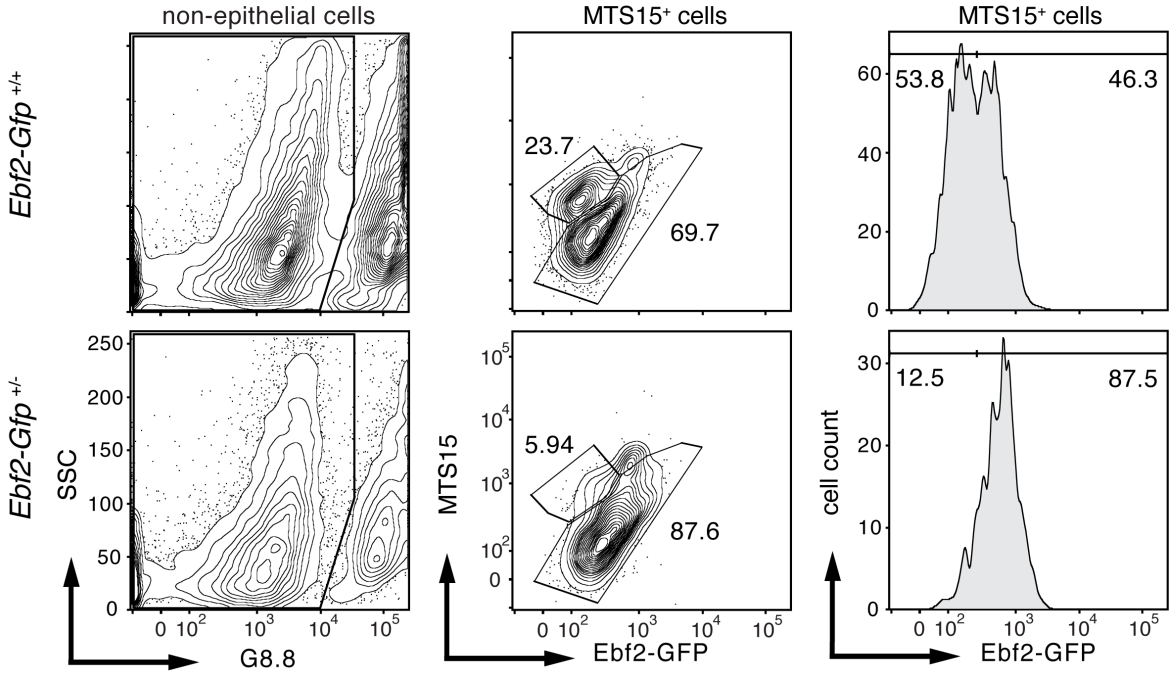

Figure 22: *Ebf2*-expressing cells are positive for the fibroblast marker MTS15. To exclude dead and hematopoietic cells a gate for DAPI$^-$ and CD45$^-$ cells was set (not shown). To gate out epithelial cells (mTECs and cTECs) a gate on G8.8 negative cells was set. Finally, cells were analyzed for *Ebf2* and MTS15. Within the MTS15 positive cells, a population of *Ebf2*-expressing Gfp positive cells shifts on the x-axis. The histogram shows that a fraction of MTS15$^+$ cells is also Gfp positive.

4.1.11 *Ebf2* in T cell development

Ebf2 is strongly expressed in thymic stromal cells and *Ebf2-LacZ*$^{-/-}$ animals show a strong decrease in thymus cellularity (Kieslinger et al., 2010). Since a distinct population of *Ebf2*-expressing mTECs and MTS15$^+$ fibroblasts was identified, we addressed the question, whether loss of *Ebf2* in thymic stromal cells affects T cell development. Therefore, the T cell profile of *Ebf2-Gfp* animals was analyzed. Investigating two to three-week-old *Ebf2-Gfp*$^{-/-}$ animals, we observed the same reduction in thymic cellularity as was published for *Ebf2-LacZ*$^{-/-}$ mice (Kieslinger et al., 2010; data not shown). A more in-depth analysis of the T cell profile, looking specifically at the percentage composition of DN, DP, CD4$^+$ and CD8$^+$ T cells, revealed a 1.6-fold reduction in the CD4$^+$ single positive T cell compartment (Figure 23).

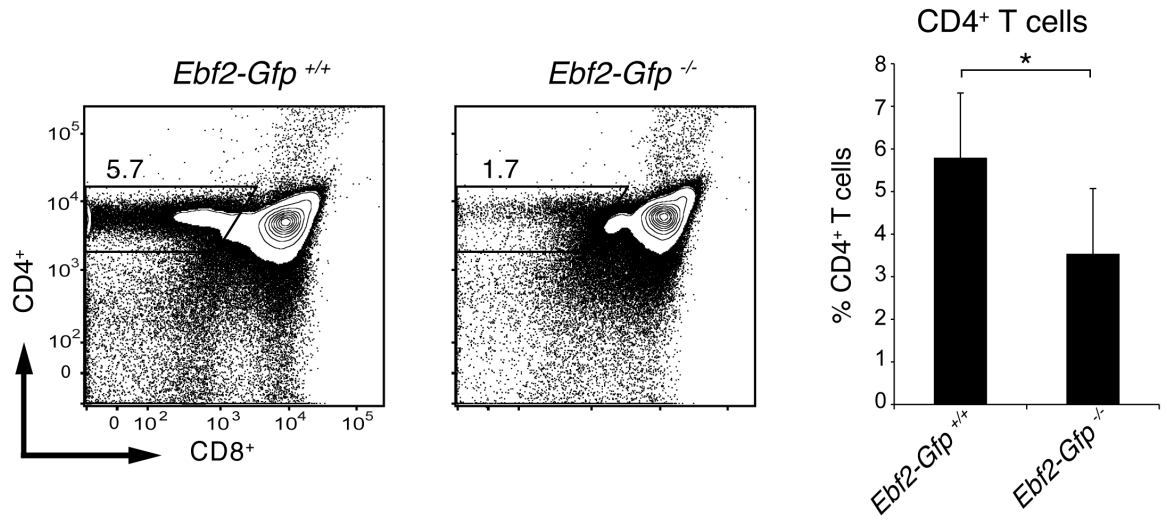

Figure 23: *Ebf2*-deficient animals show a reduction in CD4$^+$ T cells. Cells were pre-gated on DAPI$^-$ lymphocytes. Cells were then analyzed for expression of CD4 and CD8 as shown and CD4$^+$ T cells were found to be reduced 1.6-fold (n=4, p=0.05).

Since *Ebf2* is not expressed in hematopoietic cells as previously reported (Kieslinger et al., 2005, data not shown), *Ebf2*-expressing stromal cells might be important regulators of T cell proliferation, maturation and differentiation. To exclude secondary effects of *Ebf2*-deficiency, resulting in a bad health condition or defects in other organs, transplantation experiments of thymic embryonic lobes from *Ebf2-Gfp*$^{+/+}$, *Ebf2-Gfp*$^{+/-}$ (heterozygous mice are not distinguishable from wild type mice and were therefore used as controls) and *Ebf2-Gfp*$^{-/-}$ into wild type recipients were performed.

Thymic embryonic lobes (E14.5) were isolated and cultured in complete IMDM medium supplemented with deoxyguanosine. This nucleotide analogon is incorporated into the DNA of rapidly replicating cells (hematopoietic cells) thereby killing them, while slowly replicating cells (stromal cells) remain unaffected. Thereafter, lobes were transplanted under the kidney capsule of six-week-old congenic wild type recipients (Figure 24).

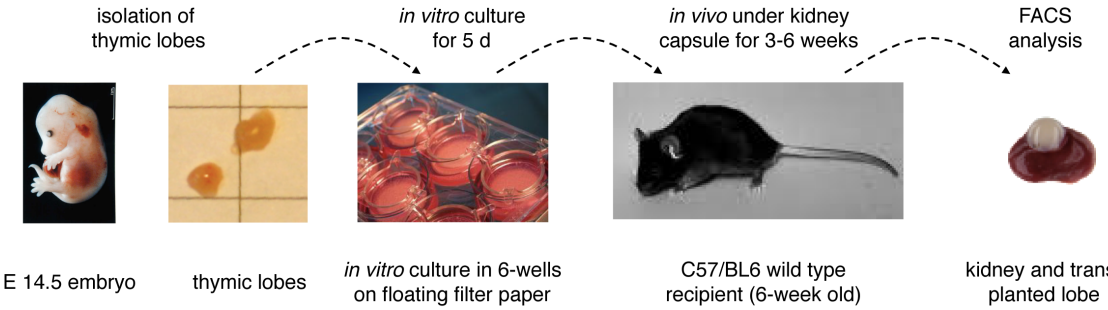

Figure 24: Schematics showing the experimental design of transplantation experiments. Embryonic lobes were isolated from E14.5 embryos and cultured on floating filter paper in complete IMDM medium supplemented with deoxyguanosine for five days. Thereafter, lobes were transplanted under the kidney capsule of C57/BL6 wild type recipients. Three and six weeks later, lobes were isolated and analyzed by FACS.

Host derived wild type CLPs repopulated the *Ebf2-Gfp*$^{-/-}$, *Ebf2-Gfp*$^{+/-}$ and *Ebf2-Gfp*$^{+/+}$ lobes and T cells were analyzed at three and six weeks after transplantation to study T cell development at different time points. The results of these experiments are shown in Figure 25. CD8^{+}, DN and DP T cell populations were found unaltered compared to control animals. The frequency of CD4^{+} T cells was also found unchanged at three and six weeks after transplantation. In summary, the reduction in thymus cellularity and CD4^{+} T cells is not transplantable.

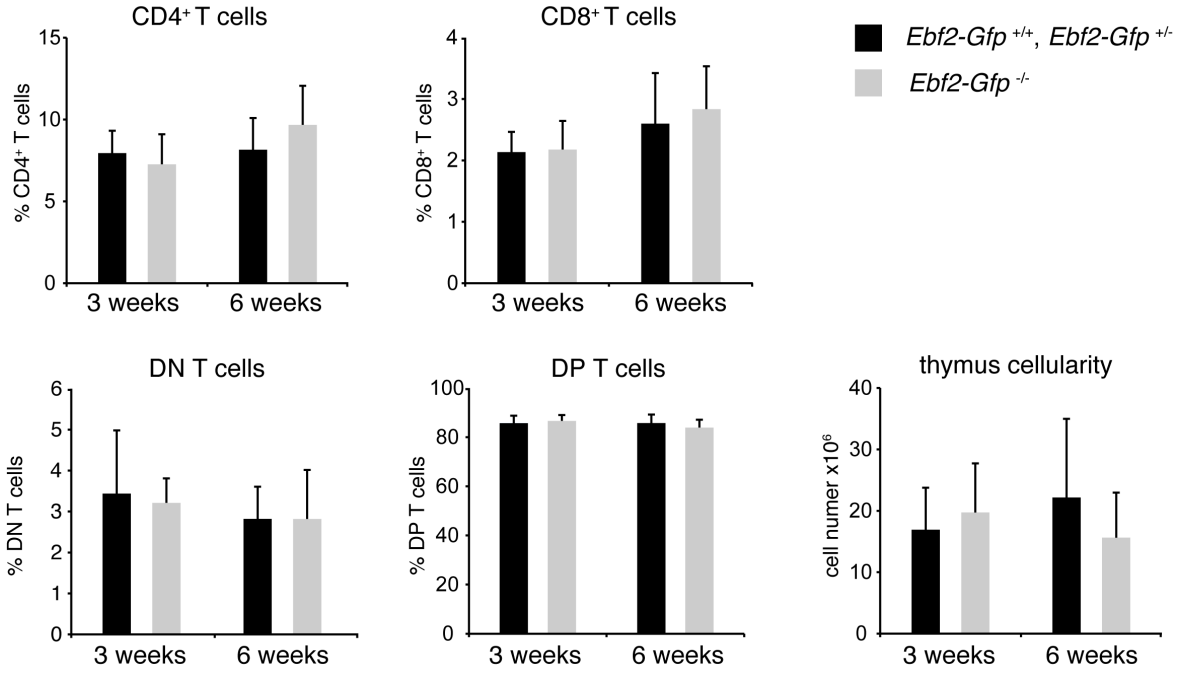

Figure 25: T cell development in transplanted *Ebf2*$^{-/-}$ thymic lobes is unchanged. Three and six weeks post transplantation thymic lobes were isolated and analyzed. The total cellularity was found unaltered. The percentage of CD4^{+}, CD8^{+}, DN and DP thymocytes in *Ebf2*$^{-/-}$ lobes is unchanged compared to controls (three weeks: wt n=7, *Ebf2*$^{-/-}$ n=10, six weeks: wt n=10, *Ebf2*$^{-/-}$ n=10, p=n.s. for all bar charts shown).

4.2 *Ebf2* in malignant hematopoiesis

IEO cells support HSCs *in vitro* in an *Ebf2*-dependent manner (Kieslinger et al., 2010). In view of the fact that the existence of CSCs was functionally proven in 1997 (Bonnet and Dick, 1997), we investigated a potential role of *Ebf2* in the maintenance of malignant B cells. Therefore, *in vitro* co-culture experiments were established and human B-CLL and B-ALL cells were co-cultured and analyzed by FACS or *in vivo* after transplantation into immunocompromised mice.

4.2.1 The support of B-CLL cells is influenced by *Ebf2*

Human B-CLL samples were taken from peripheral blood of patients, depleted for CD2/CD14 expressing cells (T cells, NK cells, macrophages, neutrophils and dendritic cells, frozen samples were provided by I. Ringshausen, TUM) and were seeded on different feeder layers. To characterize subtypes of B-CLL cells in the context of *Ebf2*, the patient samples used varied regarding their ZAP-70 status. Figure 26 shows the experimental setup.

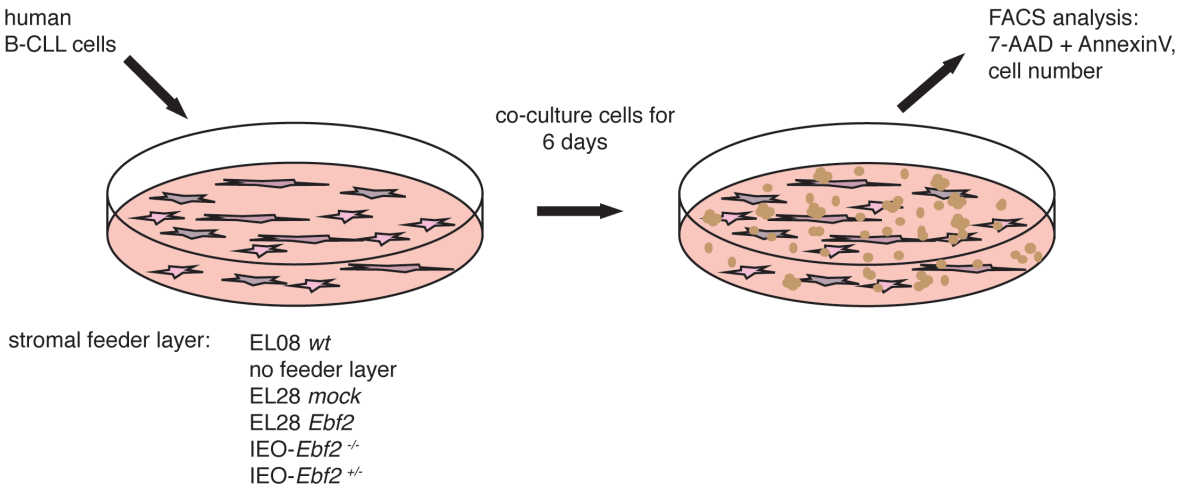

Figure 26: Schematic showing the experimental design of co-culture experiments. Human B-CLL cells were co-cultured on different stromal feeder layers for six days. Thereafter, cells were collected, stained with 7-AAD and AnnexinV and analyzed by FACS.

The stromal cell lines EL08 and EL28 were isolated from the mouse aorta gonad mesonephros (AGM) region. Single cell clones were characterized regarding their capacity to maintain HSCs *in vitro*. While EL08 cells maintain HSCs *in vitro* for weeks, their counterpart EL28 does not carry this potential (Oostendorp et al.,

2005). The same cell lines were characterized regarding their capacity to support human B-CLL cells. Interestingly, EL08 cells provide a better support than EL28 cells, as was determined by lower apoptotic rates in co-cultures (Ingo Ringshausen, personal communication). Therefore, these cell lines served as positive and negative control. Due to reports that feeder cell line mediated support of HSCs correlates with the expression of Ebf proteins (Kieslinger et al., 2010), RNA levels of *Ebf1*, *Ebf2* and *Ebf3* in EL08 and EL28 cells were compared by quantitative real time PCR. Expression levels of *Ebf1, 2* and *3* are at least 16-fold higher in the supporting EL08 cells than in non-supporting EL28 cells (Figure 27a). To investigate the importance of *Ebf2*, a gain of function experiment was carried out. EL28 cells were transduced with an *Ebf2-IRES-Gfp* or *mock-IRES-Gfp* (empty vector control) retrovirus to overexpress *Ebf2*. Any gain or loss of support in EL28 *Ebf2* cells compared to EL28 *mock* cells for human B-CLL cells would be mediated by *Ebf2*. Figure 27b shows successfully infected and non-infected control cells detected by FACS. Ebf2 protein levels in EL28 *Ebf2* compared to EL28 *mock* were analyzed by western blot (Figure 27c).

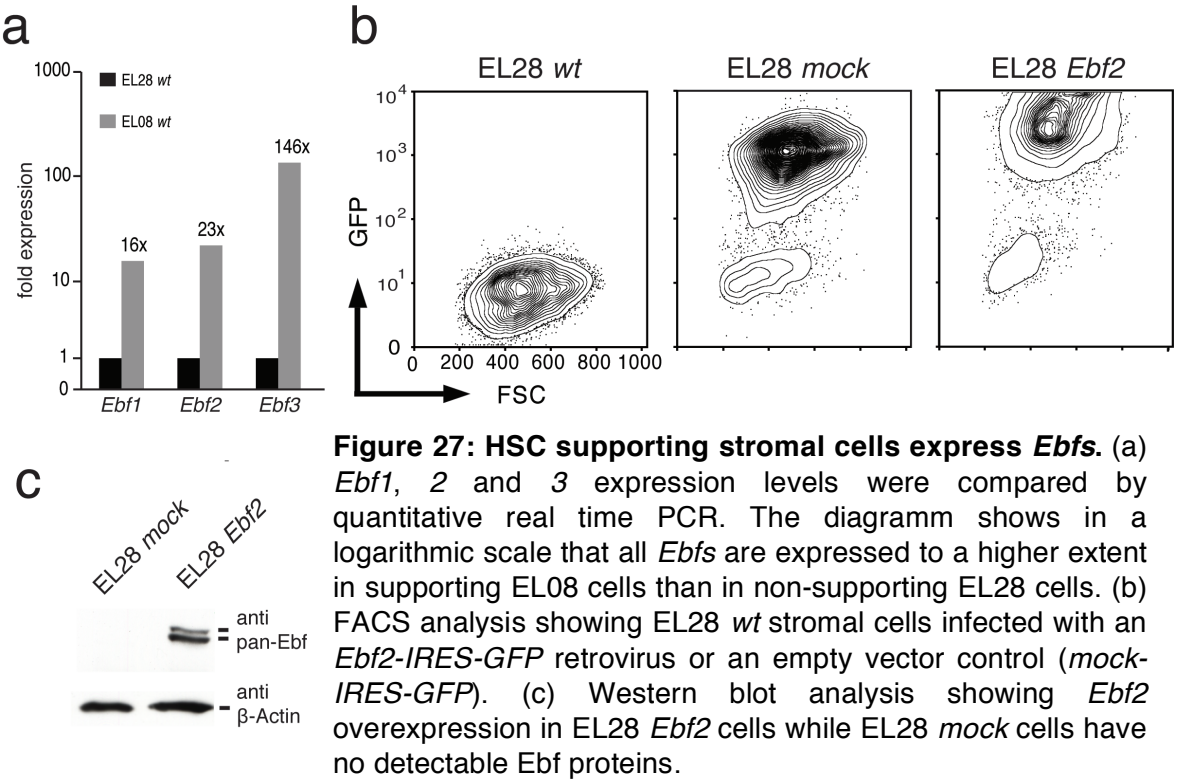

Figure 27: HSC supporting stromal cells express *Ebfs*. (a) *Ebf1*, *2* and *3* expression levels were compared by quantitative real time PCR. The diagramm shows in a logarithmic scale that all *Ebfs* are expressed to a higher extent in supporting EL08 cells than in non-supporting EL28 cells. (b) FACS analysis showing EL28 *wt* stromal cells infected with an *Ebf2-IRES-GFP* retrovirus or an empty vector control (*mock-IRES-GFP*). (c) Western blot analysis showing *Ebf2* overexpression in EL28 *Ebf2* cells while EL28 *mock* cells have no detectable Ebf proteins.

Malignant B-CLL cells were cultured on EL08 *wt*, EL28 *mock* and EL28 *Ebf2* transduced feeder layers. In parallel, B-CLL cells were cultured on mouse IEO cells isolated from *Ebf2-Gfp*$^{+/-}$ and *Ebf2-Gfp*$^{-/-}$ mice. Hence, a gain of function and a loss of function approach are tested simultaneously. With this experimental

setup any support mediated by *Ebf2* should increase cell survival in EL28 *Ebf2* over EL28 *mock*, while at the same time the level of support mediated by IEO-*Ebf2*$^{-/-}$ cells compared to IEO-*Ebf2*$^{+/-}$ should decline.

To determine the number of viable B-CLL cells after six days of co-culture, a quantitative FACS analysis using accucheck counting beads (Invitrogen) was established. A known volume of beads (type A and B beads) was added to a known volume of resuspended cells. When counting the beads along with cells, their numbers can be related. Furthermore, the beads contain two different fluorospheres in a known proportion. The accuracy of a measurement can therefore be determined by relating the counts for beads A and B. At the end of a co-culture experiment, all cells were harvested and transfered to FACS tubes for washing and staining. For analysis, beads were added and samples were measured by FACS. FSC/SSC were adjusted to have three separate populations: (1) FACS counting beads of type A and B in the upper left. (2) B-CLL cells in the lower center and (3) the majority of feeder cells scattered from center to the upper right (Figure 28).

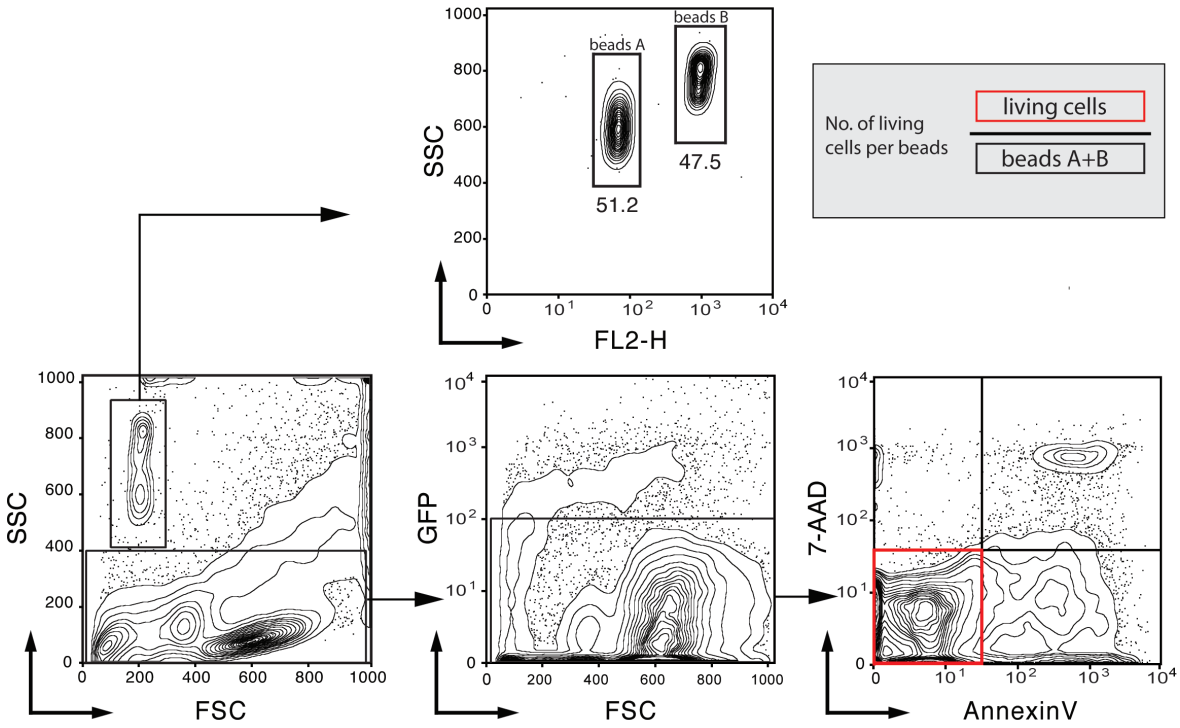

Figure 28: Gating scheme and experimental design to quantify the number of viable B-CLL cells after six days of co-culture by FACS analysis. In FSC/SCC a gate was set on FACS counting beads and a second gate on lymphocytes. Accuracy of the measurement was controlled by analysis of the ratio of the fluorescent beads A and B in

FL2/SSC. Gfp^+ feeder cells were excluded and Gfp^- lymphoid cells were analyzed with 7-AAD and AnnexinV. The ratio between viable cells and beads was calculated as shown.

To determine the number of FACS beads, they were gated and analyzed in SSC/FL2-H. The events counted within the gates for beads A and B were aggregated. For analysis of viable B-CLL cells a gate on lymphoid cells was set. To exclude Gfp-positive feeder cells a gate on Gfp-negative B-CLL cells was set. Finally, B-CLL cells were analyzed for AnnexinV (apoptotic cells) and 7-AAD (dead cells) and the events for living cells in the lower left quadrant were counted (Figure 28).

Figure 29 gives an overview on one representative experiment (patient sample V261), which was analyzed after six days of co-culture on the following feeder layers:

(1) EL08 served as a positive control
(2) No feeder layer served as negative control
(3) EL28 *mock* are transduced with an empty vector and served as control for EL28 *Ebf2* transduced cells
(4) EL28 *Ebf2* cells overexpress *Ebf2*
(5) IEO-*Ebf2*$^{-/-}$ cells represent stromal cells deleted for *Ebf2*
(6) IEO-*Ebf2*$^{+/-}$ cells represent stromal cells which express *Ebf2*

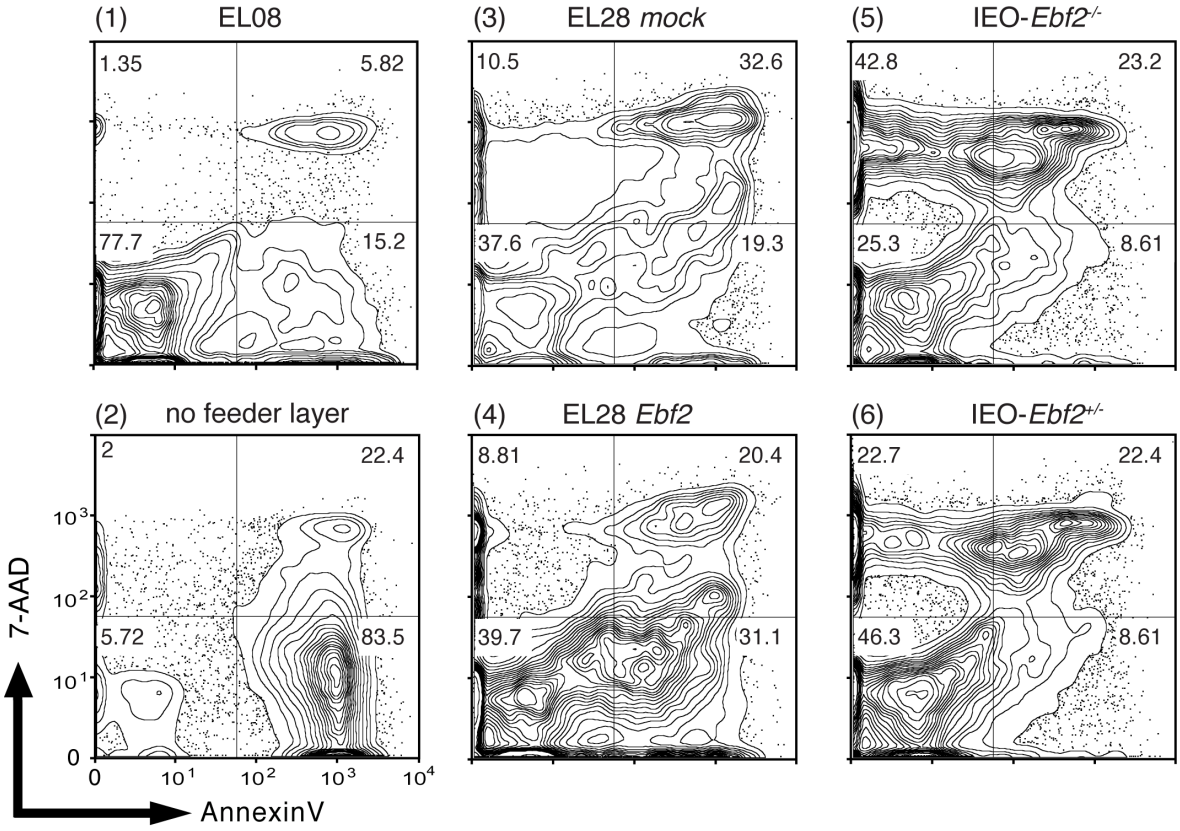

Figure 29: Representative analysis of co-cultered lymphocytes after six days under different conditions. EL08 cells and no feeder layer served as positive and negative control in co-culture experiments. EL28 feeder cells were transduced with an empty vector control (EL28 *mock*) and an Ebf2 encoding virus (EL28 *Ebf2*). Mouse stromal IEO-*Ebf2*$^{+/-}$ and IEO-*Ebf2*$^{-/-}$ cells were compared to determine the relevance of *Ebf2*. Events counted in the lower left quadrant are 7-AAD and AnnexinV negative and therefore considered viable cells.

To detect *Ebf2*-mediated support, the ratio between beads and the number of living cells after six days of co-culture was determined. Finally, the measured values were normalized and then compared: EL28 *Ebf2* was normalized to EL28 *mock* and IEO-*Ebf2*$^{-/-}$ values were normalized to IEO-*Ebf2*$^{+/-}$.

A summarizing overview on the eight patient samples tested is given in Figure 30. The detected effects are shown in percent change after normalization. Overall, three out of eight samples showed a significant response to *Ebf2* expression. Sample V 261 responded to *Ebf2* under both experimental conditions. Overexpression of *Ebf2* led to a significant increase in B-CLL cell survival (20% more viable cells) while the loss of *Ebf2* in IEO$^{-/-}$ cells resulted in 50% fewer living B-CLL cells in comparison to IEO$^{+/-}$ cells. Patient sample V 128 behaved in a similar way. We detected 20% more viable cells upon overexpression of *Ebf2* in EL28 *Ebf2* cells compared to EL28 *mock* while the loss of *Ebf2* in IEO cells resulted in a significant decrease in feeder layer-mediated support (30% fewer

living cells on IEO$^{-/-}$ cells compared to IEO$^{+/-}$ cells). A similar trend was observed for sample P 27. Finally, we detected significantly fewer living cells for patient sample D 14 when cultured on IEO$^{-/-}$ cells compared to IEO$^{+/-}$ cells. However, this sample did not respond to overexpression of *Ebf2* in EL28 *Ebf2* compared to EL28 *mock*. Out of the eight samples tested, only V 147 patient cells showed slightly increased survival in the absence of *Ebf2* (non-significant). These results show that *Ebf2* can influence the survival of B-CLL cells. However, the ZAP70-status could not be correlated with *Ebf2*-mediated support.

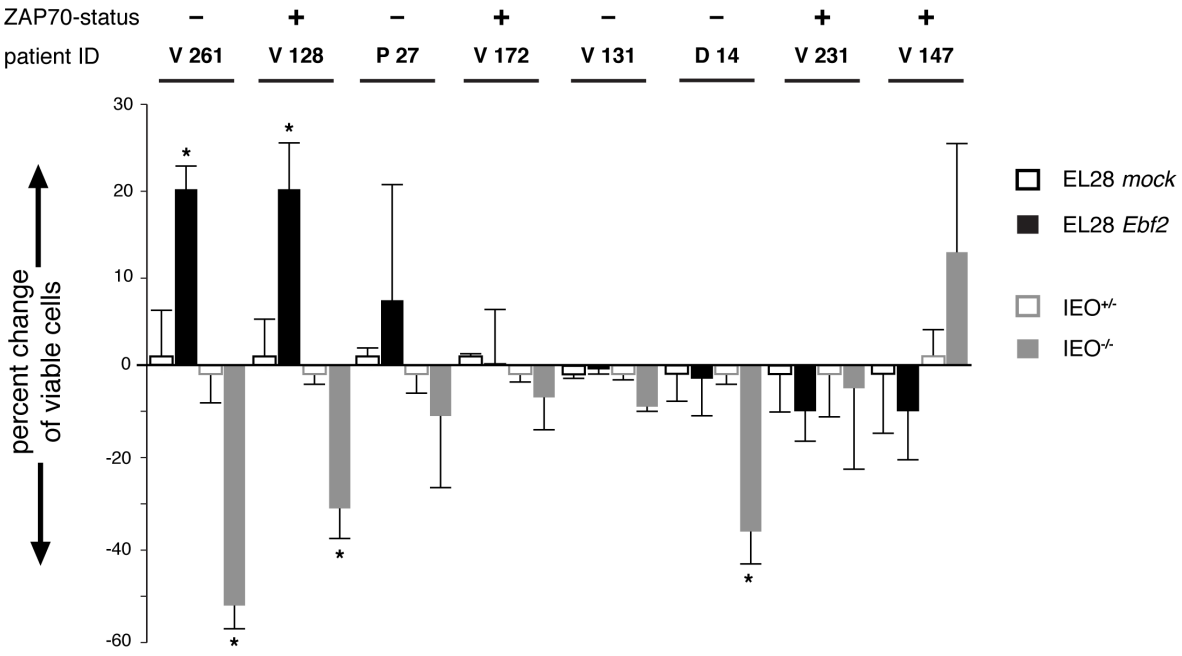

Figure 30: Increased survival of human B-CLL cells cultured on *Ebf2*-expressing stromal cells. A group of eight human patient samples with differing ZAP70-status were co-cultured for six days on mouse primary IEO-*Ebf2*$^{+/-}$ and IEO-*Ebf2*$^{-/-}$ cells as well as on *Ebf2* over-expressing and control cells (EL28 *mock*). Columns show percent change of viable B-CLL cells on *Ebf2*-expressing feeder layers relative to control cell feeder layers (significant changes (p=<0.05) are indicated with asterisks).

4.2.2 IEO cells support B-ALL CSCs *in vitro*

B-ALL is highly invasive and characterized by quickly proliferating cells. In co-culture experiments we addressed the question, whether the CSC frequency in a given B-ALL patient sample can be altered in an *Ebf2*-dependent manner. We isolated bone marrow stromal cells from *Ebf2-Gfp*$^{+/-}$ animals and sorted two cell populations: (1) bone marrow stromal cells depleted for *Ebf2*-expressing niche cells (non-IEO) and (2) *Ebf2*-expressing niche cells (IEO). These two cell

populations were cultured *in vitro* until 80% confluency was reached. Transgenic human B-ALL cells were isolated directly from the spleen of leukemic mice, counted and seeded on top of the different feeder layers. Transgenic human B-ALL cells were generated by transducing primary human B-ALL patient cells with a *Gaussia luciferase-IRES-Gfp* encoding adenovirus. After transduction the cells were injected into immunodeficient mice. Upon signs of sickness the animals were sacrificed and human B-ALL cells were isolated from the spleen and analyzed for *Gfp*-expression by FACS. Gfp-positive transgenic human B-ALL cells were then FACS-sorted and re-injected into mice. This procedure was repeated until 96-99% of the cells isolated from the spleen of a leukemic mouse were Gfp-positive. Sample P199 was generated in this way and $1x10^7$ cells were seeded on IEO and non-IEO feeder layers. After 30 days *in vitro*, B-ALL cells were harvested and counted. The number of B-ALL cells on non-IEO cells was roughly unchanged compared to the number initially seeded, while we detected a modest reduction (20%) on IEO cells. Next, the cells were washed, resuspended in PBS and injected into immunodeficient mice at different concentrations (Figure 31).

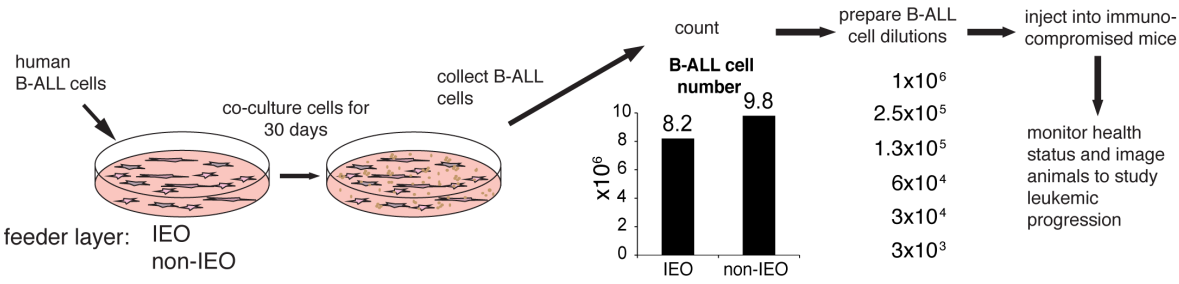

Figure 31: Outline of the experiment performed. FACS sorted IEO and non-IEO cells were co-cultured with human B-ALL patient cells for 30 days *in vitro*. Thereafter, cells were counted, prepared in limiting dilutions and injected into mice.

Engraftment and development of leukemic cells was then followed over time by imaging the animals with a CCD camera. Therefore, the animals were narcotized and injected with native coelenterazine and imaged on day 11, 21 and 34 post injection of leukemic cells. Coelenterazine serves as a substrate for Gaussia luciferase, which is expressed by the human B-ALL cells due to the stable integration of the *gaussia luciferase* encoding adenovirus. The chemiluminescence reaction can be detected with a CCD camera and signal intensities correlate with cell number (Figure 32). Animals who had received the highest dose of leukemic cells were detectably engrafted already 11 days after injection. In these mice, the

B-ALL cells engrafted femur and tibia first (scattered/weak signal from the thorax region is unspecific signal from the liver).

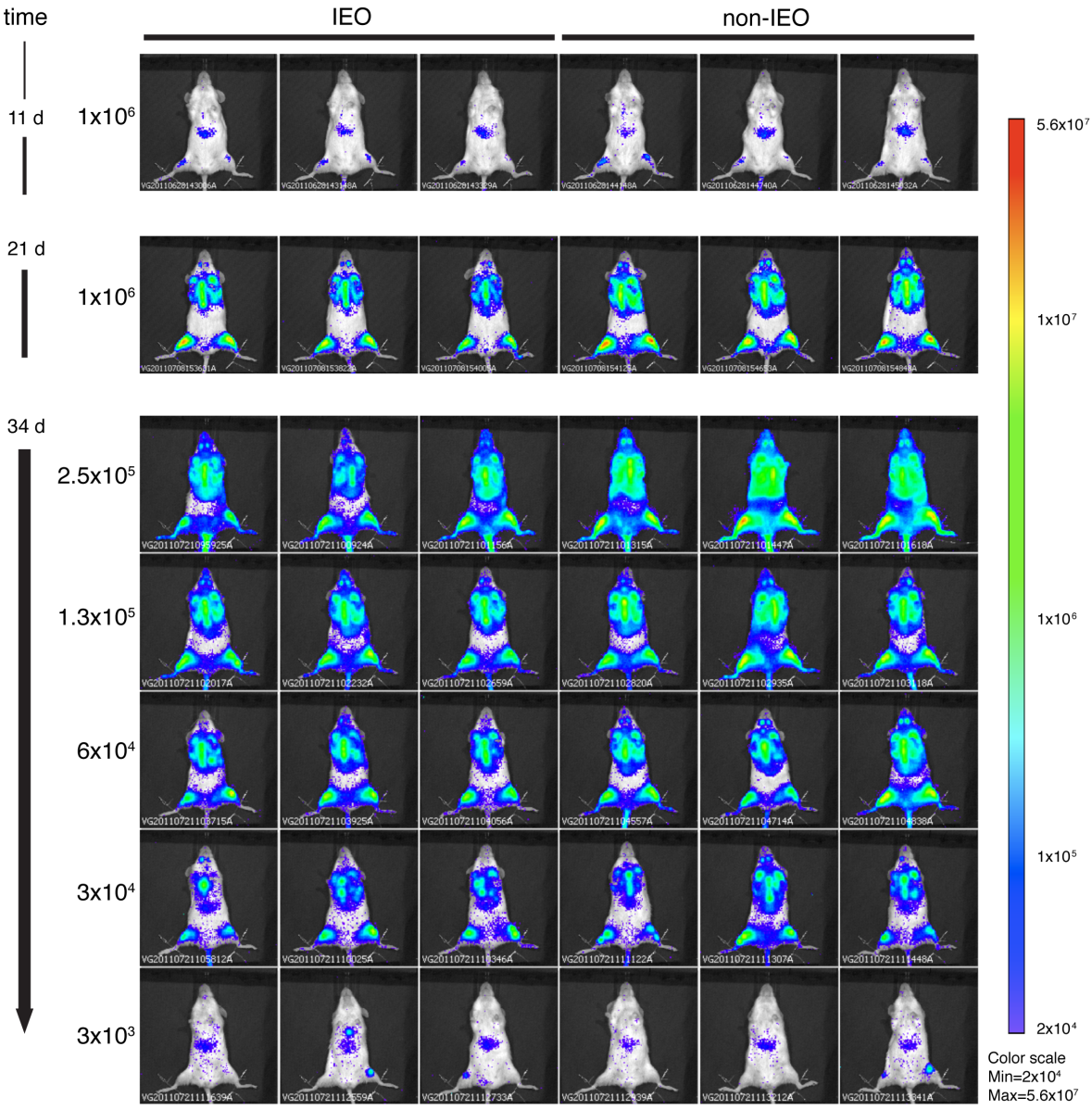

Figure 32: IEO and non-IEO cells maintain human B-ALL CSCs for at least 30 days *in vitro*. Mice were imaged 11, 21 and 34 days post injection. On day 11, only mice who had received 1x10^6 leukemic cells were engrafted. 21 days after injection, animals of that group were full with leukemic cells and were sacrificed shortly after. 34 days post injection mice within all groups were engrafted. The pattern of engraftment always followed the same order: femur/tibia, sternum, lung/axillary lymph nodes and last in cervical lymph nodes.

At 21 days, the leukemic cells in these mice had spread and infiltrated sternum, lungs, cervical and axillary lymph nodes. These animals were sacrificed shortly

after. Mice, which had been injected lower cell numbers, were not detectably engrafted at 11 days post injection (data not shown). At 34 days post injection, only animals, which had been injected the lowest cell number (3000 cells), were not engrafted throughout the experimental animal group. Only two out of three from the IEO group were engrafted, while just one out of three animals from the non-IEO group was detected positive. From these results it can be concluded that it requires about 3000 leukemic cells to successfully transplant the leukemia. Interestingly, the same cell number is at least needed to successfully transplant this human B-ALL patient sample directly from one mouse to another without *in vitro* culture.

In summary, IEO and non-IEO stromal cells maintained B-ALL cells over 30 days *in vitro*. Although the CSC frequency was not altered in an *Ebf2*-dependent manner, the leukemic potential was entirely preserved.

5 Discussion

5.1 Generation of mice with a conditional allele of *Ebf2*

Embryonic stem cell engineering enabeled researchers to study gene function in higher vertebrates. As certain biological processes or diseases are directly linked to single genes, mice deleted in this gene offer a powerful tool to investigate the underlying mechanisms. However, many phenotypes observed in knockout mice may be caused indirectly and result from complex physiological alterations in these mice. This can strongly diminish the conclusions drawn from the data obtained. The deletion of *Ebf2* is a good example because its loss in different organs and tissues results in multiple/complex phenotypes that are probably interconnected. Most obvious is the strong reduction in body weight, which could be caused by an altered metabolism due to loss of *Ebf2* in adipocytes. Deletion of *Ebf2* causes disturbance of neuronal axon migration presumably resulting in a waddling gait and mildly uncoordinated movements. In addition, *Ebf2*-deficient animals display secondary hypogonadism and strongly reduced fertility (Corradi et al., 2003; Wang et al., 2004). Together with the juvenile osteopenia phenotype (Kieslinger et al., 2005) and the observed hematopoietic defects (Kieslinger et al., 2010), *Ebf2*-deficient animals are in a poor health condition, which is reflected by a high postnatal lethality observed amongst $Ebf2^{\Delta fl/\Delta fl}$ offspring (85% died after birth, only

15% reached the age of three weeks (supplementary Figure S5). The study of developmental processes like hematopoiesis or T cell development in these animals harbors risks, because T cell progenitors emerge in the bone marrow but differentiate in the thymus. Therefore, alterations observed in the thymus may originate from the bone marrow.

In conclusion, *Ebf2* conditional knockout animals were generated for the following reasons: (1) the deletion of *Ebf2* can be restricted to hematopoietic organs, (2) *Ebf2*-mediated niche function for HSCs might be associated to a certain stromal subpopulation, and (3) if so, these mice shall be used to study malignant hematopoiesis *in vivo* (this is not possible in *Ebf2*-deficient animals, because they die from irradiation which is mandatory for transplantation experiments; personal communication Matthias Kieslinger). Furthermore, by use of certain Cre lines (e.g. inducible systems), *Ebf2* can be deleted tissue specifically and at defined time points.

While many laboratories use the BAC recombineering technology (Warming et al., 2005) to generate their congenic targeting vectors, a PCR based strategy was applied here. The generation of the arms of homology with a high fidelity polymerase using a BAC clone as template was successful and unique restriction sites used for cloning and southern blot analysis were introduced via overhangs on the primers used in the PCR reactions. This approach circumvents constraints concerning endogenous restriction sites and greatly facilitated the design of an applicable southern blot strategy. Amongst all ES clones analyzed, seven scored positive for homologous recombination. This relatively low targeting efficiency was expected from a previous targeting of the same locus, although the constructs used are slightly different (Corradi et al., 2003). As *Ebf2* is not expressed in ES cells (personal communication Silvia Hiechinger, HMGU Munich), the low efficiency most likely results from a closed chromatin structure at the *Ebf2* locus. Of the seven mutant ES cell clones obtained, two Bruce4 and two IDG3.2 that formed uniform colonies with distinct borders and had normal proliferation rates were injected into blastocysts. Surprisingly, male chimeric mice (Bruce4 and IDG3.2 ES cells were generated from male animals) were only obtained from the two Bruce4 ES cell clones. This result was unexpected, because all four ES cell clones formed uniform, rotund colonies with distinct borders. This assessment was independently confirmed by our collaborators who injected the ES cells into blastocysts (personal communication, A. Tasdemir, HMGU Munich). However, at this point in time no conclusions can be drawn whether Bruce4 ES cells should be preferred over IDG3.2, as the number of experiments performed is too low. From breedings of male chimeras with wild type C57/BL6 females, we obtained offspring

with black fur color, which must derive from the injected Bruce4 ES cells. Together with the results obtained from southern blot analysis and genotyping PCR this led us to progress further and we crossed newly generated *Ebf2*$^{+/fl}$ animals with *Del*^{Cre} transgenic mice, which express Cre recombinase in all tissues including the germline. Heterozygous *Ebf2*$^{+/\Delta fl}$ animals were then intercrossed to generate *Ebf2*$^{\Delta fl/\Delta fl}$ mice, which should fully recapitulate the phenotypes observed in *Ebf2-LacZ*$^{-/-}$ animals. We isolated RNA from thymic stromal cells of wild type and *Ebf2*$^{\Delta fl/\Delta fl}$ mice and were not able to amplifiy *Ebf2* transcript on cDNA of *Ebf2*$^{\Delta fl/\Delta fl}$ animals while control reactions were successful. Although we did not analyze whether the chosen strategy led to activation of the NMD pathway, we assume that no truncated protein is expressed. This question could not be addressed experimentally, because an Ebf2 specific antibody is not available.

Ebf2$^{\Delta fl/\Delta fl}$ animals move with a waddling gait, display reductions in body weight, bone size and bone firmness as reported for *Ebf2-LacZ*$^{-/-}$ mice (Corradi et al., 2003; Kieslinger et al., 2005). When we analyzed the hematopoietic system of *Ebf2*$^{\Delta fl/\Delta fl}$ animals, we detected the previously described reduction in total cellularity of hematopoietic organs and KSL frequency for *Ebf2-LacZ*$^{-/-}$ and *Ebf2-Gfp*$^{-/-}$ mice (Hiechinger, S., 2010; Kieslinger et al., 2010). Interestingly, some of the phenotypes observed in *Ebf2*$^{\Delta fl/\Delta fl}$ animals were slightly more severe than previously reported (e.g. KSL frequency and survival rates). In the first publication of *Ebf2-LacZ* animals, no juvenile mortality of *Ebf2*-deficient mice is mentioned (Corradi et al., 2003). In contrast, animals even reached the age of 2 years (personal communication G. G. Consalez, ISR Milan). Interestingly, the ES cells used in the reported gene targeting were derived from the 129Sv mouse strain and although offspring were bred with C57/BL6 animals for five generations, the studies were not performed in a pure genetic background (Corradi et al., 2003). Without control (SNP analysis) it takes about ten generations to achieve a clean genetic background. However, in 2002 *Ebf2-LacZ* mice were transferred to our laboratory and since then are further backcrossed onto a C57/BL6 background. While premature death was rarely observed during first generations of backcrossing (personal communication, Matthias Kieslinger), the frequency increased over the years and we rarely obtain *Ebf2*-deficient animals older than three weeks nowadays (own observation). More or less the same holds true for *Ebf2-Gfp*$^{-/-}$ mice for which R.Reed reported a 25% postnatal lethality rate (Wang et al., 2004). Remarkably, the *Ebf1* deletion is not reported to be lethal neither (Lin and Grosschedl, 1995). However, the chances to obtain an *Ebf1*$^{-/-}$ animal in our laboratory and the laboratory of Harinder Singh (personal communication Chauncey Spooner, Genentech) on a pure C57/BL6 background are dramatically low. Therefore, we speculate that some phenotypes caused by the deletion of *Ebf1*

and *Ebf2* are more severe in a pure C57/BL6 background. As *Ebf2*$^{\Delta fl/\Delta fl}$ animals were generated from pure C57/BL6 ES cells, this might explain the increased reduction in KSL frequency from two- to fourfold (Kieslinger et al., 2010) to the level of roughly sevenfold described here. It has to be mentioned here, though, that the number of animals analyzed was only three. Differences in litter sizes and different levels of parental care may influence the severity of some phenotypes. With regard to the high mortality rate it should also be kept in mind that animals that survived till the age of three weeks were most likely naturally pre-selected for a mild phenotype.

In preparation of stromal cell type specific deletions, we analyzed the phenotype of *Ebf2*$^{fl/fl}$ animals. In this way, the functionality of the conditional allele of *Ebf2* is controlled. *Ebf2*$^{fl/fl}$ animals have unchanged KSL frequencies (data not shown). They are born at the expected Mendelian ratios and they are indistinguishable from wild type littermates. Therefore, we conclude that the introduction of *LoxP* sites does not lead to phenotypic changes.

In summary, the data discussed in this chapter led to the conclusion that we successfully generated mice carrying a conditional allele of *Ebf2* because the phenotypes we observe after complete Cre-mediated deletion, but not before that, are comparable to those described for *Ebf2-LacZ*$^{-/-}$ and *Ebf2-Gfp*$^{-/-}$ mice (Corradi et al., 2003; Kieslinger et al., 2005; Hiechinger, S., 2010; Kieslinger et al., 2010).

Bioinformatic analysis on the mouse genome indicates the presence of cryptic or pseudo *LoxP* sites with a frequency of 1.2 per megabase. Although these sequences are recombined by Cre recombinase with rather low efficiency compared to consensus *LoxP* sites, their recombination can result in DNA damage causing cell death or altered proliferation rates in Cre expressing cells. Therefore, expression of Cre recombinase alone may result in an *in vivo* phenotype (Schmidt-Supprian et al., 2007). Due to these reports on Cre toxicity, we used Cre expressing littermates as controls.

5.2 *Prx*^{Cre} driven deletion of *Ebf2*

Mesenchymal stem cells were shown to constitute an essential component of the HSC niche (Mendez-Ferrer et al., 2010). We used *Prx*^{Cre} transgenic mice to delete *Ebf2* specifically in MSCs for two reasons. First, these analyses provide new insights into the role of *Ebf2* expressed by MSCs and second, the deletion in MSCs serves as a backup for osteoblast and adipocyte specific deletion

experiments because both cell types derive from MSCs. If adipocytes and osteoblasts equally contribute to HSC support in the bone marrow, deletion of *Ebf2* in only one of these cell types may result in a very mild phenotype.

The observation that ten-week-old $Prx^{Cre}Ebf2^{fl/fl}$ animals show a wild type phenotype was very surprising and unexpected. No alterations in body weight, bone size or hematopoietic organs were observed. Prx^{Cre} animals are widely used to study processes of skeletal development involving MSCs, chondrocytes and osteoblasts (Kimura et al., 2010; Seo and Serra, 2007). In the first report on Prx^{Cre} animals, Cre expression was characterized in whole mount stainings using LacZ-reporter animals. Cre expression in E10.5 embryos was detected throughout the limbs, interlimb flanks and craniofacial mesenchyme (Logan et al., 2002). We concluded that Cre is expressed in MSCs and decided to use Prx^{Cre} animals to delete *Ebf2* in every mesenchymal cell deriving from a MSC, including adipocytes and osteoblasts (Figure 2). Detection of a recombined $Ebf2^{\Delta fl}$ allele by PCR on gDNA isolated from bone marrow of tibia and femur proved the functionality of the conditional *Ebf2* allele and the expression of *Cre* recombinase (supplementary Figure S2). However, Prx^{Cre} driven deletion of *Ebf2* most likely resulted only in a partial deletion of *Ebf2* in certain skeletal areas. Although all skeletal elements derive from MSCs, the *Prx* enhancer used to drive Cre expression is presumably not generally active in MSCs but mainly in MSCs of the lateral plate mesoderm (Martin et al., 1995). The lateral plate mesoderm forms the appendicular skeleton (pelvis, pectoral girdle and long bones of limbs) and *Prx* is expressed in these tissues. However, *Prx* seems expressed to a lesser extent (if at all) in paraxial mesoderm that forms the somites, which give rise to the axial skeleton. Therefore, *Ebf2* is probably still expressed in the spinal cord and parts of the skull and rip cage of $Prx^{Cre}Ebf2^{fl/fl}$ mice. These skeletal elements contribute to hematopoiesis.

Although we cannot exclude that *Ebf2* expressed by MSCs contributes to HSC niche function, results within this thesis show that *Ebf2* expressed by osteoblasts is required for HSC homeostasis in three- to four-week-old $Osx^{Cre}Ebf2^{fl/fl}$ mice. As osteoblasts derive from MSCs, *Ebf2* should be deleted in osteoblasts of $Prx^{Cre}Ebf2^{fl/fl}$ mice. As none of the previously described phenotypes observed in *Ebf2*-deficient animals was detected in $Prx^{Cre}Ebf2^{fl/fl}$ mice, we speculate that the deletion efficiency within the IEO population is very low in $Prx^{Cre}Ebf2^{fl/fl}$ animals. However, it requires analysis of additional mice and furthermore it is mandatory to study three- to four-week-old $Prx^{Cre}Ebf2^{fl/fl}$ mice before any conclusion can be drawn.

To determine the deletion efficiency, we will combine the mouse strains available to generate *Prx*^{Cre}*Ebf2*$^{fl/Gfp}$ mice. By FACS sorting of Gfp positive cells, we will determine the deletion efficiency within the IEO population by quantitative real time PCR. In a similar approach, one could use a reporter mouse strain carrying a *LoxP* flanked stop cassette in front of the human *CD2* gene. *Prx*^{Cre}-mediated recombination of the *LoxP* sites would activate expression of *hCD2* (which encodes a membrane bound surface molecule for which antibodies are available) and the analysis of stromal cells from hipbone, tibia and vertebrae would provide valuable information on the deletion efficiency.

5.3 *AP2*^{Cre}-mediated deletion of *Ebf2*

Ebf2-deficient mice show a strong reduction in body weight and seem to have reduced subcutaneous fat (although we did not investigate this experimentally, supplementary figure S6). *Ebf2* carries adipogenic differentiation potential (Jimenez et al., 2007) and we speculated that *Ebf2* might play an important role in the metabolic function of adipocytes. Remarkably, *AP2*^{Cre}*Ebf2*$^{fl/fl}$ animals were not reduced in body weight and had normal amounts of subcutaneous fat (own observation). These findings argue that *Ebf2* is dispensable for the metabolic function of adipocytes. This assumption is supported by the detection of an *Ebf2*$^{\Delta fl}$ allele in gDNA isolated from adipose tissue of *AP2*^{Cre}*Ebf2*$^{fl/fl}$ animals (supplementary Figure S3). Moreover, the numbers of IEO cells isolated from *Ebf2-Gfp*$^{+/-}$ and *Ebf2-Gfp*$^{-/-}$ animals are comparable, suggesting that the loss of *Ebf2* does not result in a differentiation block of bone marrow adipocytes in *Ebf2*-deficient mice. Furthermore, no difference between IEO-*Ebf2*$^{+/-}$ and IEO-*Ebf2*$^{-/-}$ cells is observed in cell culture and adipocytes are detected at similar frequencies (own observation). These thoughts and speculations are reinforced by the fact that we observed a strong body weight reduction in young *Osx*^{Cre}*Ebf2*$^{fl/fl}$ animals arguing that the body weight reduction is not related to the function of *Ebf2* in adipocytes. This assumption is supported further by the fact that *Osx*^{Cre}*Ebf2*$^{fl/fl}$ mice had a normal body weight at the age of ten weeks. Although *Osx*^{Cre} mice are not reported to delete in adipocytes (Rodda and McMahon, 2006) we want to prove this by PCR on gDNA isolated from adipose tissue of *Osx*^{Cre}*Ebf2*$^{fl/fl}$ mice. To draw final conclusions regarding the deletion efficiency in *AP2*^{Cre}*Ebf2*$^{fl/fl}$ animals we will perform a quantitative PCR analysis on gDNA of sorted adipocytes from *AP2*^{Cre}*Ebf2*$^{fl/fl}$ mice.

Interestingly, *Ebf1* and *Ebf2* are described to carry an equal adipogenic potential (Jimenez et al., 2007). Due to relatively high expression levels of all Ebf family

members in this tissue, it is possible that redundancy among the family members can compensate for the loss of a single Ebf protein. Deletion of *Ebf1* or *Ebf2* might be compensated, resulting only in non-significant reductions of adipocyte numbers. Intercrossing *Ebf1*- and *Ebf2*-deficient mice to produce double deficient animals would be one possibility to address whether adipogenesis requires both transcription factors.

When we examined hematopoietic organs and HSC frequencies in ten-week-old $AP2^{Cre}Ebf2^{fl/fl}$ animals, they were comparable to those in control mice. In summary, we could not detect any of the phenotypes observed in three-week-old $Ebf2^{\Delta fl/\Delta fl}$ mice in the ten-week-old $AP2^{Cre}Ebf2^{fl/fl}$ mice analyzed. However, we need to extend the number of animals analyzed before any conclusions can be drawn. Interestingly, adiponectin was amongst the most deregulated genes in our DNA microarray analysis on IEO cells isolated from $Ebf2\text{-}Gfp^{+/-}$ and $Ebf2\text{-}Gfp^{-/-}$ mice. Adiponectin is exclusively expressed by adipocytes and was shown to be important for HSC proliferation (DiMascio et al., 2007). Therefore, we plan to analyze three-week-old $AP2^{Cre}Ebf2^{fl/fl}$ mice in the near future.

5.4 Osx^{Cre}-mediated deletion of *Ebf2*

Many of the cytokines mediating homing, proliferation, and quiescence of HSCs were shown to be expressed in osteoblasts (Lymperi et al., 2010) and the number of HSCs directly correlates to the number of osteoblasts in the bone marrow, indicating their importance in hematopoiesis (Calvi et al., 2003; Zhang et al., 2003). Osx^{Cre} transgenic animals were crossed with $Ebf2^{fl/fl}$ mice to investigate the function of *Ebf2* expressed by osteoblasts. Our observation that the deletion of *Ebf2* in osteoblastic cells resulted in severe weight reduction was very surprising. Although this reduction was observed in *Ebf2*-deficient animals, the cause remained unclear and like others (personal communication, G. G. Consalez, ISR Milan) we speculated that the neuronal defects might lead to reduced food uptake by the animals. Moreover, the severe osteopenia phenotype and the displayed hunchback might be an indicator of pain during movement and stretching for food pellets in *Ebf2*-deficient animals. We detected a similar reduction in bone length in $Osx^{Cre}Ebf2^{fl/fl}$ animals and counteracted the potentially reduced maneuverability by feeding the animals pulp and providing water via a long neck of bottle. However, the average body weight of $Osx^{Cre}Ebf2^{fl/fl}$ animals was still decreased. There were exceptions of animals, which developed relatively normal. The reason may be low deletion efficiency. In summary, the fact, that $Osx^{Cre}Ebf2^{fl/fl}$ animals are vivid and healthy but still show reduced body weight strongly suggests a direct connection

between *Ebf2* expressed by osteoblasts and early corporal/physic development. Anyhow, as the role of *Ebf2* in hematopoiesis is the main focus of this thesis we did not investigate this phenotype any further.

The post-natal development of the hematopoietic system in the bone marrow is completed at the age of eight to ten weeks and this time point was, therefore, chosen as time point for analysis (Beerman et al., 2010; Warren and Rossi, 2009). When we determined the total bone marrow cellularity of ten-week-old $Osx^{Cre}Ebf2^{fl/fl}$ mice, we detected a slight reduction compared to control animals (non-significant). Spleenic weights were mildly reduced (non-significant) while thymi remained unaffected. At the same time KSL frequencies in ten-week-old $Osx^{Cre}Ebf2^{fl/fl}$ mice were not reduced compared to control animals. These results were very surprising, because three-week-old *Ebf2*-deficient animals show reduced KSL frequencies compared to controls and we assumed that the severity of the hematopoietic phenotype would increase over time. As IEO cells mainly display characteristics of osteoblasts, we expected the deletion of *Ebf2* in osteoblasts would cause defects in HSC homeostasis. Anyhow, we could not detect a reduction in KSL cells and, moreover, the reductions in total bone marrow cellularity were minor. Although more animals need to be analyzed, our data indicate that in some way the relevance of *Ebf2* for hematopoiesis is time point dependent. Interestingly, R.Reed and colleagues report that 50% of the $Ebf2\text{-}Gfp^{-/-}$ mutant mice died by P30 (Wang et al., 2004). However, animals that survived to adulthood grew to normal size. In the future, we want to follow hematopoietic development over time (with gradual gaps of two weeks) from the age of two to ten weeks.

Ebf2-deficient and $Osx^{Cre}Ebf2^{fl/fl}$ animals show a reduction in body weight during the first three to four weeks after birth. However, while *Ebf2*-deficient animals die at the age of roughly three to six weeks, the severity of the body weight phenotype observed in Osx^{Cre} deleted animals starts to decline from that age onwards. In consequence of this observation we decided to analyze three to four-week-old $Osx^{Cre}Ebf2^{fl/fl}$ animals and detected a reduction in total bone marrow cellularity and a significant decrease in KSL frequencies. These results strongly indicate that the transcription factor *Ebf2* expressed in osteoblastic lineage cells regulates HSC homeostasis.

During embryogenesis, the sites of hematopoiesis change and at E13 the fetal liver carries the highest hematopoietic potential and serves as the primary hematopoietic organ (Morrison et al., 1995). The last step in hematopoietic development requires the switch from fetal liver- to bone marrow-based

hematopoiesis, which starts at E16-E18 and parallels the ossification of bones. The importance of osteoblastic cells for this process was shown in *Runx2*-deficient mice. Deletion of this transcription factor leads to a maturational arrest of osteoblastic differentiation at a very early stage (Komori et al., 1997). *Runx2*$^{-/-}$ animals have no functional osteoblasts and lack calcified bone. At E18.5, *Runx2*-deficient mice show congenital lack of bone marrow, which causes excessive extramedullary hematopoiesis in spleen and liver. Remarkably, hematopoiesis in mutant embryos at E16 is normal (Deguchi et al., 1999). This data strongly indicates that factors expressed by osteoblasts are required to establish bone marrow based hematopoiesis. *Ebf2* is expressed at sites of adult hematopoiesis (bone marrow, spleen and thymus), but not in the fetal liver. Interestingly, the development of B and T lymphocytes during embryogenesis of *Ebf2*-deficient animals shows no significant defects (Kieslinger et al., 2010). Therefore, we speculate that *Ebf2* may affect the switch from fetal liver to adult bone marrow based hematopoiesis. During early hematopoietic development, fetal liver and bone marrow contribute to the formation of mature blood cells. Fetal liver HSCs (Lin$^-$, Mac1$^+$, Sca1$^+$) have a different CD phenotype than adult HSCs (Lin$^-$, Sca1$^+$, c-Kit$^+$), and when the frequencies of fetal liver HSCs were determined in three-week-old *Ebf2*-deficient animals, they were found to be increased two- to threefold. At the same time the number of adult phenotype HSCs is decreased two- to fourfold (Kieslinger et al., 2010). These findings argue that hematopoiesis in three-week-old *Ebf2-LacZ*$^{-/-}$ animals is maintained in part by fetal liver derived HSCs. Interestingly, the number of CAFCs (cobblestone-area-forming cells) of wild type KSL cells cultured on IEO cells isolated from *Ebf2-LacZ*$^{+/-}$ and *Ebf2-LacZ*$^{-/-}$ mice was reduced by 50% on the *Ebf2*-deficient feeder layer (Kieslinger et al., 2010). This indicates less proliferation in the absence of *Ebf2*. The observations presented in this thesis may partly be explained by the list of down regulated genes obtained from our DNA microarray experiment on IEO stromal cells isolated from *Ebf2-Gfp*$^{+/-}$ and *Ebf2-Gfp*$^{-/-}$ mice.

Matrix metalloproteinases (MMP) remodel the extracellular matrix and are involved in the regulation of HSC activity through release of membrane-bound cytokines in the bone marrow. MMP-9, which was found to be downregulated in *Ebf2*-deficient IEO cells is required to release membrane bound VEGF, which stimulates hematopoiesis and hematopoietic cell mobilization (LeCouter et al., 2004). Interestingly, *VEGF* itself is also expressed in IEO cells and was detected to be downregulated in IEO-*Ebf2*$^{-/-}$ cells compared to IEO-*Ebf2*$^{+/-}$ cells (personal communication, Matthias Kieslinger).

Another MMP family member, MMP-13 (also downregulated in *Ebf2*-deficient IEO cells) was shown to play an important role during processes of angiogenesis via VEGF in tumor formation (Lederle et al., 2010). Remarkably, blood vessels in one *Ebf2*$^{\Delta fl/\Delta fl}$ animal analyzed seem less pronounced compared to the wild type littermate, which could result from the detected deregulation in MMPs (supplementary Figure S6). However, unchanged bone morphology, including bone marrow vasculature, in *Ebf2-LacZ*$^{-/-}$ animals strongly argue against this (Kieslinger et al., 2005).

Deletion of the chemokine *SDF-1* results in hematopoietic failure and premature death at E18.5 or postnatally (Nagasawa et al., 1996). The expression level of *SDF-1* is reduced in IEO-*Ebf2*$^{-/-}$ cells compared to IEO-*Ebf2*$^{+/-}$ cells indicating that the transcription factor *Ebf2* is involved in mediating the switch from fetal liver to bone marrow based hematopoiesis via *SDF-1*. This result is reinforced by the fact that *SDF-1* is a direct target of Ebf2 (Lagergren et al., 2007). This data could be confirmed by quantitative real time PCR on IEO-*Ebf2*$^{+/-}$ and IEO-*Ebf2*$^{-/-}$ cells in our laboratory (personal communication, Bettina Groll, HMGU). While *SDF-1* plays an important role in HSC homing to the bone marrow niche, SCF promotes HSC proliferation via the c-Kit receptor expressed on hematopoietic cells (Ikuta et al., 1992; Miller et al., 1996; Miller et al., 1997). Under physiologic conditions, SCF is membrane bound and needs to be cleaved for signaling via c-Kit. This process is partly mediated by MMP-9 (Heissig et al., 2002), which was also found to be downregulated in *Ebf2*-deficient IEO cells in our DNA microarray experiment. This downregulation was independently confirmed on sorted IEO cells from *Ebf2-Gfp*$^{+/-}$ and *Ebf2-Gfp*$^{-/-}$ cells in our laboratory (personal communication, Johanna Knallinger, HMGU Munich). Hence, we speculate based on these results that IEO-*Ebf2*$^{-/-}$ cells have a reduced capability to recruit HSCs to their bone marrow niche due to reduced *SDF-1* expression levels. In addition reduced levels of MMP-9 result in decreased amounts of SCF leading to reduced proliferation of HSCs in the bone marrow. This interpretation is supported by the observation that fetal liver HSCs proliferated three times less when co-cultured on IEO-*Ebf2*$^{-/-}$ compared to IEO-*Ebf2*$^{+/-}$ stromal cells (preliminary data, supplementary Figure S7). In summary, the observed phenotype in young *Osx*^{Cre}*Ebf2*$^{fl/fl}$ is most likely a consequence of reduced homing to the bone marrow and delayed expansion of HSCs. Therefore, we presume that the establishment of adult hematopoiesis partly depends on signals mediated by the transcription factor *Ebf2*.

In a set of experiments we want to further investigate the HSC phenotype by looking at more defined stem cell populations and investigate proliferative rates of these populations in *Osx*^{Cre}*Ebf2*$^{fl/fl}$ mice. Our *in vivo* data shall be further confirmed

by using the Tet-Off gene expression system available in the *Osx*^{Cre} transgenic mice used in this study (Gossen et al., 1992; Rodda and McMahon, 2006). The expression of Cre recombinase will be inhibited by administration of doxycycline during embryonic and early postnatal development of *Osx*^{Cre}*Ebf2*$^{fl/fl}$ animals. Thereby, the deletion of *Ebf2* is prevented until withdrawal of doxycycline. Analysis of the KSL frequency in *Osx*^{Cre}*Ebf2*$^{fl/fl}$ mice, who received doxycycline until different time points after birth will provide new insights. In another approach, we want to transplant fetal liver HSCs and adult HSCs into lethally irradiated young *Osx*^{Cre}*Ebf2*$^{fl/fl}$ animals. This experiment may provide answers whether *Ebf2* is differentially required by fetal liver and adult HSCs. We speculate that signals mediated by *Ebf2* are important for the maturation of fetal liver derived HSCs and the establishment of adult bone marrow-based hematopoiesis.

5.5 *Ebf2* in T cell development

Ebf2 is expressed at all sites of adult hematopoiesis (bone marrow, spleen and thymus; Kieslinger et al., 2010). While the nature of these stromal cells in the bone marrow is rather well defined, the role and function of *Ebf2*-expressing cells in spleen and thymus is unknown. Based on the overall reduction in thymic cellularity observed in *Ebf2-Gfp*$^{-/-}$, *Ebf2*$^{\Delta fl/\Delta fl}$ and *Ebf2-LacZ*$^{-/-}$ animals (Kieslinger et al., 2010) we speculated that *Ebf2* might be of functional relevance at all sites of adult hematopoiesis. Thus, we characterized which thymic stromal cells express *Ebf2* and investigated how they could be responsible for the observed phenotype.

Medullary thymic epithelial cells (mTECs) promiscuously express genes from all tissues, a process that assures T cell tolerance to antigens normally not present in the thymus. This function is mainly mediated by the transcription factor *AIRE*. As a result, mTECs present an enormous repertoire of self-antigens to T cells on MHCI and MHCII molecules and thereby negatively select self-reactive T cells. We found that in particular the CD80^{high} fraction expresses *Ebf2*. This population represents mature mTECs that also express AIRE. As a consequence *Ebf2*, expressed in these cells could simply represent a promiscuously expressed gene, which therefore would have no function in mTECs except tolerance induction. However, it has been shown that a single promiscuously expressed gene is present only in a very small fraction (1-3%) of mTECs (Derbinski et al., 2001). As we detected about 6% Gfp positive cells within the mTEC population, it is most unlikely, that this cell population results from promiscuous gene expression. We think that this population of *Ebf2*-expressing mTECs represents a true distinct population with specific function. To address this question Gfp positive and Gfp negative mTECs

of *Ebf2-Gfp*$^{+/-}$ animals will be isolated by FACS sorting. Measurement of *Ebf2* transcript levels within the sorted populations will show whether Gfp expression correlates with *Ebf2* expression and in case it does, *Ebf2*-expressing mTECs represent a true population.

Ebf2 expression was also detected in thymic fibroblasts. The importance of thymic fibroblasts was demonstrated in a previous study, which showed that growth factors provided by these cells are important for thymic regeneration after chemically induced atropy (Alpdogan et al., 2006). Furthermore they support early T cell development by providing extracellular matrix components (Anderson et al., 1997) but their precise functional role is still poorly understood. Interestingly, *Ebf2*-expressing fibroblasts are positive for the surface marker MTS15, which is specific to a unique population of thymic fibroblasts (Gray et al., 2007). MTS15 expressing fibroblasts line blood vessels at the corticomedullary junction, which is the entry site for common lymphoid progenitors (CLPs) from the peripheral blood stream into the thymus. Unlike the bone marrow, the thymus has no self-renewing potential and depends on the constant migration of CLPs from bone marrow into the thymus. Upon immigration into this zone, CLPs reside here for up to ten days (Petrie et al., 2007). MTS15^{+} cells express high levels of cytokines, e.g. SCF, IL-7 and IL-6 (Gray et al., 2007). Therefore, we speculated that *Ebf2* could potentially not only play an important role for the support of hematopoiesis in the bone marrow, but also in the thymus. However, our analysis of T cell development were performed in compromised animals with a strong HSC phenotype. As T cell progenitors derive from the bone marrow the T cell phenotype could be secondary. Therefore we transplanted thymic lobes into wild type animals.

Upon transplantation, we could not observe the same phenotype, namely the reduction in total cellularity and CD4^{+} T cells. Furthermore, no reduction in any of the early T cell stages (DN1-DN4) was observed (data not shown), also arguing against a functional role for *Ebf2* in the thymus. However, these results might also be explained by the observation that mesenchymal stem cells (MSCs) from the periphery can invade the thymus (Chamberlain et al., 2007). By this mechanism *Ebf2*-deficient cells could be replaced with host derived MTS15^{+} cells. The fact that we could detect Gfp positive mTECs, but no MTS15/Gfp double positive cells (data not shown) after transplantation argues that these cells were replaced by host-derived cells.

Due to the fact that we observed a reduction of thymic weights in four-week-old *Osx*^{Cre}*Ebf2*$^{fl/fl}$ mice (the *osterix* promotor is specific to osteoblasts; Rodda and McMahon, 2006), it is most likely that indeed the defect in T cell development is a

secondary phenotype and originates from the bone marrow. Similarly to the bone marrow phenotype, alterations in thymic weights were only detected in four-week-old *Osx*^{Cre}*Ebf2*$^{fl/fl}$ animals but not in ten-week-old *Osx*^{Cre}*Ebf2*$^{fl/fl}$ mice. The fact that *Ebf2* transcript could be detected in thymic stromal cells of *Osx*^{Cre}*Ebf2*$^{fl/fl}$ mice (data not shown) argues against an essential role for *Ebf2* in T cell development. It is more likely that the number of CLPs entering the thymus is decreased and therefore T cell development is affected. While this may explain the reduction in total cellularity it does not explain why CD4$^+$ T cells were reduced to a stronger extent than other T cell lineages. As no fibroblast specific cre lines are available, *Ebf2*$^{fl/fl}$ mice cannot be used to address this question. It would require the transplantation of *Ebf2-LacZ*$^{-/-}$ thymic lobes into *Ebf2-Gfp*$^{+/-}$ mice to gain further insights whether *Ebf2*-expressing stromal cells can populate transplanted thymi.

5.6 *Ebf2* influences the survival of B-CLL cells

The aim of this project was to determine the relevance of *Ebf2* in the support of human B-CLL cells. B-CLL is characterized by the accumulation of malignant B cells in the bone marrow and peripheral blood. Over time, these cells start to outgrow normal hematopoietic cells, leading to decreased immune function and bone marrow failure. A striking feature of B-CLL is that unlike other leukemia, B-CLL rarely infiltrates other organs, which is strong evidence that bone marrow derived factors are required for cell proliferation and survival. As *Ebf2* supports normal hematopoietic cells and is expressed in bone marrow stromal cells, we established an *in vitro* approach to address the question whether B-CLL cells respond to *Ebf2* expressed by different stromal cells. In the clinic, zeta-chain-associated protein kinase 70 (ZAP70) serves as a prognostic marker and ZAP70$^+$ B-CLL cases show a faster disease progression (Chiorazzi et al., 2005). Therefore we investigated patient samples with differing ZAP70 status to find out whether subtypes of B-CLL depend more or less on *Ebf2* expressed by stromal cells.

In the experiments performed we used two different feeder layers in a gain and loss of function approach. Bone marrow derived IEO-*Ebf2*$^{+/-}$ cells were compared to IEO *Ebf2*$^{-/-}$ cells (loss of function). In parallel the stromal cell line EL28 (*Ebf2* non-expressing) was compared to EL28 *Ebf2*, which were transduced to overexpress *Ebf2* (gain of function). In this experimental setup, *Ebf2*-mediated survival should be detectable in either experiments. Because certain studies indicate that only a very small fraction of B-CLL cells in the bone marrow proliferate and that the number of malignant cells generated is marginal compared to the amount of normal hematopoietic cells emerging every day (Chiorazzi et al.,

2007), we decided to measure the apoptotic rate of the bulk population instead of investigating cell proliferation. Apoptosis is often used as final read out in such experiments but bears the problem that it is a very fast event and occurs within hours (Elmore et al., 2007). Due to the fact that the co-culture experiments performed in this study lasted for several days, we decided to measure the number of living cells at the end of co-culture instead of counting apoptotic events as readout for *Ebf2*-mediated effects. To do so, we combined an AnnexinV/7-AAD apoptosis assay with a quantitative FACS analysis. Thereby, the experimental readout becomes time independent. In an ideal experimental setting, apoptosis should be determined consistently every 12-24 hours, but the patient material provided was not sufficient.

Eight patient samples were tested under two conditions. Three human samples responded to *Ebf2* expression with increased survival while just one sample survived slightly better on *Ebf2*-deficient stromal cells (non-significant). Interestingly, two out of eight samples responded under both experimental conditions. Taking into account that B-CLL is a very heterogeneous disease, our results show the trend, that *Ebf2* plays a role in the support of B-CLL cells. Furthermore, our data indicate that a differing ZAP70 status does not change the dependency on *Ebf2*. However, more samples need to be tested in this assay to draw final conclusions. Furthermore these results should be confirmed using other cell lines (HSC supporting and non-supporting counterpart) and should be strengthened by knockdown experiments.

B-CLL mouse models offer a great tool to study the nature of the disease and new ways of treatment (Pekarsky et al., 2007; Santanam et al., 2010). Newly generated $Osx^{Cre}Ebf2^{fl/fl}$ animals may be used to study the function of *Ebf2* in B-CLL progression. Therefore, one could transplant bone marrow from B-CLL mouse models into $Osx^{Cre}Ebf2^{fl/fl}$ animals of different age to address the role of *Ebf2 in vivo*.

5.7 Long-term culture of B-ALL cells

While prolonged survival of malignant cells in peripheral blood and bone marrow is a hallmark of B-CLL, B-ALL is characterized by high proliferation rates and aggressive invasion of lung, liver and lymphoid tissues by lymphoblasts. In a co-culture based experiment we addressed the following questions: (1) whether CSCs can be maintained *in vitro*, (2) if CSCs depend on the same specialized bone marrow niche cells like non-malignant immature hematopoietic cells do and (3)

how their frequency changes on *Ebf2*-expressing and non-expressing feeder layers. Therefore we used a well-characterized human B-ALL patient sample with a known CSC frequency (originally determined by directly transplanting the leukemic cells from a mouse into another without *in vitro* culture) and plated these cells on confluent IEO (express *Ebf2*) and non-IEO (whole bone marrow stromal cells depleted for *Ebf2*-expressing niche cells) feeder layers isolated from *Ebf2-Gfp*$^{+/-}$ mice. These co-cultures were then run for one month.

As the CD phenotype of CSCs in B-ALL is unknown, a FACS analysis would not provide all information needed and we decided to use an *in vivo* readout system. Therefore the human B-ALL cells were transplanted into NOD/LtSz-*scid IL2Rγ*^{null} mice (NSG) mice (Shultz et al., 2005). In this animal model the polygenic NOD/ShiLtJ strain (Anderson and Bluestone, 2005) was combined with the severe combined immune deficiency (*Prkdc*^{scid}) mutation (Blunt et al., 1995) and the targeted IL2 receptor gamma chain (*Il2rg*^{tm1Wjl}) deficiency (Cao et al., 1995). As a consequence, NSG mice lack mature B and T cells and have almost no NK cells. Furthermore they have defects in innate immunity and cytokine signaling pathways. As human cells develop normally upon transplantation, this animal model is widely used in the studies of hematopoietic stem cells and human disease like HIV, EBV and various types of cancer.

Co-cultures were examined under the microscope every week and no signs of cell death or proliferation were observed. Therefore, B-ALL cells were most likely resting in G_0 phase during co-culture. After four weeks the total B-ALL cell number was determined. We detected a mild reduction in total cell numbers on the IEO feeder layer compared to the numbers initially seeded while the number of B-ALL cells cultured on non-IEO stromal cells were almost unchanged. This indicates that IEO cells do not support the main B-ALL cell population as well as non-IEO cells do. However, no conclusion regarding the CSC frequency can be drawn from this result. To determine the CSC frequency, the harvested B-ALL cells were transplanted at limiting dilutions into NSG mice. Disease progression is driven by CSCs and their frequency is indirectly determined at the threshold limit, where the transplanted cell number does not cause leukemia in NSG mice.

11 days post injection, animals that had been injected the highest dose of leukemic cells were detectably engrafted in the bone marrow (fluorescent signal from the knee). Although the B-ALL cells were originally isolated from the spleen of leukemic mice, they home to the bone marrow first. This is the regular pattern of engraftment detected in FACS analysis on prepared organs from leukemic mice (personal communication, Catarina Alves, HMGU). This result suggests, that the

B-ALL cells are very potent and survive in the spleen, but preferably home to the bone marrow where they originate from. Interestingly, in those mice injected with higher cell numbers, B-ALL cells cultured on non-IEO cells engrafted slightly better, leading to faster disease progression. This argues, that either the CSC frequency was maintained better or their number even increased on non-IEO cells compared to IEO cells. However, at lower cell numbers non-significant differences were observed.

At the lowest cell number not all mice were engrafted one-month post injection. Based on these results the CSC frequency was calculated (about one in $3x10^3$ B-ALL cells) and was found to be unchanged compared to the initial frequency of the sample without *in vitro* culture. These results implicate that B-ALL cells do not specifically depend on the support of IEO niche cells but can be maintained on whole bone marrow stromal cells. This argues that they do not depend on the same niches like normal HSCs but they can be maintained in these niches.

The detection of an unaltered CSC frequency after one month *in vitro* is a very interesting finding and has not previously been reported in the literature. In future experiments, we want to use this experimental setup to study different types of feeder layers to elucidate the minimal needs of B-ALL cells. This will provide valuable information why B-ALL can aggressively infiltrate other organs.

6 Outlook

Within the course of this study, we applied gene targeting in murine embryonic stem cells to generate mice with a conditional allele of *Ebf2*. Functional testing of this mouse model proved its functionality and confirmed an important functional role for the transcription factor *Ebf2* in hematopoietic stem cell homeostasis. Furthermore, our results obtained from stromal cell type-specific deletions implicate, that specifically *Ebf2*-expressing osteoblastic cells are required for HSC homeostasis. However, our data suggest that this support is required only at certain stages of development and at the present point in time the contribution of other cell types cannot be excluded.

Therefore, we will breed $Ebf2^{fl/fl}$ mice with additional stromal Cre lines and analyze these animals at the age of three to four weeks. As we speculate, based upon our DNA microarray data, that *Ebf2* is required specifically for the homing and

proliferation of hematopoietic cells, it may be worth to investigate the hematopoietic recovery in adult *Ebf2* conditional knockout mice after bone marrow suppression with 5-fluorouracil (5-FU). 5-FU is a chemotherapeutic drug that kills actively cycling bone marrow cells resulting in a partial bone marrow ablation. The recovery from this challenge requires intensive proliferation of hematopoietic stem- and progenitor cells and this process may require *Ebf2*.

Our results obtained from the B-CLL co-cultures show, that the transcription factor *Ebf2* can induce or repress genes that affect the survival of malignant B-CLL cells. To identify molecules that mediate this increased survival and reveal pathways of communication between feeder and B-CLL cells, we will analyze the gene expression profiles of EL28 *mock*- and EL28 *Ebf2*-transduced cells by DNA microarray. This data shall then be combined with the results from the DNA microarray experiment performed on IEO-*Ebf2*$^{+/-}$ and IEO-*Ebf2*$^{-/-}$ cells. In-depth bioinformatic analysis will allow for the identification of the signals provided by *Ebf2*-expressing stromal cells and may help to identify new *Ebf2* target genes.

To extend our knowledge on the minimal needs of B-ALL cells, we plan to perform additional co-culture experiments to test more B-ALL patient samples and different feeder layers. Finally, we want to find out whether this co-culture system could be used in drug development. Therefore, we will add well-established B-ALL drugs into co-cultures and study their effect on B-ALL cell proliferation and apoptosis by FACS. Influences on the CSC frequency will be determined by transplanting B-ALL cells at limiting dilutions into immunocompromised mice.

7 Material and Methods

7.1 Material

7.1.1 Chemicals

Chemicals were purchased from the following companies: Applied Biosystems, BD Biosciences, Biochrom (Berlin, Germany), BioRad (Munich, Germany), Eppendorf (Hamburg, Germany), GE Healthcare, Invitrogen , MBI-Fermentas (Thermo Scientific Inc.), Merck, Roth (Karlsruhe, Germany), Roche Applied Science, Sigma-Aldrich, Stratagene.

7.1.2 Instruments and devices

Device	Manufacturer
Agarose gel chambers	Peqlab Biotechnologie GmbH
Accuracy weighing machine	CP2245, Sartorius AG
Bacterial incubator	B6120, Heraeus, Thermo Scientific
Blotting chamber	Trans-Blot Semi-Dry Transfer Cell, Biorad
Blotting paper	Whatman 3mm, Schleicher & Schuell GmbH
Cell culture material	various, Nunc GmbH & Co KG
	verschiedene, Falcon
Cell counter	CASY TTC, Innovatis
Centrifuges	Rotina 38R, Hettich
	Micro 200R, Hettich
	Eppendorf centrifuge, 5424, Eppendorf
CO_2-inkubator	CB150, Binder
Cryo-tubes	Nunc GmbH & Co KG
Cuvette	Uvette, 220 nm, Eppendorf
Film developer	Cawomat 2000IR, Cawo
Electroporation cuvettes	Gene Pulser, Bio-Rad
Electroporation system	Gene Pulser, Bio-Rad
FACS machines	FACSCalibur, Becton Dickinson
	FACSAriaIII, Becton Dickinson
	FACSCanto, Becton Dickinson
Glass ware	Schott, Braun
Heating block	Thermomixer Compact, Eppendorf
Ice machine	Scotsman AF 200, Scotsman Icesytem
Improved counting chamber	Karl Hecht GmbH&Ko KG
Refrigerator and freezer	Liebherr GmbH
	Privileg, Quelle

Device	Manufacturer
Laminar flow	Herasafe KS12, Heraeus
Magnet stirer	RCT basic safety control (IKA)
Microwave	Panasonic
Microscope	Axiovert25, Zeiss
Nitrocellulose membrane	Protran, Whatman
PCR machine	DNA Engine, Bio-Rad
SDS-PAGE chamber	Mini-Protean, Bio-Rad
Spectro photometer	BioPhotometer, Eppendorf
Powersupply	Power Pack, Bio-Rad
Pipettes	Gilson
pH meter	763 Multi Calimolic, Knick
Reaction vessels	0,2 ml PCR-reaction tube, Biozym Diagnostik
	15 ml, 50 ml, Falcon
	0,5 ml, 1,5 ml, 2 ml, Eppendorf
Shakers	Polymax 1040, Heidolph
	Reax2, Heidolph
Thermo cycler	Light Cycler 480II, Roche
UV-Crosslinker	Stratalinker 1800, Stratagene
UV-Transilluminator	San Gabriel
Vacuum pump	BVC 21, Vacuubrand
Vortexer	Vortex Genius (IKA)
Waterbath	Sub6, Grant

7.1.3 Software

Adobe Photoshop CS5, Adobe Illustrator CS5, MacVector, CellquestPro, Endnote, FlowJo, Microsoft Excel, Microsoft Word

7.1.4 Statistics

P-values were calculated using „complete one-way analysis of variance“ (ANOVA). If the calculated P-values are > 0.05 for the statistical comparison the graph is marked as n.s. (=non-significant).

7.1.5 Enzymes

Enzyme	Manufacturer
Collagenase typeIA	Sigma-Aldrich
Dispase II	Roche
Fire-Pol DNA polymerase	Solis BioDyne
Phusion DNA polymerase	Finnzymes, Thermo Scientific
Proteinase K	Roth
Restriction enzymes	MBI Fermentas, New England Biolabs
T4 DNA ligase	Invitrogen
Taq DNA polymerase	Invitrogen

7.1.6 Western blot antibodies

Antibody	Manufacturer
Anti-β-actin antibody, clone AC-74	Sigma-Aldrich
Anti-EBF antibody, clone 6G6	E. Kremmer, HMGU, R. Grosschedl
Goat-anti-mouse IgG (Fc-spec.)	Sigma-Aldrich
Goat-anti-rat peroxidase conjugated	Jackson Immuno Research

7.1.7 FACS antibodies

Antigen	Manufacturer	Clone
CD8a, FITC	BD Biosciences	clone 53-6.7
CD4, FITC	BD Biosciences	rm4-5

Antigen	Manufacturer	Clone
CD11b, FITC	BD Biosciences	M1/70
Ter119, FITC	BD Biosciences	TER119
Gr1, FITC	BD Biosciences	RB6-8C5
B220, FITC	BD Diosciences	RA3-6B2
G8.8 (EpCAM)	Hybridoma supernatant	
Sca1, PE	BD Biosciences	D7
CD4, APC	BD Biosciences	cloneGK1.5
c-Kit, APC	BD Biosciences	2B8
CD45	BD Biosciences	A20
Ly51	BD Biosciences	BP-1
CD80	BioLegend	B7.1
MTS15	Hybridoma supernatant	

7.1.8 Size markers

Name	Manufacturer
1 kb Ladder (DNA)	Fermentas
100 bp Plus DNA Ladder, 100-3000	Fermentas
Prestained SDS-PAGE Standard	Fermentas

7.1.9 Kits

Name	Manufacturer
Plasmid Miniprep Kit	Sigma-Aldrich
Plasmid Plus Midi Columns	Qiagen GmbH
EndoFree Plasmid Maxi Kit	Qiagen GmbH
Wizard SV Gel and PCR Clean-Up	Promega
Random Prime Labeling Kit	Amersham Bioscience
Illustra G-50 Micro Columns	GE Healthcare
Illumina RNA amplification Kit	Illumina

Name	Manufacturer
CloneJET PCR Cloning Kit	Fermentas
Ki67 proliferation detection Kit	BD Pharmingen

7.1.10 DNA Microarray

Name	Manufacturer
MouseWG v2.0 Expression Beadchip	Illumina

7.1.11 Plasmids and BAC clones

Name	Description
MSCV-IRES-GFP (Dr. R. Moriggl)	This vector encodes the murine stem cell virus and was used to generate retroviral packaging cell lines.
pEZ FrtLox DT (Dr. M. Schmidt-Supprian)	This plasmid contains 2x *Frt* and 2x *LoxP* sequences, a PGK-neomycin selection cassette and the *diphteria toxin A* gene to avoid random integration. This vector served as backbone for the *Ebf2* targeting.
pJET1.2/blunt (Fermentas)	This vector was used for subcloning and sequencing of PCR products.
RP23-148l22 (imaGenes GmbH)	C57BL/6 BAC clone containing region 67.845.129-67.865.129 of chromosome 14. Used as template in PCR reactions to generate left and right arm of homology, insert region and both southern blot probes.

7.1.12 Southern blot probes

Name	Application
BglII probe (chr. 14: 67.861.329-67.861.550)	Probe used in southern blot to identify ES cell clones positive for homologous recombination at the *Ebf2* locus. The probe was generated by PCR. Hybridisation temperature: 56°C. Washing: 3x 10 minutes at 58°C with 0.1% SSC, 0.5% SDS.
SpeI probe (chr. 14: 67.850.279-67.850.624)	Probe used in southern blot to identify ES cell clones positive for homologous recombination at the *Ebf2* locus. The probe was generated by PCR. Hybridisation temperature: 58°C. Washing: 3x 10 minutes at 60°C with 0.2% SSC, 0.5% SDS.

7.1.13 Oligonucleotides

7.1.13.1 Oligonucleotides used in quantitative real time PCR

Name	Sequence
Actin Fw	tgt ggt ggt gaa gct gta gc
Actin Rw	gac gac atg gag aag atc tgg
Ebf1 Fw	gtc acc aca agc atg aat gg
Ebf1 Rw	tct gac aac tgg tgc gaa ag
Ebf2 Fw	tgg aga atg aca aag agc aag
Ebf2 Rw	ggg ttt ccc gct gtt ttc aaa
Ebf3 Fw	aga gcc gaa caa cga gaa aa
Ebf3 Rw	gca cat ctc cgg att ctt gt
GFP Fw	gcc cga agg tta tgt aca gg
GFP Rw	tga tgc cat tct ttg gtt tg

Name	Sequence
HPRT Fw	tgc tgg tga aaa gga cct ctc g
HPRT Rw	tct ggg gac gca gca act ga

7.1.13.2 Oligonucleotides used to genotype mice

Name	Sequence
Cre Fw	ccc acc gtc agt acg tga gat atc
Cre Rw	cgc ggt ctg gca gta aaa act atc
Ebf2 GFP Fw	ggc ctg ggt tgt agt aac cat
Ebf2 GFP Ko	ctg agc atg atc ttc cat cac
Ebf2 GFP Rw	ttc aga gct ggt cct ctt cc
Ebf2 cko 1	caa ctc tga acc agg cgt tt
Ebf2 cko 3	cag tcg ctg gga gag taa gc
Ebf2 cko I	ctg ttt taa ccg agc aaa gac t
Ebf2 cko III	gcc gca agc tta taa ctt cgt at
Ebf2 LacZ Fw	gag gcg gca gat ctg aag
Ebf2 LacZ Rw	cca atg ctg cca gca aat g
Ebf2 LacZ Ko	cat tca ggc tgc gca act gtt

7.1.13.3 Oligonucleotides used for cloning

Name	Sequence
BglII probe B2 Fw	tca gac tga gac cag ggc ttt
BglII probe B2 Rw	gcc tct cct ccc tat gga atc
Insert Fw	gtc gac tgg ttg att ccg ttt tat g
Insert Rw	gtc gac aat gaa gcc tgg ccc aac
LHR Fw	atc gat aag gcc gac tgc tcc tct at
LHR Rw	gcg gcc gca act agt ccc ctg ccc tct tt
RHR Fw	ctc gag tta gat ctg gga cga ggg ctc
RHR rw	ctc gag gtc tag tca gcc aaa ctc cagc
SpeI probe short Fw	gag tta gtt gtg ggg tga ggg

Name	Sequence
SpeI probe short Rw	gag tct cgc gtt cca tcc tcg

7.1.13.4 Oligonucleotides used in RT-PCR

Name	Sequence
Ebf2 cko RT Fw	cct tta cag caa cgg tgt cc
Ebf2 cko RT Rw	tat ggg ctg ttt ggt gac ag

7.1.14 Bacteria

Name	Genotype
XL-1 blue Competent Cells	recA1 endA1 gyrA96 thi-1 hsdR17 supE44 relA1 lac [F′ proAB lacIqZΔM15 Tn10 (Tetr)], Stratagene.

7.1.15 Cell lines

Name	Description
Bruce4	C57BL/6 murine embryonic stem cells. (Kindly provided by PD Dr. U. Zimber-Strobl, HMGU)
EL08	Stromal cell line isolated from mouse AGM region. This cell line was used as a positive control in co-culture experiments. (Kindly provided by Dr. R.Oostendorp, TUM)
EL28	Stromal cell line isolated from mouse AGM region. This cell line was used as a negative control in co-culture experiments. (Kindly provided by Dr.

Name	Description
	R.Oostendorp, TUM)
GP+E86	This fibroblast cell line was used to produce retroviruses to infect murine stromal cell lines.
HEK293T cells	Modified from HEK293 cells, this cell line expresses the SV40 large T antigen. HEK293T cells were used to generate retroviruses to infect GP+E86 cells.
MEF	Generated from pSV2 neo/PEP-IL 4 C57BL/6 mice these mouse embryonic fibroblasts carry a neomycin resistenz. (Kindly provided by Dr. R.Kühn, HMGU)

7.1.16 Mouse strains

Name	Description
B6;SJL-Tg(ACTFLPe)9205Dym/J (Within this thesis we used the name: *FlpE*)	Transgenic mouse strain expressing Flp recombinase under control of the human beta actin promotor. Flp recombinase is active in all tissues, including the germ line.
B6.C-Tg(CMV-cre)1Cgn/J (Within this thesis we used the name: Del^{Cre})	Transgenic mouse strain expressing Cre recombinase under control of the minimal human cytomegalovirus promotor. Cre recombinase is active in all tissues, including the germ line.
B6.Cg-Tg(Fabp4-cre)1Rev/J (Within this thesis we used the name: $AP2^{Cre}$)	Transgenic mouse strain expressing Cre recombinase under control of the fatty acid binding protein 4 promotor.

Name	Description
	Cre recombinase expression is detected in brown and white gonadal and subcutaneous adipose tissue.
B6.Cg-Tg(Prrx1-cre)1Cjt/J (Within this thesis we used the name: *Prx*^{Cre})	Transgenic mouse strain expressing Cre recombinase under control of the paired related homeobox 1 promotor. Cre recombinase expression is detected in early limb bud mesenchyme.
B6.Cg-Tg(Sp7-tTA,tetOEGFP/cre)1-Amc/J (Within this thesis we used the name: *Osx*^{Cre})	Transgenic mouse strain expressing Cre recombinase under control of the mouse Sp7 (formerly called osterix) promotor. Cre recombinase expression is detected in the osteoblast lineage.
C57BL/6 (Charles River, WIGA)	C57BL/6 wild type mice were used in all breedings.
Ebf2$^{+/neo\text{-}fl}$	Transgenic mouse strain carrying 2 *Frt* sequences, 2 loxP sequences and a PGK-neomycin resistenz cassette in one allele of the *Ebf2* gene.
Ebf2$^{+/fl}$	Transgenic mouse strain with one conditional allele of *Ebf2* carrying 2 loxP sites.
Ebf2$^{+/\Delta fl}$	Transgenic mouse strain with recombined *LoxP* sites. *Ebf2* encoding exons 4-6 were thereby deleted.
Ebf2-Gfp$^{+/-}$	Transgenic mouse strain expressing Gfp under control of the endogenous *Ebf2* promotor (Dr. R. Reed, JHMI Baltimore).

Name	Description
Ebf2-LacZ$^{+/-}$	Transgenic mouse strain expressing beta-galactosidase under control of the endogenous *Ebf2* promotor (Dr. G. G. Consalez, ISR Milan).
NOD.Cg-Prkdcscid Il2rgtm1Wjl/SzJ	NOD.Scid.IL2-receptor γ knockout. Mice show reduced dendritic cell function, defective macrophages, no mature T and B cells, blocked signaling from 6 distinct interleukins to prevent NK cell development and were used for xenograft transplants.

7.2 Cell culture

7.2.1 Generell cell culture techniques

In context of this work human and murine primary cells and cell lines were cultured. Cells were kept in an incubator (Binder) at 37°C, 5% CO_2 and 100% relative humidity. Cells were passaged when 80% confluency, being defined here as 80% of the cell culture dish surface being covered with cells, was reached. If not stated otherwise, cells were spun down at 250 *g*, for 6 minutes at room temperature. Any manipulation or treatment of cells was performed under a sterile laminar flow (Heraeus). All working steps were performed with sterile material according to sterile working practices.

7.2.2 Cell culture media

Primary osteoblastic cells

500 ml	MEMalpha (Gibco)
10% (50 ml)	FCS (PAA)
1% (6 ml)	Glutamine (Gibco)
1% (6 ml)	Penicillin/Streptomycin (10000 U/ml, 10000U/ml, Gibco)

Murine embryonic stem cells

500 ml	DMEM (Dulbecco´s Modified Eagle´s Medium, Gibco)
12% (75 ml)	FCS (ES cell approved, PAA)
2% (12 ml)	HEPES (Gibco)
1% (6 ml)	Sodium Pyruvate (Gibco)
1.5 % (9 ml)	Glutamine (Gibco)
50 mM	Beta-mercaptoethanol (Gibco)
2000 Units	LIF (leukemia inhibitory factor)

GP+E86

500 ml	DMEM (Dulbecco´s Modified Eagle´s Medium, Gibco)
10% (50 ml)	FCS (PAA)
1% (6 ml)	Glutamine (Gibco)
1% (6 ml)	Penicillin/Streptomycin (10000 U/ml, 10000U/ml, Gibco)

Thymic embryonic lobes

500 ml	IMDM (Iscove´s Modified Dulbecco´s Medium)
10% (50 ml)	FCS (PAA)
200 mM	Deoxyguanosine (Sigma-Aldrich)

Murine embryonic fibroblasts

500 ml	DMEM (Dulbecco´s Modified Eagle´s Medium, Gibco)
10% (50 ml)	FCS (PAA)
1% (6 ml)	Glutamine (Gibco)

Adherent cell lines (EL08, EL28) and co-cultures (B-CLL and B-ALL)

500 ml	RPMI (Gibco)
10% (50 ml)	FCS (PAA)
1% (6 ml)	Glutamine (Gibco)
1% (6 ml)	Penicillin/Streptomycin (10000 U/ml, 10000U/ml, Gibco)

7.2.3 Passaging of cells

Description of the general procedure for a 10 cm cell culture dish: culture medium was removed and cells were washed with 10 ml PBS. To detach the cells, 3 ml trypsin was added and the cells were transferred to a 37°C incubator for 5-10 minutes (depends on cell type). After optical control with a microscope (all cells need to swim in medium) the reaction was stopped by addition of 7 ml of complete cell culture medium (7.2.2). Cells were then vigorously pipetted up and down to generate a single cell suspension, transferred to a falcon tube and harvested by centrifugation (250 *g*, 6 min at room temperature). The pellet was then resuspended in fresh medium and cells were plated onto a new culture dish.

7.2.4 Cell countings

Cells were counted with a CASY TTC cell counter (Innovatis) according to the manufacturer´s protocol. Briefly, an aliquot of 50 µl trypsinized cells was transferred to a 15 ml Falcon tube with 10 ml PBS. Tube was inverted a few times before measurement. Parameters on the device were adjusted specifically for each cell type and the final cell number was the average, calculated from three independent measurements.

For ES cell culture the cells were counted under a microscope using an improved counting chamber (Hecht).

7.2.5 Thawing and freezing of cells

For long-term storage, cells were trypsinized and harvested as described (7.2.3). After centrifugation, $1x10^6$ cells were resuspended in 1 ml freezing medium (90% FCS, 10% DMSO) and transferred to a cryo-tube. Immediatly afterwards, vials

were put into a pre-cooled freezing box (Nunc, Thermo Scientific) and moved to a -80°C freezer. The next day cells were moved into a liquid nitrogen tank.

To thaw cells, cryo-vials (Nunc, Thermo Scientific) were removed from liquid nitrogen and subsequently put in a 37°C waterbath until still partly frozen. Cells were then resuspended in 10 ml of complete medium and harvested. After centrifugation, cells were resuspended in fresh medium and plated.

7.2.6 Mitotic inactivation of MEFs

Prior to co-culture experiments with ES cells, MEFs were mitotically inactivated by incubation in 10 mg/ml Mitomycin C (Sigma-Aldrich) for 2 hours. After treatment, cells were washed 3 times with PBS and replated at a density of $2.5x10^6$ cells per 10 cm dish. ES cells were added at the earliest 6 hours after treatment.

7.2.7 Co-cultures

To maintain their pluripotency, murine embryonic stem (ES) cells were cultured on mouse embryonic fibroblasts. Therefore, MEFs were mitotically inactived by Mitomycin C treatment (7.2.6). Thereafter, $0.8x10^6$ ES cells were added and provided with fresh ES cell medium every 24 hours. ES cells were passaged as described (7.2.3) when colonies reached a certain size and were round-shaped with distinct borders, using trypsin supplemented with 3% chicken serum (Gibco).

Human ALL and CLL patient cells were cultured on mouse aorta-gonad-mesonephros (AGM) derived adherent cell lines EL08 and EL28. Prior to co-cultures cell lines were plated into 48-well plates ($5x10^4$ cells/well). On the next day ALL or CLL cells were added. Immature *Ebf2* expressing osteoblastic (IEO) cells were plated at 2500 cells per 48-well and cultured till 80% confluency was reached before ALL or CLL cells were added. Cells were fed every 48 hours by a partial medium exchange (50%) and kept in culture for up to 30 days.

7.2.8 Separation of blood leukocytes by Ficoll gradient

B-CLL cells from frozen human peripheral blood samples were isolated by ficoll gradient centrifugation. Therefore, samples were thawed, cells were resuspended in 20 ml medium and transferred to a 50 ml falcon with 10 ml of ficoll. After centrifugation (490 *g*, 20 minutes at RT with the centrifuge´s brake disabled) cells were harvested from the intermediary phase with a 20 ml pipette. Residues of ficoll

were removed by two PBS washing steps before cells were harvested, resuspended in RPMI and used in co-cultures.

7.2.9 Flow cytometry

For fluorescence activated cell sorting, single cell suspensions were prepared. Unspecific antibody binding was inhibited by Fc-block (20 minutes pre-incubation of the cells with a monoclonal CD16/CD32 rat anti-mouse antibody at room temperature). Stainings were performed in FACS buffer (1x PBS, 1.5% FCS) for 20 minutes at 4°C in the dark. Prior to analysis, cells were washed twice with cold FACS buffer and propidium iodide (10 μg/ml final concentration) was added just before measurement. For FACS sorting, a FACSAriaIII (Becton Dickinson) was used. All other experiments were recorded on a FACSCalibur (Becton Dickinson) and FACSCanto (Becton Dikinson). Software for recording was Cellquest (Becton Dickinson) and FACSDiva (Becton Dickinson). FlowJo 9.3 (Treestar) was used to analyze data.

7.2.10 Detection of apoptosis

Early apoptotic cells in co-culture experiments were detected with an AnnexinV apoptosis detection kit (Becton Dickinson). Experimental procedures were performed according to the manufacturer´s protocol. Briefly, cells were harvested by centrifugation and resuspended in 95 μl AnnexinV staining buffer supplemented with 5 μl AnnexinV and 5 μl 7-AAD. Tubes were vortexed and kept in the dark at RT for 15 minutes. Then 400 μl AnnexinV staining solution was added and samples were analyzed by flow cytometry.

7.2.11 Quantitative flow cytometry

To determine the number of living cells at the end of co-culture experiments, PCB 100 Accu Check Counting Beads (Invitrogen) were used. Prior to FACS measurements 30 μl (1000 Beads per μl) of FACS beads were added to each sample.

7.2.12 Transfection of ES cells

To generate stably transfected ES cell clones, cells were grown to a density of about $0.7x10^7$ ES cells per 10 cm dish on a MEF feeder layer (about 50% of MEFs are covered with ES cell clones). Cells were harvested, washed and $1x10^7$ cells

were resuspendend in 700 µl of RPMI without phenol red and transferred to an electroporation cuvette (Gene Pulser cuvette, 0.4 cm electrode, Bio-Rad). 20 µg of the linearized pEZ FrtLox DT Ebf2 cko plasmid were resuspended in 100 µl of RPMI without phenol red and were added to the cells. Transfection was performed with an electroporator (Gene Pulser, Biorad) at 230 V, 500 µF. Cells were plated on MEFs and 32-48 hours after transfection G418 (Gibco) was added to start selection. Concentrations of G418 were increased by 10 mg/ml every day (lowest 180 mg/ml, highest 220 mg/ml).

7.2.13 Isolation and expansion of stably transfected ES cell clones

7-9 days after transfection, single ES cell colonies were transferred to round bottom 96-well plates with a 200 µl pipette. Therefore the ES cell medium was removed and replaced with PBS. Next, the plate was put under a microscope and each colony was isolated by scratching the colony from the plate with the pipette tip while simultaneously sucking the clone into the tip with 25 µl PBS. The decision on which clones to pick was based on two main criteria: size (all clones should have a similar size (this is important for later freezing)) and appearance (round shaped and distinct borders). Colonies were then trypsinized in 50 µl trypsin (3% chicken serum) at 37°C for 10 minutes and passaged on three 96-well plates (plate A, B and C) with MEFs ($1.8x10^6$ per 96-well plate). 2-3 days after picking, cells on plate A were frozen by trypsinisation and addition of freezing medium (final DMSO concentration was 10%). Plate B was frozen about 36 hours later. Cells on plate C were passaged on two gelatinized 96-well plates, grown to confluency and analyzed for homologous recombination by southern blot.

7.2.14 Retroviral infection

Retroviral producer cell lines were generated based on the murine stem cell virus (MSCV). HEK-293 cells were electroporated with *MSCV-mock-IRES-GFP* / *MSCV-Ebf2-IRES-GFP* and a helper-Plasmid (encodes viral *gag*-, *pol*- *env*-genes) to generate retroviruses. On three consecutive days, supernatant of freshly transfected HEK-293 cells was transfered onto proliferating GP+E86 cells and polybrene (6 mg/ml, Millipore) was added to increase the infection rate. Next, cells were harvested and 300.000 highly GFP positive GP+E86 cells were FACS sorted and expanded on a new 10 cm dish till 80% confluency. This procedure was repeated three times. Finally, the supernatent of GP+E86 cells was passed through a 0.22 µm filter and was put on proliferating stromal cells. This procedure

was repeated every 12 hours on three consecutive days and polybrene (6 mg/ml, Millipore) was added each time to increase infection rates.

7.3 Molecular biology

7.3.1 Working with RNA

7.3.1.1 Lysis of eukaryotic cells

Adherent cells were harvested by trypsinisation and $1x10^6$ cells were transferred to a 15 ml falcon and collected by centrifugation (250 *g*, 6 min at 4°C). After removal of the supernatant, cells were lysed in 2 ml peqGOLD Trifast. RNA was extracted as described (7.3.1.3).

7.3.1.2 Lysis of primary cells after FACS sorting (DNA microarray)

IEO cells were sorted right into a 1.5 ml tube containing 1 ml of peqGOLD Trifast and RNA was extracted as described (7.3.1.3).

7.3.1.3 RNA extraction

To 1 ml of peqGOLD Trifast, 0.2 ml chloroform were added. Samples were mixed vigorously and incubated at RT for 5 minutes. The organic and aqueous phases were seperated by centrifugation (12000 *g*, 5 min at 4°C). 0.5 ml of the upper aqueous phase were transferred into a new 1.5 ml tube and mixed with 0.5 ml chilled isopropanol and 1 µl of glycogen (Ambion). After incubtion for 30 minutes on ice, RNA was precipitated by centrifugation (12000 *g*, 15 min at 4°C). The supernatant was removed and the RNA pellet washed with 1 ml 70% (v/v) ethanol (DEPC water). After harvesting the RNA pellet by centrifugation (12000 *g*, 5 min at 4°C), the supernatant was thoroughly removed and the pellet was dried for 1 minute at 50°C. Right afterwards the RNA pellet was resuspended in 20 µl of RNAse free water. Samples were either directly used in a downstream application or frozen on dry ice for storage at -80°C.

7.3.1.4 RNA processing for DNA microarray experiments

RNA samples were prepared as described (7.3.1.3). Prior to amplification the RNA quality was determined using the Bioanalyzer 2100 plattform (Agilent Technologies) and an „Agilent RNA 6000 Nano Kit“ (Agilent Technologies). Thereafter, a RNA amplification- and labeling step was performed using Illumina® TotalPrepTM-96 RNA Amplification Kit (Illumina) according to the manufacturer´s protocol. Genexpression profile analyses were performed using MouseWG v2.0

Expression Beadchips (Illumina). Arrays were scanned using an iScan System (Illumina) and data was analyzed using BeadStudio Data Analysis Software (Illumina).

7.3.1.5 cDNA synthesis from total RNA

cDNA was synthesized according to the manufacturer´s protocol for first strand cDNA synthesis, using Superscript II (Invitrogen). First, the RNA was dissolved in 10 µl water. Next, 1 µl oligo dT primer (500 µg/ml, Fermentas) and 1 µl of 10 mM dNTPs were added. The mixture was incubated at 65°C for 5 minutes, cooled to 4°C before 4µl first strand synthesis buffer, 1 µl of 0.1 mM DTT and 1 µl of RNAsin were added. The solution was incubated at 42°C for 2 minutes. Right afterwards 1 µl of Superscript II RT was added and cDNA was synthesized during incubation at 42°C for 50 minutes. Heat inactivation of the enzyme was secured by a 15 minute incubation step at 70°C.

7.3.1.6 Quantitative real time PCR

Gene expression analyses were performed according to the manufacturer´s protocol for the Lightcycler 480 Real Time PCR System (Roche). Oligonucleotides were designed to be intron spanning using tools provided on the manufacturer´s website. Measured values were normalized to hypoxanthine guanine phosphoribosyl transferase 1 (Hprt1) expression levels. Each experiment was performed in technical triplicates. The average and standard deviation were calculated based on the Cp values of the triplicates.

7.3.2 Working with DNA

7.3.2.1 Plasmid DNA isolation

For cloning purposes plasmid DNA was isolated from bacterial cultures using GenElute Plasmid Miniprep Kit (Sigma-Aldrich). Isolation was performed according to the manufacturer´s protocol.

7.3.2.2 Extraction of genomic DNA for genotyping

Mouse-tails were suspended in 100 µl tailbuffer (1x Fire Polymerase Buffer, Solis BioDyne) supplemented with 50 mg/ml proteinase K and incubated at 56°C O/N. After heat-inactivation at 95°C for 15 minutes on the next day, 1 µl of the solution was used in PCR reactions.

7.3.2.3 Extraction of genomic DNA from ES cell clones (96-well format)

Confluent ES cell clones were lysed by addition of 50 µl ES cell lysis buffer (10 mM Tris pH 7.4, 10 mM EDTA, 10 mM NaCl, 0.5% SDS, 1 mg/ml proteinase K) and O/N incubation at 56°C in a humidified atmosphere. On the next day, DNA was precipitated with 100 µl ice-cold pure ethanol. After ethanol removal and two washing steps with 70% ethanol, the DNA was air dried and resuspended in 30 µl water.

7.3.2.4 Extraction of genomic DNA from ES cell clones (10 cm dish)

For ES cell clone sequencing purposes, clones were grown till confluency on 10 cm plates, washed twice with 10 ml PBS and lysed in 5 ml ES cell lysis buffer (7.3.2.3). After transfer to a 50 ml falcon tube, cells were incubated at 56°C O/N. DNA was precipitated (7.3.2.6) and used in PCR reactions.

7.3.2.5 Extraction of DNA

1 volume of phenol/chloroform (1:1) was added to the DNA sample, mixed vigorously and centrifuged (14000 rpm, 10 min at 4°C). The upper aqueous phase was transferred to a new tube and 1 volume of chloroform was added. After centrifugation (14000 rpm, 15 min at 4°C) the upper aqueous phase was transferred to a new tube and DNA was precipitated (7.3.2.6).

7.3.2.6 Precipitation of DNA

DNA was precipitated by the addition of 1/10 volume of sodium acetate (3 M, pH 5.2) and 2 ½ volumes of pure Ethanol. After mixing, the solution was incubated on ice for 30 minutes. DNA was harvested by centrifugation (14000 *g*, 30 min at 4°C) and the DNA pellet was washed in 70% ethanol and once again centrifuged (14000 *g*, 30 min at 4°C). The supernatant was discarded and the DNA pellet was air dried and dissolved in 100 µl water.

7.3.2.7 Restriction analysis of DNA

For cloning and southern-blot analysis, DNA was cut with restriction enzymes. If not stated otherwise, reactions were performed according to the manufacturer´s protocol.

7.3.2.8 Restriction analysis of genomic DNA (96-well plate)

In context of southern-blot analysis, genomic DNA was cut in 96-wells (prepared as described 7.3.2.3). For this purpose, dissolved DNA was supplemented with 1 mM spermidin, 1 mM DTT, 100 mg/ml RNAse, 5 µl 10x restriction buffer and 50

units of the desired restriction enzyme. After sealing the plate with parafilm, reactions were incubated O/N at 37°C.

7.3.2.9 Agarose gel electrophoresis

DNA fragments derived from PCR reactions and restriction reactions were separated on gels: 1xTAE buffer (40 mM Tris/HCl, 20 mM Acetate, 1 mM EDTA, pH 8.5) supplemented with 0.8-3% Agarose. 1x TAE buffer served as running buffer. Separation was performed at 42-180 V for 0.5-16 hours. To detect DNA fragments 10 μl ethidium bromide (5 mg/ml) per 100 ml gel were added. A size marker supplemented with bromphenolblue was used for orientation.

7.3.2.10 Southern blot analysis

DNA was separated by agarose gel electrophoresis (7.3.2.9). Next, gel slices were shaken in 0.25 M HCl for 20 minutes, were briefly washed with water and subsequently incubated in alkaline transfer buffer (0.4 M NaOH, 0.6 M NaCl). Blotting of DNA from the gel onto a nylon membrane (Immobilon, Millipore) was performed overnight from top to bottom by capillary pressure of the transfer buffer. The next day, slots were marked directly on the membrane using a soft pencil. Thereafter, the basic membrane was neutralized in 2x SSC (0.3 M NaCl, 0.03 M sodium citrate, pH 6.5) for 20 minutes at RT. DNA crosslinking was performed with UV-light (Stratalinker, Stratagene) according to the manufacturer´s protocol.

Prior to hybridization with a radioactively labeled probe, membranes were pre-hybridized by incubation in warm (56°C) Church buffer (0.4 M Na_2HPO_4, 0.1 M NaH_2PO_4, 7% SDS, 0.1 mM EDTA). 50-100 ng of a specific probe were radioactively labeled using Amersham Ready-To-Go DNA labeling Beads (GE Healthcare) according to the manufacturer´s protocol. Non-incorporated radioactivity was removed using illustra sephadex G-50 DNA grade columns (GE Healthcare). Prior to hybridization, probes were denaturated by incubation at 95°C for 4 minutes, followed by subsequent quenching at 4°C for 2 minutes. Probes were pipetted directly into the hot Church buffer and were hybridized (7.1.12) with the membranes over night. The next day, the buffer was removed and membranes were washed (7.1.12).

7.3.2.11 Polymerase chain reaction (PCR)

DNA fragments were amplified in PCR reactions for genotyping, cloning, sequencing, RT-PCR and southern-blot purposes. Except for clonings and sequencing all experiments were performed with FirePol DNA polymerase (Solis BioDyne). Phusion High-Fidelity DNA polymerase (Thermo Scientific) was used for

PCR reactions related to sequencing and cloning. Experiments were performed according to the guidelines given in the manufacturer´s protocols. Annealing temperature was adjusted to the oligonucleotides used. Elongation time was adjusted to product lengths. Oligonucleotides used are listed under (7.1.13).

7.3.3 Protein methods

7.3.3.1 Protein extraction

$1x10^6$ cells were harvested, washed and resuspended in 200 µl lysis buffer (50 mM tris/HCl, pH 8; 150 mM NaCl; 1 % Nonidet™ P 40 substitute (Sigma)). Thereafter, lysates were incubated on ice for 40 min. To prevent protein degradation complete, mini, EDTA-free tablettes (Roche) were added according to the manufacturer´s protocol. Finally, lysates were centrifuged (18600 *g*, 5 min at 4°C) and supernatants were used in downstream applications or were shock frozen in liquid nitrogen.

7.3.3.2 Western blot analysis

Protein concentrations were determined with a BCA protein Assay Kit (Pierce) following the instructions given in the manufacturer´s protocol. Briefly, reagent A and B were mixed (50:1). To generate a calibration curve, BSA (PAA laboratories) was added at different concentrations (0, 2, 4, 8, 10 and 15 µg/µl) to a total volume of 400 µl of reagent A/B. Protein concentration in cell lysates was determined by addition of 1 µl lysate to 399 µl reagent A/B . After incubation (30 min at 37°C) the optical absorbance at a wavelength of 562 nm was determined.

For protein separation according to their molecular weight up to 20 µg protein lysates were mixed with 5x Laemmli sample buffer (4% SDS; 20% glycerin; 250 mM tris, pH 6.8; 5% beta-mercaptoethanol; 0.01% bromophenolblue). Prior to separation in SDS polyacrylamide gels, samples were boiled (10 min at 95°C). Thereafter, proteins were loaded onto a SDS polyacrylamide gel comprising of a 5 % stacking gel (250 mM tris/HCl pH 6.8, 0.1% SDS, 5% acrylamide; 0.1% APS; 0.004% TEMED) and a 10-12% resolving gel (375 mM tris/HCl pH 8.8, 0.1% SDS, 10-12% acrylamide; 0.1% APS; 0.004% TEMED). Prestained Protein Ladder (Fermentas) was used as size marker. Separation of proteins was performed in a Bio-Rad electrophoresis chamber for 20 minutes at 100 V and then for 1 h at 160 V. 1xTris-Glycine SDS running buffer (25 mM tris; 1% SDS; 192 mM glycin) was used as the electrophoresis buffer during the stacking and resolve process. Subsequently, proteins in the resolving gel were transferred to a Hybond-P nitrocellulose membrane (Amersham) using 1x blotting buffer (20% EtOH, 80% 1x

SDS running buffer) and a Trans-Blot SD semi dry chamber (Bio-Rad) by applying an electric force of 11 V, 300 mA for 1 h. Efficient transfer and equal protein loadings were verified with a Ponceau S (0.1% w/v Ponceau S, 5% acetic acid) staining. Prior to incubation with specific antibodies, membranes were incubated in 5% milk-powder buffer (1x PBS, 5% (w/v) non-fat milk powder, 0.2% (v/v) Tween) for 30 minutes. For immuno detection primary antibodies were incubated with membranes in 5% milk-powder solution at 4°C O/N at moderate rolling. After washing (3x, 10 min in 15 ml 5% milk-powder solution) membranes were incubated with the secondary antibody in 5% milk-powder solution (moderate rolling for 1 hour at RT). After washing (3x, 10 min in 15 ml 5% milk-powder solution) the membrane was incubated with ECL (GE Healthcare) and chemiluminescence was detected with a photosensitive Hyperfilm (GE Healthcare).

7.4 Mice

All mice used in this study were housed under specific pathogen-free conditions and were used in accordance with institutional, state and federal guidelines. All strains were maintained or backcrossed to a pure C57BL/6 background.

7.4.1 Mouse breedings

Male chimeras were bred with C57BL/6 females for germline transmission. Offspring carrying the targeted mutation were used for breeding with either B6;SJL-Tg(ACTFLPe)9205Dym/J females for recombination of *Frt* sites to generate *Ebf2*$^{+/fl}$ or with B6.C-Tg(CMV-cre)1Cgn/J females for recombination of *LoxP* sites to generate *Ebf2*$^{+/\Delta fl}$ mice. B6.Cg-Tg(Fabp4-cre)1Rev/J, B6.Cg-Tg(Prrx1-cre)1Cjt/J and B6.Cg-Tg(Sp7-tTA,tetO-EGFP/cre)1Amc/J strains were used in combination with *Ebf2*$^{fl/fl}$ animals for cell type-specific deletions. Animals were sacrificed at 3-10 weeks of age, and unless otherwise stated, at least 3 animals were analyzed per experiment while Cre-expressing *Ebf2*$^{+/fl}$ littermates served as controls.

7.4.2 Transplantation of thymic epithelial cells

Thymic embryonic lobes (E14.5) from animals of the respective genotypes were placed on Isopore membrane filters (Millipore), floating on 3 ml IMDM with 1.35 mM deoxyguanosine and were cultured for 6 days. Lobes were washed with PBS and transplanted under the kidney capsule of 8-12 week old C57BL/6 mice.

7.4.3 Transplantation of ALL cells

Transgenic human ALL cells used in this study were kindly provided by Dr. Catarina Alves, (laboratory of PD Dr. Irmela Jeremias, HMGU). To report briefly, primary ALL cells were transduced over night with an extGLuc virus (encodes a membrane-bound Gaussia luciferase). The next day, infected cells were intravenously injected into NOD.Cg-Prkdcscid Il2rgtm1Wjl/SzJ mice (The Jackson Laboratory) for expansion. When showing symptoms of sickness, mice were sacrificed and human transgenic ALL cells were isolated from the spleen as discribed (7.4.3.4).

For co-culture experiments, $1x10^6$ ALL cells were plated on confluent IEO and non-IEO stromal feeder layers in a 48-well format. Cells were cultured as described (7.2.7). After 1 month, cells were collected by trypsinization, washed and intravenously injected into NOD/scid IL-2Rgamma^{null} mice. The following dilutions were injected into 3 mice each: $3x10^3$, $3x10^4$, $6x10^4$, $1.3x10^5$, $2.5x10^5$, $5x10^5$, $1x10^6$.

7.4.3.1 *In vivo* imaging of B-ALL cells

To monitor engraftment and development of B-ALL cells, mice were imaged using a CCD camera. To this end, aminals were anesthetized using isoflurane and each mouse was intravenously injected with 100 μg of native coelenterazine (Synchem OHG, Germany) and imaged using the IVIS Lumina II Imaging System (Caliper Life Sciences). Data were analyzed with Living Image Software 4.0 (Caliper Life Sciences) and LIC frequency was calculated using poison statistic – ELDA software (Hu and Smyth, 2009).

7.4.3.2 Isolation of total bone marrow

Total bone marrow was isolated by flushing femur and tibia with ice cold PBS. Single cell suspensions were generated by vigorous up and down pipetting before cells were passed through a 70 μm cell strainer (Falcon).

7.4.3.3 Isolation of IEO cells from *Ebf2-Gfp* animals

Hindlegs from E18.5 embryos were isolated and skin and flesh were cut away leaving all bones intact. The remaining tissue was removed with 2 consecutive incubation steps in DMEM (0.1% collagenase, Sigma-Aldrich and 0.2% dispaseII, Roche) for 20 minutes at 37°C in a rotating incubator. Peeled bones were washed with PBS and swiped clean to remove all cells from the bone surface. Thereafter bones were cut open with scissors and incubated 3 times for 30 minutes at 37°C in the described medium in a rotating incubator. Supernatants were collected. For

FACS sorting, stromal cells were collected by centrifugation, resuspended in FACS buffer and kept on ice.

7.4.3.4 Isolation of primary lymphocytes

Thymus and spleen were taken out as whole organs. To generate single cell suspensions, the organs were passed through a 70 μm cell strainer (Falcon).

7.4.3.5 Isolation of thymic epithelium

Thymi were taken out as whole organs and connective tissue and fat were removed. Using scissors, thymi were cut into very small pieces and transferred to 1 ml dissociation medium (IMDM supplemented with 0.2% collagenase (Roche) and 0.2% DispaseI (Roche), 2% FCS, 25 mM HEPES (Gibco) and 25 μg/ml DNAse I (Roche). Next, cells were dissociated out of the extracellular matrix by incubation at 37°C for 50 min in a FACS tube while pipetting the solution vigorously up and down every 10 min. The reaction was stopped with EDTA (final concentration: 5 mM). Cells were filtered with a 100 μm cell strainer (Falcon), washed in 1x PBS, resuspended in PercollTM (GE Healthcare) and transferred to a FACS tube. Next, a layer of Percoll (p 1.055) and a third layer of FACS buffer were carefully added on top. The gradient was centrifuged (1350 *g*, 30 min at 4°C) without acceleration and brake. Cells were harvested from the upper interphase with a 1 ml pipette and stained as described (7.2.9).

8 Supplementary data

8.1 Supplementary tables

Table S1: Summary of the Ebf2 targeting in IDG3.2 and Bruce4 ES cells.

ES cell line	ES clones picked	correct integration	targeting efficiency	clones injected	chimeric animals
IDG3.2	400	3	0.75%	2	1 female
Bruce4	500	4	0.8%	2	9 male, 5 female

Table S2: Gene expression profiles of IEO cells from *Ebf2-Gfp*$^{+/-}$ and *Ebf2-Gfp*$^{-/-}$ animals were compared by DNA microarray analysis. Top downgulated genes with biological relevance for the observed phenotypes are shown (downregulation is shown in -fold, values for *Ebf2-Gfp*$^{+/-}$ and *Ebf2-Gfp*$^{-/-}$ are average signal intensities detected for n=6 each).

Rank	Probe	Symbol	*Ebf2-Gfp*$^{+/-}$	*Ebf2-Gfp*$^{-/-}$	Fold change	Gene name and biological function	Secreted	Trans-membrane
1	ILMN_2757966	Cxcl4	5977,386	1043,154	5,730108881	C-X-C motif chemokine 4, interacts with integrins, promotes blood coagulation	+	
2	ILMN_1241001	Eif2s3y	1374,429	250,0238	5,497192667	Eukaryotic translation initiation factor 2, essential for spermatogenesis		
3	ILMN_1259174	Scin	2611,352	550,4852	4,743727897	Scinderin, fibroblast motility, actin remodeling		
4	ILMN_2436424	Igl-5	1684,717	375,1085	4,49127919	Immunoglobulin Lambda Like Polypeptide 5 (IGIL5)		
5	ILMN_2776603	Ccl9	1356,672	306,6503	4,424166551	Chemokine (C-C motif) ligand 9, cytokine, activates osteoclasts through CCR1	+	
6	ILMN_2599233	Scrg1	4102,959	1036,546	3,958299005	Stimulator of chondrogenesis 1, associated with the secretory pathway		
7	ILMN_2609590	Cpa3	1204,255	317,3775	3,794393112	Carboxypeptidase A3, expressed in mast cells		
8	ILMN_3160137	Aldoc	1082,401	295,9504	3,657372992	Aldolase C, expressed in hippocampus and purkinje cells		
9	ILMN_2737685	Mmp13	7804,528	2257,042	3,457856788	Collagenase 3, extracellular matrix remodeling factor	+	
10	ILMN_1226525	H2-Ab1	1332,837	394,7888	3,376076018	Histocompatibility 2 class II antigen A beta 1		x
11	ILMN_1251248	Ebf2	1346,926	409,7955	3,28682477	Early B cell factor 2, transcription, multicellular organismal development		
12	ILMN_2617468	Chac1	4082,72	1261,296	3,23692456	Cation transport regulator-like 1, pro-apoptotic component of the unfolded protein response pathway		
13	ILMN_2711075	Mmp9	5317,391	1687,816	3,150456566	Matrix Metalloproteinase 9, extracellular matrix remodeling factor	+	
14	ILMN_2721052	Panx3	5974,231	1896,88	3,149503922	Pannexin 3, gap junction protein, target of Runx2, bone development		x
15	ILMN_2883606	Ebf2	1950,457	619,8492	3,146663737	Early B cell factor 2, transcription, multicellular organismal development		

Rank	Probe	Symbol	*Ebf2-Gfp*$^{+/-}$	*Ebf2-Gfp*$^{-/-}$	Fold change	Gene name and biological function	Secreted	Trans-membrane
16	ILMN_2991799	Cpa3	807,1603	271,0061	2,97838425	Carboxypeptidase A3, expressed in mast cells		
17	ILMN_1219686	Esd	6177,165	2075,97	2,975556005	Esterase D, formylgluthatione hydrolase, possibly involved in recycling of sialic acids		
18	ILMN_2678421	Pcolce2	1647,099	574,4349	2,86733797	Procollagen C-endopeptidase enhancer 2, extracellular matrix remodeling factor	+	
19	ILMN_2565942	B930011A14Rik	972,8411	351,8075	2,76526538	Uncharacterized		
20	ILMN_2940568	Epyc	4780,46	1731,87	2,760288012	Dermatan sulfate proteoglycan 3, extracellular matrix remodeling factor	+	
21	ILMN_2738082	Adipoq	1911,28	711,1412	2,68762378	Adiponectin, fat metabolism and insulin sensitivity, HSC proliferation	+	
22	ILMN_2965669	Xlr4a	5993,713	2269,566	2,640907116	X-linked lymphocyte-regulated 4A, uncharacterized		
23	ILMN_1222219	2610528A11Rik	724,238	274,9014	2,634537329	Uncharacterized		
24	ILMN_2597332	1700123O20Rik	3191,948	1216,086	2,624771603	Uncharacterized		
25	ILMN_2498263	Hspa1b	999,5281	381,4258	2,620504696	Heat shock 70 kDa protein 1B, protein stabilization		
26	ILMN_2967037	Gpr1	790,0399	302,8622	2,608578753	G protein-coupled receptor 1, Receptor for the inflammation-associated RARRES2		x
27	ILMN_2472730	Zfp533	2100,802	820,4057	2,560686743	DNA binding protein, expressed in cardiomyocytes		
28	ILMN_2742861	Serpina3f	844,4957	331,9901	2,543737599	Serine (or cysteine) peptidase inhibitor clade A member 3F	+	
29	ILMN_1231274	Cmtm5	1380,55	559,494	2,467497417	CKLF-like MARVEL transmembrane domain containing 5, chemokine-like factor		x
30	ILMN_1227663	Sgms2	1990,848	815,4755	2,441333921	Sphingomyelin synthase 2, phosphatidylcholine metabolism, cell-signaling		x
31	ILMN_1251748	Pscdbp	1109,768	457,7377	2,424462744	Cytohesin 1 interacting protein, modulates the activation of ARF genes		
32	ILMN_2613601	2010001M09Rik	683,9405	285,2767	2,397463585	Uncharacterized		

Rank	Probe	Symbol	*Ebf2-Gfp*$^{+/-}$	*Ebf2-Gfp*$^{-/-}$	Fold change	Gene name and biological function	Secreted	Trans-membrane
33	ILMN_2485323	Trf	781,2725	331,5245	2,35660562	Telomeric repeat binding factor, inhibitor of telomerase		
34	ILMN_2848906	Rlbp1	521,5691	223,1512	2,337290142	Retinaldehyde binding protein 1, soluble retinoid carrier		
35	ILMN_2753342	Hapln1	3705,211	1603,295	2,310997664	Hyaluronan and proteoglycan link protein 1, extracellular matrix remodeling factor	+	
36	ILMN_2917280	Efcab1	1563,575	677,7128	2,307135117	EF-hand calcium binding domain 1, possibly calcium ion binding		
37	ILMN_1250001	4930583H14Rik	3901,56	1698,32	2,297305573	Uncharacterized		
38	ILMN_2613878	Prg2	1576,918	692,7039	2,276467622	Proteoglycan 2, immune response, defense response to bacterium	+	
39	ILMN_2788223	Kng1	1109,352	491,8	2,255697438	Kininogen 1, inhibitor of thiol proteases	+	
40	ILMN_2944824	Hp	1981,691	882,7574	2,24488744	Haptoglobin, combines with free plasma hemoglobin to prevent damage	+	
41	ILMN_2625377	Rgs1	450,0417	201,1044	2,237851086	Regulator of G-protein signaling 1, signal transduction		x
42	ILMN_1218240	Cd69	555,3282	249,3483	2,227118452	CD69 molecule, calcium dependent lectin superfamily type II transmembrane receptor		x
43	ILMN_1257051	Glt25d2	1004,469	451,8425	2,223051174	Glycosyltransferase 25 domain containing 2, extracellular matrix remodeling factor	+	
44	ILMN_2607675	LOC641240	786,2088	355,908	2,209022556	Uncharacterized		
45	ILMN_3006123	Asns	1239,171	567,0882	2,185146861	Asparagine synthetase, uncharacterized		
46	ILMN_2988143	Plac8	2548,588	1192,105	2,13788886	Placenta-specific 8		
47	ILMN_2913716	H2-Ab1	537,9681	253,126	2,125297678	Histocompatibility 2, class II antigen A, beta 1		x
48	ILMN_2749037	Ndg2	1097,461	525,4182	2,088738076	Coiled-coil-helix-coiled-coil-helix domain containing 10, uncharacterized		
49	ILMN_1241695	Ms4a6d	535,6003	256,5482	2,087718019	Membrane-spanning 4-domains, subfamily A, member 6E, signal transduction		x

Rank	Probe	Symbol	*Ebf2-Gfp*$^{+/-}$	*Ebf2-Gfp*$^{-/-}$	Fold change	Gene name and biological function	Secreted	Trans-membrane
50	ILMN_2846485	Vpreb1	1597,234	771,2458	2,070979187	Pre-B lymphocyte 1, associates with the Ig-mu chain		
51	ILMN_2772845	Cat	887,3517	428,8466	2,069158762	Catalase, defense against oxidative stress		
52	ILMN_2548302	2210017A09Rik	541,1469	261,5438	2,069048855	Uncharacterized		
53	ILMN_1227907	Gmfg	639,8651	310,062	2,063668234	Glia maturation factor gamma, nerve growth factor, possibly involved in angiogenesis		
54	ILMN_2827729	Calb2	429,2529	208,4879	2,058886391	Calbindin 2, message targeting and intracellular calcium buffering		
55	ILMN_2703182	Lgals7	2172,209	1064,097	2,04136371	Lectin galactoside-binding soluble 7, cell-cell and/or cell-matrix interactions		x
56	ILMN_2866856	H2-DMa	945,5711	464,325	2,036442363	Histocompatibility 2 class II locus Dma, antigen presenting cell function		x
57	ILMN_2787257	Coro1a	1003,122	497,3518	2,016926449	Coronin actin binding protein 1A, possibly a component of the cytoskeleton		
58	ILMN_2627546	LOC677369	500,382	248,5185	2,013459763	Uncharacterized		
59	ILMN_1227240	Cdkn2b	797,5409	396,5067	2,01141847	CDKN2B antisense RNA 1, uncharacterized		
60	ILMN_2737302	Cxcl12	1805,92	900,9241	2,004519582	Chemokine (C-X-C motif) ligand 12, SDF-1, chemokine	+	
61	ILMN_2754940	LOC100047808	664,4418	331,8748	2,002085726	Uncharacterized		
62	ILMN_3158250	Cxcl12	1253,633	631,1554	1,98625093	Chemokine (C-X-C motif) ligand 12, SDF-1, chemokine	+	
63	ILMN_2440194	5330423I11Rik	687,5683	346,9864	1,981542504	Uncharacterized		
64	ILMN_1225528	Trib3	2921,41	1476,323	1,978842028	Tribbles homolog 3, putative protein kinase that is induced by NF-kappaB		
65	ILMN_1221146	Cytl1	2962,408	1499,702	1,975331099	Cytokine-like 1, putative cytokine expressed in bone marrow cells	+	
66	ILMN_2613832	Mgst2	1296,353	657,7356	1,970933305	Microsomal glutathione S-transferase 2, eicosanoid and glutathione metabolism		

Rank	Probe	Symbol	*Ebf2-Gfp*$^{+/-}$	*Ebf2-Gfp*$^{-/-}$	Fold change	Gene name and biological function	Secreted	Trans-membrane
67	ILMN_3007428	Sox9	2445,267	1252,027	1,95304654	SRY, transcription factor required for normal skeletal development		
68	ILMN_2609813	Chi3l1	1706,275	874,1982	1,951817105	Chitinase 3-like 1, possibly involved in inflammation and tissue remodeling	+	
69	ILMN_2725927	Serpina3g	4443,392	2294,676	1,936391891	Serpin peptidase inhibitor, clade A member 3, inhibits neutrophil cathepsin G	+	
70	ILMN_1222471	Gmfg	556,176	287,7134	1,93309036	Glia maturation factor, gamma, uncharacterized		
71	ILMN_2855310	Mpl	461,7367	239,0909	1,93121821	Myeloproliferative leukemia virus oncogene, receptor for thrombopoietin		x
72	ILMN_1229301	LOC676779	1539,94	798,1091	1,92948558	Uncharacterized		
73	ILMN_2523169	Treml1	506,7372	263,2628	1,924834044	Triggering receptor expressed on myeloid cells-like protein 1, calcium signaling		x
74	ILMN_1221526	LOC100041516	995,4444	517,3671	1,924058178	Uncharacterized		
75	ILMN_1240728	Sh3tc2	444,1233	231,3192	1,919958655	SH3 domain and tetratricopeptide repeats 2, expressed in brain and spinal cord		
76	ILMN_2538597	LOC386405	1049,396	546,7166	1,919451504	Uncharacterized		
77	ILMN_2954824	Ppp1r1b	1168,207	609,2021	1,917601729	Protein phosphatase 1 regulatory (inhibitor) subunit 1B, signal transduction	-	
78	ILMN_2734097	Btc	755,3676	394,0275	1,917042846	Betacellulin, ligand for EGF receptor	+	
79	ILMN_1217849	Laptm5	9898,646	5180,909	1,910600244	Lysosomal protein transmembrane 5, receptor associated with lysosomes		
80	ILMN_1230680	D130057F13Rik	1930,368	1014,34	1,903077863	Uncharacterized		
81	ILMN_2723965	Edn2	477,9507	251,3001	1,901912096	Endothelin 2, initiate intracellular signaling events through endothelin receptors		x
82	ILMN_1259069	F730003H07Rik	6085,027	3200,338	1,901370105	Uncharacterized		
83	ILMN_1215877	Extl1	628,6032	331,4048	1,896783631	Exostoses (multiple)-like 1, alpha 1,4- N-acetylglucosaminyltransferase	-	

Rank	Probe	Symbol	*Ebf2-Gfp*$^{+/-}$	*Ebf2-Gfp*$^{-/-}$	Fold change	Gene name and biological function	Secreted	Trans-membrane
84	ILMN_1247592	Casp1	461,491	246,292	1,873755542	Caspase 1, apoptosis- and inflammation-related cysteine peptidase	-	
85	ILMN_1229397	Slc1a1	852,5682	457,7504	1,862517652	Solute carrier family 1, transport of L-glutamate and also L- and D-aspartate	-	
86	ILMN_2695199	St3gal6	5493,285	2955,622	1,85858848	ST3 beta-galactoside alpha-2,3-sialyltransferase 6	-	
87	ILMN_2730311	2610017I09Rik	593,4163	319,7457	1,855900799	Uncharacterized		
88	ILMN_2889899	Glt25d2	504,2467	272,9079	1,847680848	Glycosyltransferase 25 domain containing 2, extracellular matrix remodeling factor	+	
89	ILMN_2716389	Smpd3	887,7005	483,4326	1,836244597	Sphingomyelin phosphodiesterase 3, bone and dentin mineralization	+	
90	ILMN_2653132	Clec7a	522,2294	285,4149	1,829720172	C-type lectin domain family 7 member A, type II membrane receptor		x
91	ILMN_2610822	Cd79b	547,951	301,2274	1,819060949	CD79b molecule, Ig-beta protein of the B-cell antigen component		x
92	ILMN_2627013	Zfp710	637,1771	350,8797	1,81594176	Zinc finger protein 710, uncharacterized		
93	ILMN_2874084	Car9	2668,724	1471,358	1,813782913	Carbonic anhydrase IX, calcification and bone resorption		x
94	ILMN_2728729	Sdc4	3925,287	2164,892	1,813156037	Syndecan 4, proteoglycan that functions in intracellular signaling	+	x
95	ILMN_2643513	Asns	4651,297	2566,063	1,812619955	Asparagine synthetase,		
96	ILMN_1251713	Car12	3459,468	1918,224	1,803474464	Carbonic anyhydrase 12, calcification and bone resorption		x
97	ILMN_1257987	Slc7a3	727,1462	404,3141	1,798468567	Solute carrier family 7 member 3, mediates arginine uptake		x
98	ILMN_2578681	C130080K17Rik	1193,022	664,4159	1,795595199	Uncharacterized	+	
99	ILMN_2630852	Il7	444,9789	247,8374	1,795446934	Interleukin 7, essential role in lymphoid cell survival	+	
100	ILMN_2538242	LOC386144	11278,48	6286,563	1,794061397	Uncharacterized		

8.2 Supplementary figures

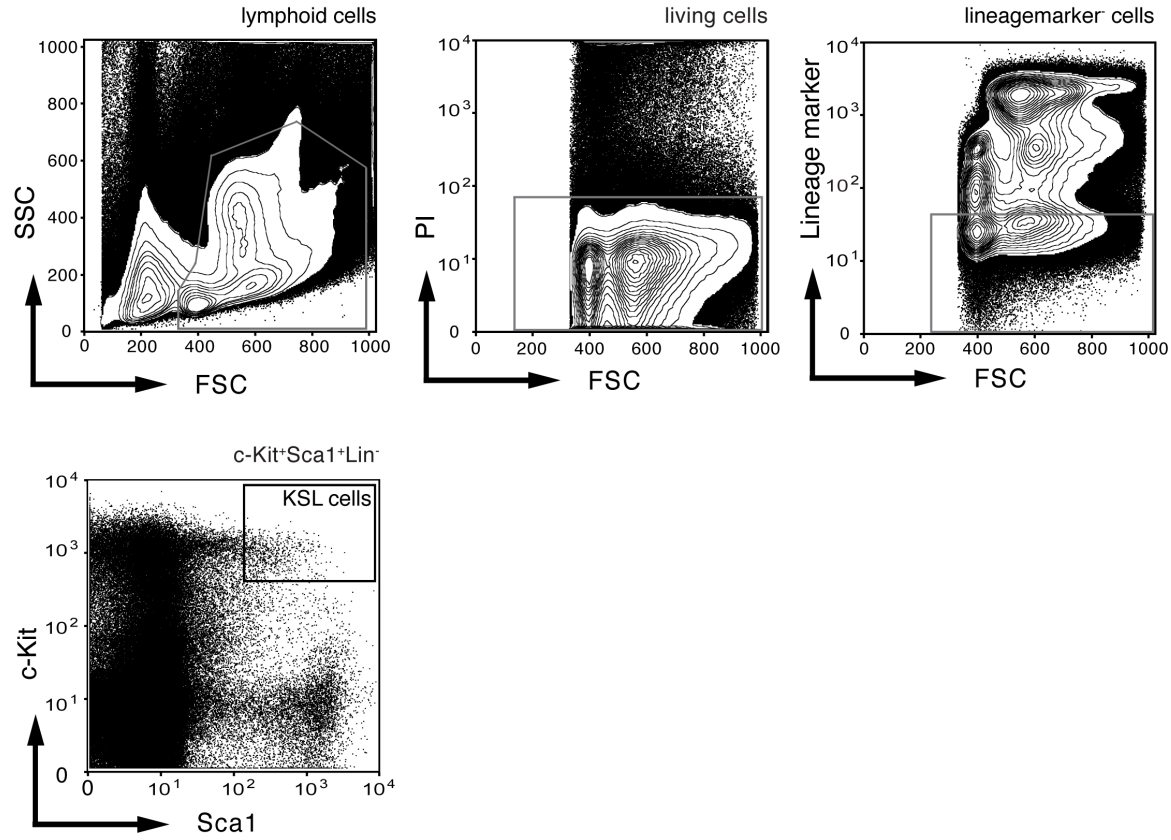

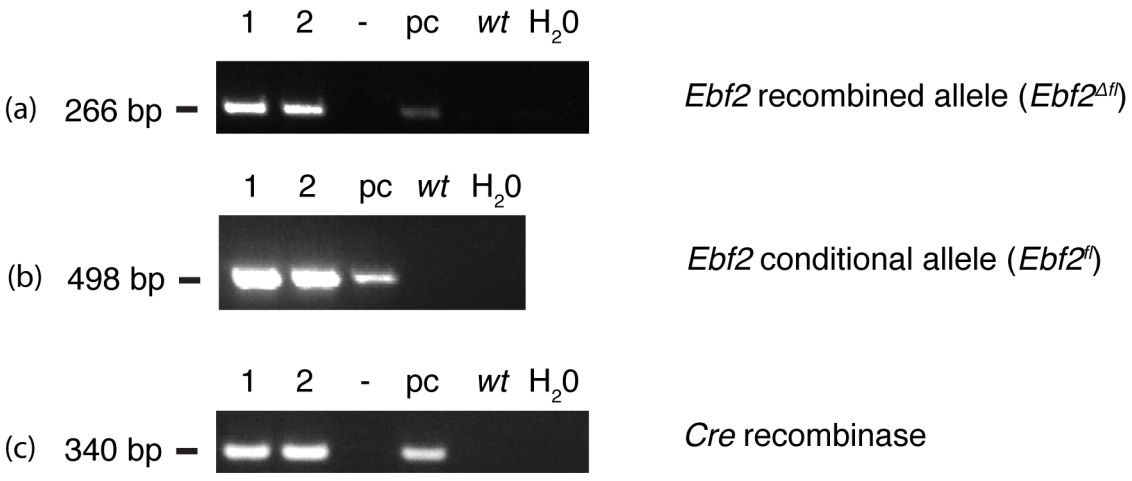

Figure S2: PCR analysis of gDNA, isolated from bone marrow cells of *Prx^{Cre}Ebf2$^{fl/fl}$* mice. Long bones of two ten-week-old *Prx^{Cre}Ebf2$^{fl/fl}$* mice were flushed with PBS and flesh on the bone surface was thoroughly removed using scissors and a scalpel. Next, the empty bones were crushed and cells from the inner bone surface were lyzed in 1 ml tail buffer at 56°C overnight. Thereafter, a PCR was performed (35 cycles) and the *Ebf2* recombined allele (a), *Ebf2* conditional allele (b) and the *Cre* recombinase gene (c) could be detected on a 2% agarose gel (- = empty lane, pc = positive control, *wt* = wild type, H_20 = water).

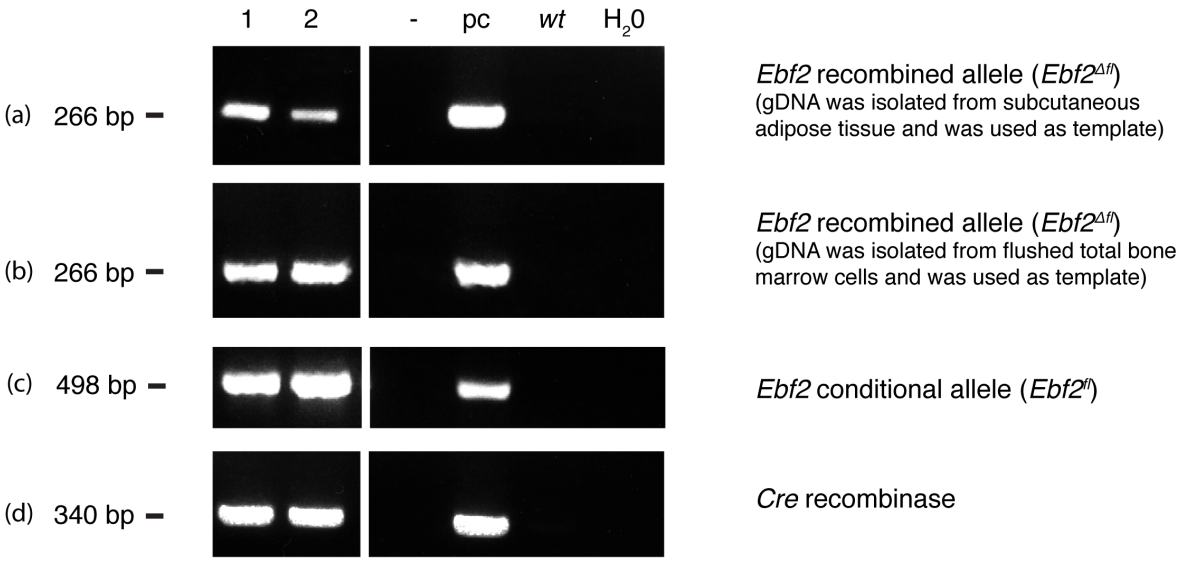

Figure S3: PCR analysis of gDNA, isolated from bone marrow cells or adipose tissue of *AP2^{Cre}Ebf2$^{fl/fl}$* mice. Long bones of two ten-week-old *AP2^{Cre}Ebf2$^{fl/fl}$* mice were flushed with PBS and cells were harvested by centrifugation. Next, cells were resuspended and lyzed in 1 ml tail buffer at 56°C overnight. Meanwhile, small pieces of subcutaneous fat were isolated from the mouse neck and waist region and the tissue was lyzed in 1 ml tail buffer at 56°C overnight. Thereafter, a PCR was performed (35 cycles) and the *Ebf2* recombined allele (a, b), *Ebf2* conditional allele (c) and the *Cre* recombinase gene (d) could be detected on a 2% agarose gel (- = empty lane, pc = positive control, *wt* = wild type, H_20 = water).

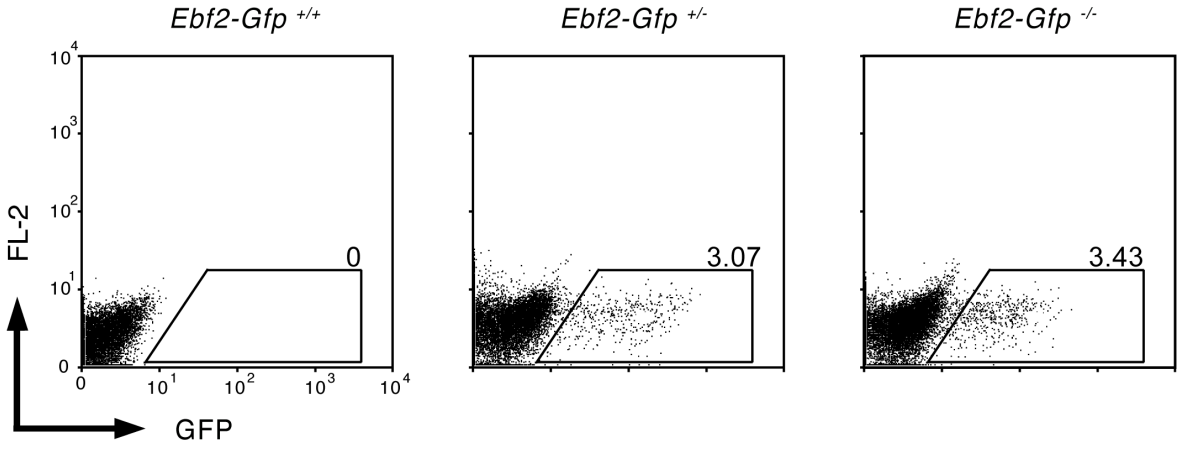

Figure S4: FACS sorting of IEO cells. Generally, timed matings between *Ebf2-Gfp$^{+/-}$* animals were setup. Males and females were put together on afternoons. Plugs were checked the next morning. Eighteen days later (E18.5) pregnant females were sacrificed and osteoblastic cell fractions were isolated as described elsewhere (7.4.3.3). For FACS sorting, cells were gated on stromal cells in FSC/SSC. Doublets were excluded in FSC/SSC-H (not shown). IEO cells are Gfp positive and were sorted into reaction tubes with medium or trizol.

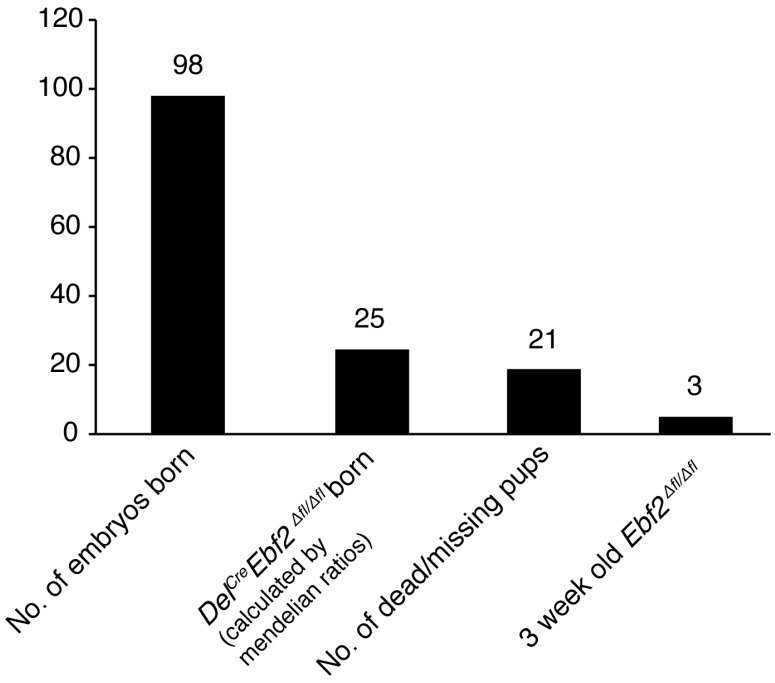

Figure S5: *Ebf2*$^{\Delta fl/\Delta fl}$ animals were born at very low frequencies. To test the newly generated mouse model, breedings of *Ebf2*$^{+/\Delta fl}$ mice were set up to generate *Ebf2*$^{\Delta fl/\Delta fl}$ animals. From 13 litters, 98 animals were born. Many pups were found dead after birth. In total, 3 *Ebf2*$^{\Delta fl/\Delta fl}$ animals reached the age of three weeks.

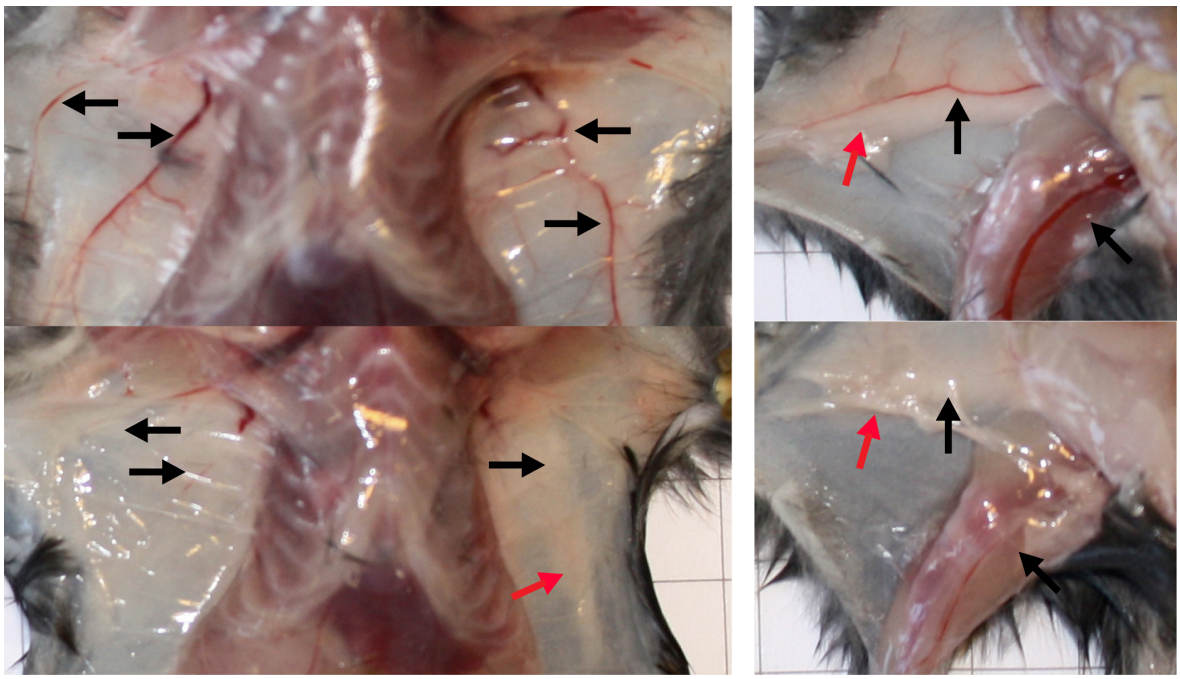

Figure S6: Indication of reduced angiogenesis and subcutaneous fat in *Ebf2*$^{\Delta fl/\Delta fl}$ animals. Upper images were taken from a wild type littermate, lower images show an *Ebf2*$^{\Delta fl/\Delta fl}$ animal. Left fotos were taken from the rip cage. Right images show ventral view on pelvis. Red arrowheads point to subcutaneous fat, black arrowheads point to absent or reduced blood vessels (analysis was performed once).

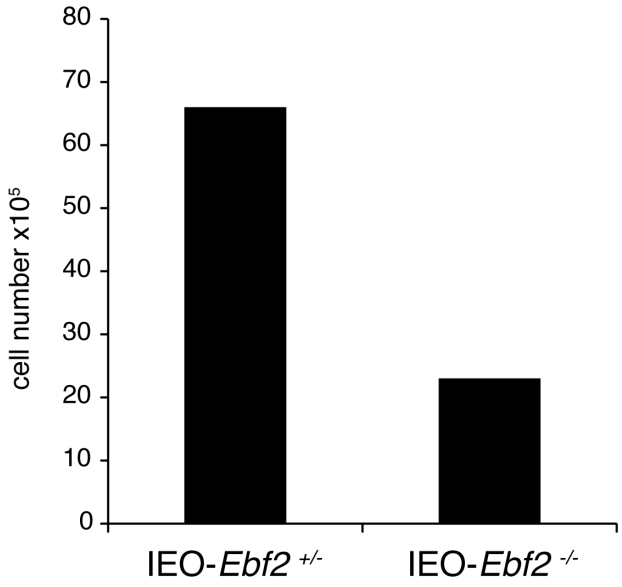

Figure S7: Fetal liver HSCs proliferate more on *Ebf2*-expressing IEO cells. Fetal liver HSCs (Lin^-, $Mac1^+$, $Sca1^+$) from wild type mice were FACS sorted and cultured in RPMI (10% FCS, 1% Glutamine) without addition of cytokines with IEO-*Ebf2*$^{+/-}$ and IEO-*Ebf2*$^{-/-}$ cells for 10 days. Cells were counted using a CASY Cell counter (experiment was performed once).

9 References

Adams, G.B., Chabner, K.T., Alley, I.R., Olson, D.P., Szczepiorkowski, Z.M., Poznansky, M.C., Kos, C.H., Pollak, M.R., Brown, E.M., and Scadden, D.T. (2006). Stem cell engraftment at the endosteal niche is specified by the calcium-sensing receptor. Nature *439*, 599-603.

Adolfsson, J., Borge, O.J., Bryder, D., Theilgaard-Monch, K., Astrand-Grundstrom, I., Sitnicka, E., Sasaki, Y., and Jacobsen, S.E. (2001). Upregulation of Flt3 expression within the bone marrow Lin(-)Sca1(+)c-kit(+) stem cell compartment is accompanied by loss of self-renewal capacity. Immunity *15*, 659-669.

Al-Hajj, M., Wicha, M.S., Benito-Hernandez, A., Morrison, S.J., and Clarke, M.F. (2003). Prospective identification of tumorigenic breast cancer cells. Proceedings of the National Academy of Sciences of the United States of America *100*, 3983-3988.

Alpdogan, O., Hubbard, V.M., Smith, O.M., Patel, N., Lu, S., Goldberg, G.L., Gray, D.H., Feinman, J., Kochman, A.A., Eng, J.M.*, et al.* (2006). Keratinocyte growth factor (KGF) is required for postnatal thymic regeneration. Blood *107*, 2453-2460.

Anderson, G., Anderson, K.L., Tchilian, E.Z., Owen, J.J., and Jenkinson, E.J. (1997). Fibroblast dependency during early thymocyte development maps to the CD25+ CD44+ stage and involves interactions with fibroblast matrix molecules. European journal of immunology *27*, 1200-1206.

Anderson, G., Owen, J.J., Moore, N.C., and Jenkinson, E.J. (1994). Thymic epithelial cells provide unique signals for positive selection of CD4+CD8+ thymocytes in vitro. The Journal of experimental medicine *179*, 2027-2031.

Anderson, M.S., and Bluestone, J.A. (2005). The NOD mouse: a model of immune dysregulation. Annual review of immunology *23*, 447-485.

Anderson, M.S., Venanzi, E.S., Klein, L., Chen, Z., Berzins, S.P., Turley, S.J., von Boehmer, H., Bronson, R., Dierich, A., Benoist, C.*, et al.* (2002). Projection of an immunological self shadow within the thymus by the aire protein. Science *298*, 1395-1401.

Arai, F., Hirao, A., Ohmura, M., Sato, H., Matsuoka, S., Takubo, K., Ito, K., Koh, G.Y., and Suda, T. (2004). Tie2/angiopoietin-1 signaling regulates hematopoietic stem cell quiescence in the bone marrow niche. Cell *118*, 149-161.

Armstrong, S.A., and Look, A.T. (2005). Molecular genetics of acute lymphoblastic leukemia. Journal of clinical oncology : official journal of the American Society of Clinical Oncology *23*, 6306-6315.

Bain, G., Maandag, E.C., Izon, D.J., Amsen, D., Kruisbeek, A.M., Weintraub, B.C., Krop, I., Schlissel, M.S., Feeney, A.J., van Roon, M.*, et al.* (1994). E2A proteins are required for proper B cell development and initiation of immunoglobulin gene rearrangements. Cell *79*, 885-892.

Banerji, J., Olson, L., and Schaffner, W. (1983). A lymphocyte-specific cellular enhancer is located downstream of the joining region in immunoglobulin heavy chain genes. Cell *33*, 729-740.

Barberan, J., Mensa, J., Llamas, J.C., Ramos, I.J., Ruiz, J.C., Marin, J.R., Tello, P.B., Massana, M.B., Vidal, J.B., Vinas, J.M.*, et al.* (2011). Recommendations for the treatment of invasive fungal infection caused by filamentous fungi in the hematological patient. Revista espanola de quimioterapia : publicacion oficial de la Sociedad Espanola de Quimioterapia *24*, 263-270.

Becker, A.J., Mc, C.E., and Till, J.E. (1963). Cytological demonstration of the clonal nature of spleen colonies derived from transplanted mouse marrow cells. Nature *197*, 452-454.

Beerman, I., Maloney, W.J., Weissmann, I.L., and Rossi, D.J. (2010). Stem cells and the aging hematopoietic system. Current opinion in immunology *22*, 500-506.

Bergers, G., Brekken, R., McMahon, G., Vu, T.H., Itoh, T., Tamaki, K., Tanzawa, K., Thorpe, P., Itohara, S., Werb, Z.*, et al.* (2000). Matrix metalloproteinase-9 triggers the angiogenic switch during carcinogenesis. Nature cell biology *2*, 737-744.

Bernard, A., Gay-Bellile, V., Amiot, M., Caillou, B., Charbord, P., and Boumsell, L. (1984). A novel human leukocyte differentiation antigen: monoclonal antibody anti-D44 defines a 28 Kd molecule present on immature hematologic cells and a subpopulation of mature T cells. J Immunol *132*, 2338-2344.

Bjerkvig, R., Tysnes, B.B., Aboody, K.S., Najbauer, J., and Terzis, A.J. (2005). Opinion: the origin of the cancer stem cell: current controversies and new insights. Nature reviews Cancer *5*, 899-904.

Bleul, C.C., Corbeaux, T., Reuter, A., Fisch, P., Monting, J.S., and Boehm, T. (2006). Formation of a functional thymus initiated by a postnatal epithelial progenitor cell. Nature *441*, 992-996.

Blunt, T., Finnie, N.J., Taccioli, G.E., Smith, G.C., Demengeot, J., Gottlieb, T.M., Mizuta, R., Varghese, A.J., Alt, F.W., Jeggo, P.A.*, et al.* (1995). Defective DNA-dependent protein kinase activity is linked to V(D)J recombination and DNA repair defects associated with the murine scid mutation. Cell *80*, 813-823.

Bonnet, D., and Dick, J.E. (1997). Human acute myeloid leukemia is organized as a hierarchy that originates from a primitive hematopoietic cell. Nature medicine *3*, 730-737.

Borkhardt, A., Cazzaniga, G., Viehmann, S., Valsecchi, M.G., Ludwig, W.D., Burci, L., Mangioni, S., Schrappe, M., Riehm, H., Lampert, F.*, et al.* (1997). Incidence and clinical relevance of TEL/AML1 fusion genes in children with acute lymphoblastic leukemia enrolled in the German and Italian multicenter therapy trials. Associazione Italiana Ematologia Oncologia Pediatrica and the Berlin-Frankfurt-Munster Study Group. Blood *90*, 571-577.

Buchman, T. G. (2008). Antibiotic overuse: the influence of social norms. Journal of the American College of Surgeons *207*, 265-275.

Buss, E.C., and Ho, A.D. (2011). Leukemia stem cells. International journal of cancer Journal international du cancer *129*, 2328-2336.

Calvi, L.M., Adams, G.B., Weibrecht, K.W., Weber, J.M., Olson, D.P., Knight, M.C., Martin, R.P., Schipani, E., Divieti, P., Bringhurst, F.R.*, et al.* (2003). Osteoblastic cells regulate the haematopoietic stem cell niche. Nature *425*, 841-846.

Cao, X., Shores, E.W., Hu-Li, J., Anver, M.R., Kelsall, B.L., Russell, S.M., Drago, J., Noguchi, M., Grinberg, A., Bloom, E.T.*, et al.* (1995). Defective lymphoid development in mice lacking expression of the common cytokine receptor gamma chain. Immunity *2*, 223-238.

Chamberlain, G., Fox, J., Ashton, B., and Middleton, J. (2007). Concise review: mesenchymal stem cells: their phenotype, differentiation capacity, immunological features, and potential for homing. Stem Cells *25*, 2739-2749.

Chen, Y., and Rice, P.A. (2003). New insight into site-specific recombination from Flp recombinase-DNA structures. Annual review of biophysics and biomolecular structure *32*, 135-159.

Chiorazzi, N. (2007). Cell proliferation and death: forgotten features of chronic lymphocytic leukemia B cells. Best practice & research Clinical haematology *20*, 399-413.

Chiorazzi, N., Hatzi, K., and Albesiano, E. (2005). B-cell chronic lymphocytic leukemia, a clonal disease of B lymphocytes with receptors that vary in specificity for (auto)antigens. Annals of the New York Academy of Sciences *1062*, 1-12.

Cobaleda, C., and Sanchez-Garcia, I. (2009). B-cell acute lymphoblastic leukaemia: towards understanding its cellular origin. BioEssays : news and reviews in molecular, cellular and developmental biology *31*, 600-609.

Coffman, R.L., and Weissman, I.L. (1981). B220: a B cell-specific member of th T200 glycoprotein family. Nature *289*, 681-683.

Collins, R.J., Verschuer, L.A., Harmon, B.V., Prentice, R.L., Pope, J.H., and Kerr, J.F. (1989). Spontaneous programmed death (apoptosis) of B-chronic lymphocytic leukaemia cells following their culture in vitro. British journal of haematology *71*, 343-350.

Corradi, A., Croci, L., Broccoli, V., Zecchini, S., Previtali, S., Wurst, W., Amadio, S., Maggi, R., Quattrini, A., and Consalez, G.G. (2003). Hypogonadotropic hypogonadism and peripheral neuropathy in Ebf2-null mice. Development *130*, 401-410.

Cox, C.V., Diamanti, P., Evely, R.S., Kearns, P.R., and Blair, A. (2009). Expression of CD133 on leukemia-initiating cells in childhood ALL. Blood *113*, 3287-3296.

Cox, C.V., Evely, R.S., Oakhill, A., Pamphilon, D.H., Goulden, N.J., and Blair, A. (2004). Characterization of acute lymphoblastic leukemia progenitor cells. Blood *104*, 2919-2925.

Derbinski, J., Schulte, A., Kyewski, B., and Klein, L. (2001). Promiscuous gene expression in medullary thymic epithelial cells mirrors the peripheral self. Nature immunology *2*, 1032-1039.

DeVita, V.T., and Schein, P.S. (1973). The use of drugs in combination for the treatment of cancer: rationale and results. The New England journal of medicine *288*, 998-1006.

DiMascio, L., Voermans, C., Uqoezwa, M., Duncan, A., Lu, D., Wu, J., Sankar, U., and Reya, T. (2007). Identification of adiponectin as a novel hemopoietic stem cell growth factor. J Immunol *178*, 3511-3520.

Dohner, H., Estey, E.H., Amadori, S., Appelbaum, F.R., Buchner, T., Burnett, A.K., Dombret, H., Fenaux, P., Grimwade, D., Larson, R.A.*, et al.* (2010). Diagnosis and management of acute myeloid leukemia in adults: recommendations from an international expert panel, on behalf of the European LeukemiaNet. Blood *115*, 453-474.

Dohner, H., Stilgenbauer, S., Benner, A., Leupolt, E., Krober, A., Bullinger, L., Dohner, K., Bentz, M., and Lichter, P. (2000). Genomic aberrations and survival in chronic lymphocytic leukemia. The New England journal of medicine *343*, 1910-1916.

Dores, G.M., Anderson, W.F., Curtis, R.E., Landgren, O., Ostroumova, E., Bluhm, E.C., Rabkin, C.S., Devesa, S.S., and Linet, M.S. (2007). Chronic lymphocytic leukaemia and small lymphocytic lymphoma: overview of the descriptive epidemiology. British journal of haematology *139*, 809-819.

Downing, J.R. (2008). Targeted therapy in leukemia. Modern pathology : an official journal of the United States and Canadian Academy of Pathology, Inc *21 Suppl 2*, S2-7.

Dubois, L., and Vincent, A. (2001). The COE--Collier/Olf1/EBF--transcription factors: structural conservation and diversity of developmental functions. Mechanisms of development *108*, 3-12.

Dunn, B. (2012). Cancer: Solving an age-old problem. Nature *483*, S2-6.

Eames, B.F., Sharpe, P.T., and Helms, J.A. (2004). Hierarchy revealed in the specification of three skeletal fates by Sox9 and Runx2. Developmental biology *274*, 188-200.

Engsig, M.T., Chen, Q.J., Vu, T.H., Pedersen, A.C., Therkidsen, B., Lund, L.R., Henriksen, K., Lenhard, T., Foged, N.T., Werb, Z.*, et al.* (2000). Matrix metalloproteinase 9 and vascular endothelial growth factor are essential for osteoclast recruitment into developing long bones. The Journal of cell biology *151*, 879-889.

Fleming, H.E., Janzen, V., Lo Celso, C., Guo, J., Leahy, K.M., Kronenberg, H.M., and Scadden, D.T. (2008). Wnt signaling in the niche enforces hematopoietic stem cell quiescence and is necessary to preserve self-renewal in vivo. Cell stem cell *2*, 274-283.

Ford, A.M., Palmi, C., Bueno, C., Hong, D., Cardus, P., Knight, D., Cazzaniga, G., Enver, T., and Greaves, M. (2009). The TEL-AML1 leukemia fusion gene dysregulates the TGF-beta pathway in early B lineage progenitor cells. The Journal of clinical investigation *119*, 826-836.

Gleissner, B., Gokbuget, N., Bartram, C.R., Janssen, B., Rieder, H., Janssen, J.W., Fonatsch, C., Heyll, A., Voliotis, D., Beck, J.*, et al.* (2002). Leading prognostic relevance of the BCR-ABL translocation in adult acute B-lineage lymphoblastic leukemia: a prospective study of the German Multicenter Trial Group and confirmed polymerase chain reaction analysis. Blood *99*, 1536-1543.

Gokbuget, N., and Hoelzer, D. (2009). Treatment of adult acute lymphoblastic leukemia. Seminars in hematology *46*, 64-75.

Goodell, M.A., Brose, K., Paradis, G., Conner, A.S., and Mulligan, R.C. (1996). Isolation and functional properties of murine hematopoietic stem cells that are replicating in vivo. The Journal of experimental medicine *183*, 1797-1806.

Gray, D.H., Tull, D., Ueno, T., Seach, N., Classon, B.J., Chidgey, A., McConville, M.J., and Boyd, R.L. (2007). A unique thymic fibroblast population revealed by the monoclonal antibody MTS-15. J Immunol *178*, 4956-4965.

Greaves, M.F., and Wiemels, J. (2003). Origins of chromosome translocations in childhood leukaemia. Nature reviews Cancer *3*, 639-649.

Gu, H., Zou, Y.R., and Rajewsky, K. (1993). Independent control of immunoglobulin switch recombination at individual switch regions evidenced through Cre-loxP-mediated gene targeting. Cell *73*, 1155-1164.

Hagman, J., Gutch, M.J., Lin, H., and Grosschedl, R. (1995). EBF contains a novel zinc coordination motif and multiple dimerization and transcriptional activation domains. The EMBO journal *14*, 2907-2916.

Hallaert, D.Y., Spijker, R., Jak, M., Derks, I.A., Alves, N.L., Wensveen, F.M., de Boer, J.P., de Jong, D., Green, S.R., van Oers, M.H.*, et al.* (2007). Crosstalk among Bcl-2 family members in B-CLL: seliciclib acts via the Mcl-1/Noxa axis and gradual exhaustion of Bcl-2 protection. Cell death and differentiation *14*, 1958-1967.

Harris, N.L., Jaffe, E.S., Diebold, J., Flandrin, G., Muller-Hermelink, H.K., Vardiman, J., Lister, T.A., and Bloomfield, C.D. (2000). The World Health Organization classification of neoplastic diseases of the haematopoietic and lymphoid tissues: Report of the Clinical Advisory Committee Meeting, Airlie House, Virginia, November 1997. Histopathology *36*, 69-86.

Harrison, C.J. (2009). Cytogenetics of paediatric and adolescent acute lymphoblastic leukaemia. British journal of haematology *144*, 147-156.

He, W., Barak, Y., Hevener, A., Olson, P., Liao, D., Le, J., Nelson, M., Ong, E., Olefsky, J.M., and Evans, R.M. (2003). Adipose-specific peroxisome proliferator-activated receptor gamma knockout causes insulin resistance in fat and liver but not in muscle. Proceedings of the National Academy of Sciences of the United States of America *100*, 15712-15717.

Heissig, B., Hattori, K., Dias, S., Friedrich, M., Ferris, B., Hackett, N.R., Crystal, R.G., Besmer, P., Lyden, D., Moore, M.A.*, et al.* (2002). Recruitment of stem and progenitor cells from the bone marrow niche requires MMP-9 mediated release of kit-ligand. Cell *109*, 625-637.

Hiechinger, S. (2010). Die Rolle von EBF2 in der haematopoietischen Stammzellnische.Ph.D. Thesis. LMU Munich: Faculty of Biology,

Hotamisligil, G.S., Johnson, R.S., Distel, R.J., Ellis, R., Papaioannou, V.E., and Spiegelman, B.M. (1996). Uncoupling of obesity from insulin resistance through a targeted mutation in aP2, the adipocyte fatty acid binding protein. Science *274*, 1377-1379.

Hu, Y., and Smyth, G.K. (2009). ELDA: extreme limiting dilution analysis for comparing depleted and enriched populations in stem cell and other assays. Journal of immunological methods *347*, 70-78.

Hulett, H.R., Bonner, W.A., Barrett, J., and Herzenberg, L.A. (1969). Cell sorting: automated separation of mammalian cells as a function of intracellular fluorescence. Science *166*, 747-749.

Jacobson, L.O. (1952). Evidence for a humoral factor (or factors) concerned in recovery from radiation injury: a review. Cancer research *12*, 315-325.

Jacobson, L.O., Marks, E.K., and et al. (1949). The role of the spleen in radiation injury. Proc Soc Exp Biol Med *70*, 740-742.

Janeway, C. M., K.; Travers, P.;Walport, M. (2008). Immunobiology, seventh edition: Garland Science.

Jenkinson, W.E., Jenkinson, E.J., and Anderson, G. (2003). Differential requirement for mesenchyme in the proliferation and maturation of thymic epithelial progenitors. The Journal of experimental medicine *198*, 325-332.

Jimenez, M.A., Akerblad, P., Sigvardsson, M., and Rosen, E.D. (2007). Critical role for Ebf1 and Ebf2 in the adipogenic transcriptional cascade. Molecular and cellular biology *27*, 743-757.

Jin, K., Jiang, H., Mo, Z., and Xiang, M. (2010). Early B-cell factors are required for specifying multiple retinal cell types and subtypes from postmitotic precursors. The Journal of neuroscience : the official journal of the Society for Neuroscience *30*, 11902-11916.

Juraskova, V., and Tkadlecek, L. (1965). Character of primary and secondary colonies of haematopoiesis in the spleen of irradiated mice. Nature *206*, 951-952.

Kampen, K.R. (2012). The discovery and early understanding of leukemia. Leukemia research *36*, 6-13.

Kay, N.E., and Shanafelt, T.D. (2007). Prognostic factors in chronic lymphocytic leukemia. Current hematologic malignancy reports *2*, 49-55.

Kessenbrock, K., Plaks, V., and Werb, Z. (2010). Matrix metalloproteinases: regulators of the tumor microenvironment. Cell *141*, 52-67.

Kiel, M.J., Yilmaz, O.H., Iwashita, T., Yilmaz, O.H., Terhorst, C., and Morrison, S.J. (2005). SLAM family receptors distinguish hematopoietic stem and progenitor cells and reveal endothelial niches for stem cells. Cell *121*, 1109-1121.

Kieslinger, M., Hiechinger, S., Dobreva, G., Consalez, G.G., and Grosschedl, R. (2010). Early B cell factor 2 regulates hematopoietic stem cell homeostasis in a cell-nonautonomous manner. Cell stem cell *7*, 496-507.

Kimura, A., Inose, H., Yano, F., Fujita, K., Ikeda, T., Sato, S., Iwasaki, M., Jinno, T., Ae, K., Fukumoto, S.*, et al.* (2010). Runx1 and Runx2 cooperate during sternal morphogenesis. Development *137*, 1159-1167.

Klein, L. (2009). Dead man walking: how thymocytes scan the medulla. Nature immunology *10*, 809-811.

Klein, L., Hinterberger, M., Wirnsberger, G., and Kyewski, B. (2009). Antigen presentation in the thymus for positive selection and central tolerance induction. Nature reviews Immunology *9*, 833-844.

Kohler, G., and Milstein, C. (1975). Continuous cultures of fused cells secreting antibody of predefined specificity. Nature *256*, 495-497.

Komori, T., Yagi, H., Nomura, S., Yamaguchi, A., Sasaki, K., Deguchi, K., Shimizu, Y., Bronson, R.T., Gao, Y.H., Inada, M.*, et al.* (1997). Targeted disruption of Cbfa1 results in a complete lack of bone formation owing to maturational arrest of osteoblasts. Cell *89*, 755-764.

Lagasse, E., Shizuru, J.A., Uchida, N., Tsukamoto, A., and Weissman, I.L. (2001). Toward regenerative medicine. Immunity *14*, 425-436.

Lagneaux, L., Delforge, A., Bron, D., De Bruyn, C., and Stryckmans, P. (1998). Chronic lymphocytic leukemic B cells but not normal B cells are rescued from apoptosis by contact with normal bone marrow stromal cells. Blood *91*, 2387-2396.

Lanasa, M.C. (2010). Novel insights into the biology of CLL. Hematology / the Education Program of the American Society of Hematology American Society of Hematology Education Program *2010*, 70-76.

Lapidot, T., Sirard, C., Vormoor, J., Murdoch, B., Hoang, T., Caceres-Cortes, J., Minden, M., Paterson, B., Caligiuri, M.A., and Dick, J.E. (1994). A cell initiating human acute myeloid leukaemia after transplantation into SCID mice. Nature *367*, 645-648.

Li, C., Heidt, D.G., Dalerba, P., Burant, C.F., Zhang, L., Adsay, V., Wicha, M., Clarke, M.F., and Simeone, D.M. (2007). Identification of pancreatic cancer stem cells. Cancer research *67*, 1030-1037.

Liberg, D., Sigvardsson, M., and Akerblad, P. (2002). The EBF/Olf/Collier family of transcription factors: regulators of differentiation in cells originating from all three embryonal germ layers. Molecular and cellular biology *22*, 8389-8397.

Lin, H., and Grosschedl, R. (1995). Failure of B-cell differentiation in mice lacking the transcription factor EBF. Nature *376*, 263-267.

Lin, K.K., and Goodell, M.A. (2011). Detection of hematopoietic stem cells by flow cytometry. Methods in cell biology *103*, 21-30.

Logan, M., Martin, J.F., Nagy, A., Lobe, C., Olson, E.N., and Tabin, C.J. (2002). Expression of Cre Recombinase in the developing mouse limb bud driven by a Prxl enhancer. Genesis *33*, 77-80.

Lombard, M., Pastoret, P.P., and Moulin, A.M. (2007). A brief history of vaccines and vaccination. Rev Sci Tech *26*, 29-48.

Long, F. (2012). Building strong bones: molecular regulation of the osteoblast lineage. Nature reviews Molecular cell biology *13*, 27-38.

Lorenz, E., Uphoff, D., Reid, T.R., and Shelton, E. (1951). Modification of irradiation injury in mice and guinea pigs by bone marrow injections. Journal of the National Cancer Institute *12*, 197-201.

Lymperi, S., Ferraro, F., and Scadden, D.T. (2010). The HSC niche concept has turned 31. Has our knowledge matured? Annals of the New York Academy of Sciences *1192*, 12-18.

Maitland, N.J., and Collins, A.T. (2008). Prostate cancer stem cells: a new target for therapy. Journal of clinical oncology : official journal of the American Society of Clinical Oncology *26*, 2862-2870.

Makinodan, T. (1956). Circulating rat cells in lethally irradiated mice protected with rat bone marrow. Proc Soc Exp Biol Med *92*, 174-179.

Malavasi, F., Deaglio, S., Damle, R., Cutrona, G., Ferrarini, M., and Chiorazzi, N. (2011). CD38 and chronic lymphocytic leukemia: a decade later. Blood *118*, 3470-3478.

Malgaretti, N., Pozzoli, O., Bosetti, A., Corradi, A., Ciarmatori, S., Panigada, M., Bianchi, M.E., Martinez, S., and Consalez, G.G. (1997). Mmot1, a new helix-loop-helix transcription factor gene displaying a sharp expression boundary in the embryonic mouse brain. The Journal of biological chemistry *272*, 17632-17639.

Malin, S., McManus, S., and Busslinger, M. (2010). STAT5 in B cell development and leukemia. Current opinion in immunology *22*, 168-176.

Martin, J.F., Bradley, A., and Olson, E.N. (1995). The paired-like homeo box gene MHox is required for early events of skeletogenesis in multiple lineages. Genes & development *9*, 1237-1249.

Massa, G., Wyllie, J.P., Pratt, A.M., Molineux, G., and Schofield, R. (1987). Marrow repopulation in mice treated with busulphan or isopropyl methane sulphonate and bone marrow. British journal of haematology *66*, 11-14.

Matloubian, M., Lo, C.G., Cinamon, G., Lesneski, M.J., Xu, Y., Brinkmann, V., Allende, M.L., Proia, R.L., and Cyster, J.G. (2004). Lymphocyte egress from thymus and peripheral lymphoid organs is dependent on S1P receptor 1. Nature *427*, 355-360.

McGregor, S., McNeer, J., and Gurbuxani, S. (2012). Beyond the 2008 World Health Organization classification: the role of the hematopathology laboratory in the diagnosis and management of acute lymphoblastic leukemia. Seminars in diagnostic pathology *29*, 2-11.

Mendez-Ferrer, S., Michurina, T.V., Ferraro, F., Mazloom, A.R., Macarthur, B.D., Lira, S.A., Scadden, D.T., Ma'ayan, A., Enikolopov, G.N., and Frenette, P.S. (2010). Mesenchymal and haematopoietic stem cells form a unique bone marrow niche. Nature *466*, 829-834.

Mercier, F.E., Ragu, C., and Scadden, D.T. (2012). The bone marrow at the crossroads of blood and immunity. Nature reviews Immunology *12*, 49-60.

Michiels, J.J., De Raeve, H., Hebeda, K., Lam, K.H., Berneman, Z., Schroyens, W., and Schwarz, J. (2007). WHO bone marrow features and European clinical, molecular, and pathological (ECMP) criteria for the diagnosis of myeloproliferative disorders. Leukemia research *31*, 1031-1038.

Morrison, S.J., Hemmati, H.D., Wandycz, A.M., and Weissman, I.L. (1995a). The purification and characterization of fetal liver hematopoietic stem cells. Proceedings of the National Academy of Sciences of the United States of America *92*, 10302-10306.

Morrison, S.J., Uchida, N., and Weissman, I.L. (1995b). The biology of hematopoietic stem cells. Annual review of cell and developmental biology *11*, 35-71.

Muller-Sieburg, C.E., Whitlock, C.A., and Weissman, I.L. (1986). Isolation of two early B lymphocyte progenitors from mouse marrow: a committed pre-pre-B cell and a clonogenic Thy-1-lo hematopoietic stem cell. Cell *44*, 653-662.

Nagasawa, T., Hirota, S., Tachibana, K., Takakura, N., Nishikawa, S., Kitamura, Y., Yoshida, N., Kikutani, H., and Kishimoto, T. (1996). Defects of B-cell lymphopoiesis and bone-marrow myelopoiesis in mice lacking the CXC chemokine PBSF/SDF-1. Nature *382*, 635-638.

Nakashima, K., Zhou, X., Kunkel, G., Zhang, Z., Deng, J.M., Behringer, R.R., and de Crombrugghe, B. (2002). The novel zinc finger-containing transcription factor osterix is required for osteoblast differentiation and bone formation. Cell *108*, 17-29.

Naveiras, O., Nardi, V., Wenzel, P.L., Hauschka, P.V., Fahey, F., and Daley, G.Q. (2009). Bone-marrow adipocytes as negative regulators of the haematopoietic microenvironment. Nature *460*, 259-263.

Nehls, M., Pfeifer, D., Schorpp, M., Hedrich, H., and Boehm, T. (1994). New member of the winged-helix protein family disrupted in mouse and rat nude mutations. Nature *372*, 103-107.

Nelson, B.P., Gupta, R., Dewald, G.W., Paternoster, S.F., Rosen, S.T., and Peterson, L.C. (2007). Chronic lymphocytic leukemia FISH panel: impact on diagnosis. American journal of clinical pathology *128*, 323-332.

Nowell, P.C., Cole, L.J., Habermeyer, J.G., and Roan, P.L. (1956). Growth and continued function of rat marrow cells in x-radiated mice. Cancer research *16*, 258-261.

Nowell, P.C., and Hungerford, D.A. (1960). Chromosome studies on normal and leukemic human leukocytes. Journal of the National Cancer Institute *25*, 85-109.

Nutt, S.L., and Kee, B.L. (2007). The transcriptional regulation of B cell lineage commitment. Immunity *26*, 715-725.

O'Brien, C.A., Pollett, A., Gallinger, S., and Dick, J.E. (2007). A human colon cancer cell capable of initiating tumour growth in immunodeficient mice. Nature *445*, 106-110.

Onciu, M. (2009). Acute lymphoblastic leukemia. Hematology/oncology clinics of North America *23*, 655-674.

Oostendorp, R.A., Robin, C., Steinhoff, C., Marz, S., Brauer, R., Nuber, U.A., Dzierzak, E.A., and Peschel, C. (2005). Long-term maintenance of hematopoietic stem cells does not require contact with embryo-derived stromal cells in cocultures. Stem Cells *23*, 842-851.

Osawa, M., Hanada, K., Hamada, H., and Nakauchi, H. (1996). Long-term lymphohematopoietic reconstitution by a single CD34-low/negative hematopoietic stem cell. Science *273*, 242-245.

Ovcharenko, I., Nobrega, M.A., Loots, G.G., and Stubbs, L. (2004). ECR Browser: a tool for visualizing and accessing data from comparisons of multiple vertebrate genomes. Nucleic acids research *32*, W280-286.

Pantelouris, E.M. (1968). Absence of thymus in a mouse mutant. Nature *217*, 370-371.

Parmar, K., Mauch, P., Vergilio, J.A., Sackstein, R., and Down, J.D. (2007). Distribution of hematopoietic stem cells in the bone marrow according to regional hypoxia. Proceedings of the National Academy of Sciences of the United States of America *104*, 5431-5436.

Peault, B., Weissman, I.L., Buckle, A.M., Tsukamoto, A., and Baum, C. (1993). Thy-1-expressing CD34+ human cells express multiple hematopoietic potentialities in vitro and in SCID-hu mice. Nouvelle revue francaise d'hematologie *35*, 91-93.

Peitz, M., Pfannkuche, K., Rajewsky, K., and Edenhofer, F. (2002). Ability of the hydrophobic FGF and basic TAT peptides to promote cellular uptake of recombinant Cre recombinase: a tool for efficient genetic engineering of mammalian genomes. Proceedings of the National Academy of Sciences of the United States of America *99*, 4489-4494.

Pekarsky, Y., Zanesi, N., Aqeilan, R.I., and Croce, C.M. (2007). Animal models for chronic lymphocytic leukemia. Journal of cellular biochemistry *100*, 1109-1118.

Peschon, J.J., Morrissey, P.J., Grabstein, K.H., Ramsdell, F.J., Maraskovsky, E., Gliniak, B.C., Park, L.S., Ziegler, S.F., Williams, D.E., Ware, C.B.*, et al.* (1994). Early lymphocyte expansion is severely impaired in interleukin 7 receptor-deficient mice. The Journal of experimental medicine *180*, 1955-1960.

Petit, I., Szyper-Kravitz, M., Nagler, A., Lahav, M., Peled, A., Habler, L., Ponomaryov, T., Taichman, R.S., Arenzana-Seisdedos, F., Fujii, N.*, et al.* (2002). G-CSF induces stem cell mobilization by decreasing bone marrow SDF-1 and up-regulating CXCR4. Nature immunology *3*, 687-694.

Pittenger, M.F., Mackay, A.M., Beck, S.C., Jaiswal, R.K., Douglas, R., Mosca, J.D., Moorman, M.A., Simonetti, D.W., Craig, S., and Marshak, D.R. (1999). Multilineage potential of adult human mesenchymal stem cells. Science *284*, 143-147.

Polak, P., Cybulski, N., Feige, J.N., Auwerx, J., Ruegg, M.A., and Hall, M.N. (2008). Adipose-specific knockout of raptor results in lean mice with enhanced mitochondrial respiration. Cell metabolism *8*, 399-410.

Rawstron, A.C., Bennett, F.L., O'Connor, S.J., Kwok, M., Fenton, J.A., Plummer, M., de Tute, R., Owen, R.G., Richards, S.J., Jack, A.S.*, et al.* (2008). Monoclonal B-cell lymphocytosis and chronic lymphocytic leukemia. The New England journal of medicine *359*, 575-583.

Reya, T., Morrison, S.J., Clarke, M.F., and Weissman, I.L. (2001). Stem cells, cancer, and cancer stem cells. Nature *414*, 105-111.

Rezzani, R., Bonomini, F., and Rodella, L.F. (2008). Histochemical and molecular overview of the thymus as site for T-cells development. Progress in histochemistry and cytochemistry *43*, 73-120.

Rieger, M.A., Hoppe, P.S., Smejkal, B.M., Eitelhuber, A.C., and Schroeder, T. (2009). Hematopoietic cytokines can instruct lineage choice. Science *325*, 217-218.

Ringrose, L., Chabanis, S., Angrand, P.O., Woodroofe, C., and Stewart, A.F. (1999). Quantitative comparison of DNA looping in vitro and in vivo: chromatin increases effective DNA flexibility at short distances. The EMBO journal *18*, 6630-6641.

Rodda, S.J., and McMahon, A.P. (2006). Distinct roles for Hedgehog and canonical Wnt signaling in specification, differentiation and maintenance of osteoblast progenitors. Development *133*, 3231-3244.

Rodewald, H.R., Ogawa, M., Haller, C., Waskow, C., and DiSanto, J.P. (1997). Pro-thymocyte expansion by c-kit and the common cytokine receptor gamma chain is essential for repertoire formation. Immunity *6*, 265-272.

Rodriguez, C.I., Buchholz, F., Galloway, J., Sequerra, R., Kasper, J., Ayala, R., Stewart, A.F., and Dymecki, S.M. (2000). High-efficiency deleter mice show that FLPe is an alternative to Cre-loxP. Nature genetics *25*, 139-140.

Rosen, J.M., and Jordan, C.T. (2009). The increasing complexity of the cancer stem cell paradigm. Science *324*, 1670-1673.

Sabio, G., Das, M., Mora, A., Zhang, Z., Jun, J.Y., Ko, H.J., Barrett, T., Kim, J.K., and Davis, R.J. (2008). A stress signaling pathway in adipose tissue regulates hepatic insulin resistance. Science *322*, 1539-1543.

Sambandam, A., Maillard, I., Zediak, V.P., Xu, L., Gerstein, R.M., Aster, J.C., Pear, W.S., and Bhandoola, A. (2005). Notch signaling controls the generation and differentiation of early T lineage progenitors. Nature immunology *6*, 663-670.

Santanam, U., Zanesi, N., Efanov, A., Costinean, S., Palamarchuk, A., Hagan, J.P., Volinia, S., Alder, H., Rassenti, L., Kipps, T.*, et al.* (2010). Chronic lymphocytic leukemia modeled in mouse by targeted miR-29 expression. Proceedings of the National Academy of Sciences of the United States of America *107*, 12210-12215.

Sauer, B., and Henderson, N. (1988). Site-specific DNA recombination in mammalian cells by the Cre recombinase of bacteriophage P1. Proceedings of the National Academy of Sciences of the United States of America *85*, 5166-5170.

Schatton, T., Murphy, G.F., Frank, N.Y., Yamaura, K., Waaga-Gasser, A.M., Gasser, M., Zhan, Q., Jordan, S., Duncan, L.M., Weishaupt, C.*, et al.* (2008). Identification of cells initiating human melanomas. Nature *451*, 345-349.

Schnutgen, F., Stewart, A.F., von Melchner, H., and Anastassiadis, K. (2006). Engineering embryonic stem cells with recombinase systems. Methods in enzymology *420*, 100-136.

Schofield, R. (1978). The relationship between the spleen colony-forming cell and the haemopoietic stem cell. Blood cells *4*, 7-25.

Schriever, F., and Huhn, D. (2003). New directions in the diagnosis and treatment of chronic lymphocytic leukaemia. Drugs *63*, 953-969.

Schwenk, F., Baron, U., and Rajewsky, K. (1995). A cre-transgenic mouse strain for the ubiquitous deletion of loxP-flanked gene segments including deletion in germ cells. Nucleic acids research *23*, 5080-5081.

Seita, J., and Weissman, I.L. (2010). Hematopoietic stem cell: self-renewal versus differentiation. Wiley interdisciplinary reviews Systems biology and medicine *2*, 640-653.

Seo, H.S., and Serra, R. (2007). Deletion of Tgfbr2 in Prx1-cre expressing mesenchyme results in defects in development of the long bones and joints. Developmental biology *310*, 304-316.

Shultz, L.D., Lyons, B.L., Burzenski, L.M., Gott, B., Chen, X., Chaleff, S., Kotb, M., Gillies, S.D., King, M., Mangada, J.*, et al.* (2005). Human lymphoid and myeloid cell development in NOD/LtSz-scid IL2R gamma null mice engrafted with mobilized human hemopoietic stem cells. J Immunol *174*, 6477-6489.

Siminovitch, L., McCulloch, E.A., and Till, J.E. (1963). The Distribution of Colony-Forming Cells among Spleen Colonies. Journal of cellular physiology *62*, 327-336.

Simsek, T., Kocabas, F., Zheng, J., Deberardinis, R.J., Mahmoud, A.I., Olson, E.N., Schneider, J.W., Zhang, C.C., and Sadek, H.A. (2010). The distinct metabolic profile of hematopoietic stem cells reflects their location in a hypoxic niche. Cell stem cell *7*, 380-390.

Singh, S.K., Clarke, I.D., Terasaki, M., Bonn, V.E., Hawkins, C., Squire, J., and Dirks, P.B. (2003). Identification of a cancer stem cell in human brain tumors. Cancer research *63*, 5821-5828.

Spangrude, G.J., Heimfeld, S., and Weissman, I.L. (1988). Purification and characterization of mouse hematopoietic stem cells. Science *241*, 58-62.

Staal, F.J., Weerkamp, F., Baert, M.R., van den Burg, C.M., van Noort, M., de Haas, E.F., and van Dongen, J.J. (2004). Wnt target genes identified by DNA microarrays in immature CD34+ thymocytes regulate proliferation and cell adhesion. J Immunol *172*, 1099-1108.

Starr, T.K., Jameson, S.C., and Hogquist, K.A. (2003). Positive and negative selection of T cells. Annual review of immunology *21*, 139-176.

Takahama, Y. (2006). Journey through the thymus: stromal guides for T-cell development and selection. Nature reviews Immunology *6*, 127-135.

Trumpp, A., Essers, M., and Wilson, A. (2010). Awakening dormant haematopoietic stem cells. Nature reviews Immunology *10*, 201-209.

Uchida, N., Jerabek, L., and Weissman, I.L. (1996). Searching for hematopoietic stem cells. II. The heterogeneity of Thy-1.1(lo)Lin(-/lo)Sca-1+ mouse hematopoietic stem cells separated by counterflow centrifugal elutriation. Experimental hematology *24*, 649-659.

USSBS, 1945. United States Strategic Bombing Survey (Pacific War). Chapter II: The Effects of the Atomic Bombings [online]. Available from: http://www.ibiblio.org/hyperwar/AAF/USSBS/AtomicEffects/AtomicEffects-2.html [Accessed 26 November 2011].

van den Brink, M.R., Alpdogan, O., and Boyd, R.L. (2004). Strategies to enhance T-cell reconstitution in immunocompromised patients. Nature reviews Immunology *4*, 856-867.

Visvader, J.E., and Lindeman, G.J. (2008). Cancer stem cells in solid tumours: accumulating evidence and unresolved questions. Nature reviews Cancer *8*, 755-768.

Vu, T.H., and Werb, Z. (2000). Matrix metalloproteinases: effectors of development and normal physiology. Genes & development *14*, 2123-2133.

Wadleigh, M., and Tefferi, A. (2010). Classification and diagnosis of myeloproliferative neoplasms according to the 2008 World Health Organization criteria. International journal of hematology *91*, 174-179.

Wagers, A.J., Sherwood, R.I., Christensen, J.L., and Weissman, I.L. (2002). Little evidence for developmental plasticity of adult hematopoietic stem cells. Science *297*, 2256-2259.

Wang, M.M., Tsai, R.Y., Schrader, K.A., and Reed, R.R. (1993). Genes encoding components of the olfactory signal transduction cascade contain a DNA binding site that may direct neuronal expression. Molecular and cellular biology *13*, 5805-5813.

Wang, S.S., Lewcock, J.W., Feinstein, P., Mombaerts, P., and Reed, R.R. (2004). Genetic disruptions of O/E2 and O/E3 genes reveal involvement in olfactory receptor neuron projection. Development *131*, 1377-1388.

Warming, S., Costantino, N., Court, D.L., Jenkins, N.A., and Copeland, N.G. (2005). Simple and highly efficient BAC recombineering using galK selection. Nucleic acids research *33*, e36.

Warren, L.A., and Rossi, D.J. (2009). Stem cells and aging in the hematopoietic system. Mechanisms of ageing and development *130*, 46-53.

Weissman, I.L. (2002). The road ended up at stem cells. Immunological reviews *185*, 159-174.

Weissman, I.L., Anderson, D.J., and Gage, F. (2001). Stem and progenitor cells: origins, phenotypes, lineage commitments, and transdifferentiations. Annual review of cell and developmental biology *17*, 387-403.

Whitlock, C.A., and Witte, O.N. (1982). Long-term culture of B lymphocytes and their precursors from murine bone marrow. Proceedings of the National Academy of Sciences of the United States of America *79*, 3608-3612.

WHO, 2006. Health, history and hard choices: Health, history and hard choices: Funding dilemmas Funding dilemmas in a fast-changing world in a fast-changing world [online]. Available from: http:// www.who.int/kms/initiatives/indiana.pdf [Accessed 28 November 2011].

Wilson, A., Laurenti, E., Oser, G., van der Wath, R.C., Blanco-Bose, W., Jaworski, M., Offner, S., Dunant, C.F., Eshkind, L., Bockamp, E.*, et al.* (2008). Hematopoietic stem cells reversibly switch from dormancy to self-renewal during homeostasis and repair. Cell *135*, 1118-1129.

Wing, K., and Sakaguchi, S. (2010). Regulatory T cells exert checks and balances on self tolerance and autoimmunity. Nature immunology *11*, 7-13.

Yeoh, E.J., Ross, M.E., Shurtleff, S.A., Williams, W.K., Patel, D., Mahfouz, R., Behm, F.G., Raimondi, S.C., Relling, M.V., Patel, A., et al. (2002). Classification, subtype discovery, and prediction of outcome in pediatric acute lymphoblastic leukemia by gene expression profiling. Cancer cell 1, 133-143.

Yoshihara, H., Arai, F., Hosokawa, K., Hagiwara, T., Takubo, K., Nakamura, Y., Gomei, Y., Iwasaki, H., Matsuoka, S., Miyamoto, K.*, et al.* (2007). Thrombopoietin/MPL signaling regulates hematopoietic stem cell quiescence and interaction with the osteoblastic niche. Cell stem cell *1*, 685-697.

Zelent, A., Greaves, M., and Enver, T. (2004). Role of the TEL-AML1 fusion gene in the molecular pathogenesis of childhood acute lymphoblastic leukaemia. Oncogene *23*, 4275-4283.

Zhang, J., Niu, C., Ye, L., Huang, H., He, X., Tong, W.G., Ross, J., Haug, J., Johnson, T., Feng, J.Q.*, et al.* (2003). Identification of the haematopoietic stem cell niche and control of the niche size. Nature *425*, 836-841.

Zhang, S., Balch, C., Chan, M.W., Lai, H.C., Matei, D., Schilder, J.M., Yan, P.S., Huang, T.H., and Nephew, K.P. (2008). Identification and characterization of ovarian cancer-initiating cells from primary human tumors. Cancer research *68*, 4311-4320.

Zou, Y.R., Kottmann, A.H., Kuroda, M., Taniuchi, I., and Littman, D.R. (1998). Function of the chemokine receptor CXCR4 in haematopoiesis and in cerebellar development. Nature *393*, 595-599.

10 Acknowledgements

Zunächst bedanke ich mich herzlichst bei Allen, die zum Gelingen dieser Arbeit beigetragen haben. Es ist eine grosse Zahl an Personen, aber jede Unterstützung hatte in der jeweiligen Projektphase seine besondere Bedeutung. Einige Personen möchte ich allerdings namentlich hervorheben.

Mein herausragender Dank gilt Herrn Dr. Matthias Kieslinger: Für sein Vertrauen bei der Überlassung dieses anspruchsvollen Forschungsthemas, seine sich daran anschliessende mehrjährige wissenschaftliche Betreuung und Ausbildung, sein fortwährendes Interesse am Gelingen der Projekte im Team, seine motivierenden Worte und die Bereitstellung eines Arbeitsplatzes in seinem Labor. Darüber hinaus hat er mir zahlreiche Kooperationen in Mailand, München und Umgebung ermöglicht.

Gleichfalls von herausragender Bedeutung war die exzellente Betreuung meiner Dissertation durch Frau Prof. Dr. Berit Jungnickel. Mein besonderer Dank gilt ihr für die vielfältigen Hinweise, die stete Diskussionsbereitschaft und schliesslich die Übernahme des Erstgutachtens. Ihre tatkräftige Unterstützung hat wesentlich zum Gelingen dieser Arbeit beigetragen. Darüber hinaus möchte ich mich herzlichst bedanken für die Organisation des „Thesis Advisory Committees“ – und damit auch allen denen, die darin mitgewirkt haben.

Mein besonderer Dank gilt Herrn Prof. Dr. Michael Schleicher für seine Bereitschaft, das Zweitgutachten zu übernehmen.

Ein ganz besonderer Dank gilt Herrn PD Dr. Joseph Mautner für seine großartige Unterstützung, vor allem auch in den diffizilen Phasen der Versuchs-durchführungen.

Vielen Dank an Herrn Dr. Marc Schmidt-Supprian für die Begleitung dieser Arbeit als Mitglied des TA-Committees und seine großartige Unterstützung.

Ein großer Dank geht an Frau PD Dr. Ursula Strobl für Ihre Hilfe bei der Ausarbeitung der Targeting Strategie, Ihre Anleitung in der ES Zellkultur sowie an die Herren Dr. Gerhard Laux, Dr. Vigo Heissmeyer und Dr. Andreas Moosmann fuer die Unterstuetzung und stete Diskussionsbereitschaft, die sie mir und meinem Projekt entgegen gebracht haben.

Vielen Dank an die Professoren Wolfgang Hammerschmidt, Dirk Eick und Georg Bornkamm für die stets offene Tür und viele freundliche Gespräche.

Ein ganz besonderer Dank gilt auch meinen Kolleginnen und Kollegen in der AG Kieslinger; allen vorran Frau Dr. Inga Ludenberg für die wissenschaftlichen Diskussionen, den guten Zusammenhalt und das Füttern meiner (ES) Zellen ☺ Ferner Katharina Zettl, Dr. Gerald Burgstaller, Jehee Kim, Qiongman Wang, Dr. Silvia Hiechinger, Torsten Willert und der gesamten KMOLBI für die enge Zusammenarbeit, das inspirierende und stets freundliche Arbeitsumfeld.

Vielen Dank an Michael Hagemann, Franziska Liebel, Sabine Schlink, Martina Münichsdorfer, Daniela Golanski und Albert Geisshauser für die erfolgreiche Zusammenarbeit!

Ein Dank auch an meine Kollegen Dr. Medhanie Assmelash Mulaw, Simon Jochum, Dr. Dinesh Adhikary, Dr. Catarina Alves, Sebastian Grömminger und Dr. Kai Höfig für die Unterstützung bei Auswertung und kritischen Diskussion der Daten.

Last but least: Ein besonders herzlicher Dank geht natürlich an Familie, Freunde und vor allem Elke, die auch in schwierigen Projektphasen mir immer motivierend und unterstützend zur Seite gestanden sind. Vielen Dank!

11 Contribution

Characterization of *Ebf2*-expressing thymic fibroblasts, thymic transplantation experiments and analysis of the T cell profile were performed in cooperation with Dr. Maria Hinterberger (AG Klein, LMU).

DNA Microarray experiments were performed in cooperation with Dr. Holger Prokisch, Dr. Gertrud Eckstein, Katharina Heim and Katja Junghans (IHG, Neuherberg).

Blastocysts were harvested and ES cells were injected by Adrianne Tasdemir and Susanne Heidemann (IDG, Neuherberg).

Experiments with human ALL samples were performed in cooperation with PD Dr. Irmela Jeremias, Dr. Catarina Alves and Volker Groiß (AGV, Großhadern).

Human B-CLL patient samples and EL08/EL28 cell lines were provided by PD Dr. Ingo Ringshausen.

FACS sortings were performed mainly by Katharina Krüger and Torsten Willert.

12 Curriculum Vitae

Personal Data

Name: Christoph Hinzen

Birth place and date:

Contact information:

Email: Christoph.Hinzen@Helmholtz-muenchen.de

Phone: 089-7099541 or +49-177-2384594

Work address: Helmholtz Zentrum München, Marchioninistr. 25, 81375 München, Germany

Education

2008-2012: PhD studies at the Ludwig Maximilians-University (Munich, Germany) working at the Helmholtz Center Munich, Institute for Clinical and Molecular Tumor biology

2000-2007: Diploma studies at the Westfälische Wilhelms-University, Münster. Major subjects: biotechnology, zoology/cell biology, management and economics

1996-1999: Abitur, German International School Budapest, Hungary. (A-levels with a final total mark of 1.9 „good“ (in 1.0 (top) – 6.0 (bottom) scale)

Academic degree

2007: Final exam (Diplom) with a total mark of 1.1 „passed with distinction“